

KAUNAS UNIVERSITY OF TECHNOLOGY

EDVINAS CHALECKAS

NON-INVASIVE TECHNOLOGIES FOR BRAIN  
PROTECTION AGAINST FUNCTIONAL  
DAMAGE DURING CARDIAC SURGERY

Doctoral dissertation  
Technological Sciences, Electrical and Electronics Engineering (T 001)

2024, Kaunas

This doctoral dissertation was prepared at Kaunas University of Technology, Health Telematics Science Institute during the period of 2019–2023. The studies were supported by the Research Council of Lithuania.

**Scientific Supervisor:**

Prof. Dr. Arminas RAGAUSKAS (Kaunas University of Technology, Technological Sciences, Electrical and Electronics Engineering, T 001).

Edited by: English language editor Brigita Brasiënė (Publishing House *Technologija*), Lithuanian language editor Aurelija Gražina Rukšaitė (Publishing House *Technologija*).

**Dissertation Defense Board of Electrical and Electronics Engineering Science Field:**

Prof. Dr. Vaidotas MAROZAS (Kaunas University of Technology, Technological Sciences, Electrical and Electronics Engineering, T 001) – **chairperson**;

Prof. Dr. Hab. Arūnas LUKOŠEVIČIUS (Kaunas University of Technology, Technological Sciences, Electrical and Electronics Engineering, T 001);

Dr. Peter SMIELEWSKI (University of Cambridge, United Kingdom, Medical and Health Sciences, Medicine, M 001);

Prof. Dr. Antanas VAITKUS (Lithuanian University of Health Sciences, Medical and Health Sciences, Medicine, M 001);

Prof. Dr. Algimantas VALINEVIČIUS (Kaunas University of Technology, Technological Sciences, Electrical and Electronics Engineering, T 001).

The public defense of the dissertation will be held at 1 p.m. on 20 May, 2024 at the public meeting of Dissertation Defense Board of Electrical and Electronics Engineering Science Field in the Rectorate Hall at Kaunas University of Technology.

Address: K. Donelaičio 73-402, LT-44249 Kaunas, Lithuania

Phone: (+370) 608 28 527; e-mail [doktorantura@ktu.lt](mailto:doktorantura@ktu.lt)

The doctoral dissertation was sent out on 19 April, 2024.

The doctoral dissertation is available on the internet <http://ktu.edu> and at the library of Kaunas University of Technology (Gedimino 50, LT-44239 Kaunas, Lithuania).

© E. Chaleckas, 2024

KAUNO TECHNOLOGIJOS UNIVERSITETAS

EDVINAS CHALECKAS

SMEGENŲ FUNKCIJŲ APSAUGOS NUO  
PAŽEIDIMŲ KARDIOCHIRURGIJOJE  
NEINVAZINĖS TECHNOLOGIJOS

Daktaro disertacija  
Technologijos mokslai, elektros ir elektronikos inžinerija (T 001)

2024, Kaunas

Disertacija rengta 2019–2023 metais Kauno technologijos universiteto Sveikatos telematikos mokslo institute. Mokslinius tyrimus rėmė Lietuvos mokslo taryba.

**Mokslinis vadovas:**

prof. dr. Arminas RAGAUSKAS (Kauno technologijos universitetas, technologijos mokslai, elektros ir elektronikos inžinerija, T 001).

Redagavo: anglų kalbos redaktorė Brigita Brasienė (leidykla „Technologija“), lietuvių kalbos redaktorė Aurelija Gražina Rukšaitė (leidykla „Technologija“).

**Elektros ir elektronikos inžinerijos mokslo krypties disertacijos gynimo taryba:**

prof. dr. Vaidotas MAROZAS (Kauno technologijos universitetas, technologijos mokslai, elektros ir elektronikos inžinerija, T 001) – **pirmininkas**;

prof. habil. dr. Arūnas LUKOŠEVIČIUS (Kauno technologijos universitetas, technologijos mokslai, elektros ir elektronikos inžinerija, T 001);

dr. Peter SMIELEWSKI (Kembridžo universitetas, Jungtinė Karalystė, medicinos ir sveikatos mokslai, medicina, M 001);

prof. dr. Antanas VAITKUS (Lietuvos sveikatos mokslų universitetas, medicinos ir sveikatos mokslai, medicina, M 001);

prof. dr. Algimantas VALINEVIČIUS (Kauno technologijos universitetas, technologijos mokslai, elektros ir elektronikos inžinerija, T 001).

Disertacija bus ginama viešame Elektros ir elektronikos inžinerijos mokslo krypties disertacijos gynimo tarybos posėdyje 2024 m. gegužės 20 d. 13 val. Kauno technologijos universiteto Rektorato salėje.

Adresas: K. Donelaičio g. 73-402, LT-44249 Kaunas, Lietuva.

Tel: (+370) 608 28 527; el. paštas [doktorantura@ktu.lt](mailto:doktorantura@ktu.lt)

Disertacija išsiųsta 2024 m. balandžio 19 d.

Su disertacija galima susipažinti interneto svetainėje <http://ktu.edu> ir Kauno technologijos universiteto bibliotekoje (Gedimino g. 50, LT-44239 Kaunas, Lietuva).

© E. Chaleckas, 2024

## **Table of Contents**

LIST OF FIGURES .....	8
LIST OF TABLES .....	14
LIST OF ABBREVIATIONS AND TERMS .....	15
INTRODUCTION .....	16
1. THE CONCEPT OF CEREBRAL AUTOREGULATION.....	21
1.1. INTRODUCTION .....	21
1.2. SLOW WAVES OF STATIC CA .....	23
1.3. CONCEPT OF DYNAMIC CEREBRAL AUTOREGULATION .....	23
1.3.1. THIGH CUFF METHOD.....	24
1.3.2. CAROTID ARTERY COMPRESSION .....	25
1.3.3. VALSALVA MANEUVER .....	25
1.3.4. SPONTANEOUS PULSATIONS EVALUATION.....	26
1.3.5. SQUAT-STAND MANEUVER.....	27
CONCLUSIONS .....	28
2. NEUROPROTECTION BY MONITORING CEREBRAL BLOOD FLOW AUTOREGULATION .....	30
2.1. INTRODUCTION.....	30
2.2. CA EVALUATION METHODS .....	30
2.2.1. INVASIVE CA EVALUATION BY USING PRESSURE REACTIVITY INDEX (PRX) .....	30
2.2.2. NON-INVASIVE CA EVALUATION METHODS.....	31
2.2.2.1. NON-INVASIVE ICP ASSESSMENT BY ARMINAS RAGAUSKAS MODEL.....	31
2.2.2.2. NON-INVASIVE ICP ASSESSMENT BY BERNARD SCHMIDT MODEL.....	32
2.2.2.3. MEAN FLOW AUTOREGULATION INDEX (MX).....	32
2.2.2.4. CEREBRAL OXIMETRY INDEX (COX).....	34
2.2.2.5. VOLUMETRIC REACTIVITY INDEX (VRX).....	34

2.2.2.6. THE CONCEPT OF OPTIMAL CEREBRAL PERFUSION PRESSURE	35
2.2.2.7. PREVIOUS CLINICAL STUDY FINDINGS .....	36
CONCLUSIONS .....	38
2. HEART AND LUNG MACHINE OPERATIONAL MODES.....	39
3.1. INTRODUCTION .....	39
3.2. CONSTANT FLOW MODE.....	39
3.3. PULSATILE MODE .....	40
3.4. SINUS FLOW MODE.....	41
3.5. RECTANGULAR SEQUENCE FLOW MODE.....	41
CONCLUSIONS .....	43
4. METHODS AND MATERIALS .....	44
4.1. DATA COLLECTION .....	44
4.2. COGNITIVE TESTS.....	44
4.3. PATIENTS' DEMOGRAPHICS .....	45
4.4. SIGNAL MORPHOLOGY .....	45
4.5. RECTANGULAR WAVE FILTERING.....	47
4.6. CHALLENGES OF RECTANGULAR WAVE MODULATION .....	49
4.6.1. ALIASING BETWEEN NORADRENALINE AND RECTANGULAR WAVE MODULATION .....	49
4.6.2. ALIASING BETWEEN HEART PULSATION AND RECTANGULAR WAVE MODULATION .....	50
4.7. TRANSIENT FUNCTION INDEX (TFX) .....	51
4.8. MEAN FLOW INDEX (MX).....	53
4.9. PUMP INDUCED WAVE ANALYSIS (EX).....	53
4.10. RECTANGULAR WAVE ENVELOPE REACTIVITY INDEX (EX2).	55
4.11. NORADRENALINE INDUCED WAVE INDEX MX2 .....	59
4.12. COMPARISON OF NEW DERIVED ENVELOPE-BASED SIGNALS	60
CONCLUSIONS .....	62
5. RESULTS.....	63

5.1. TFX .....	63
5.2. MX.....	64
5.3. EX.....	66
5.4. EX2.....	68
5.5. MX2.....	70
CONCLUSIONS .....	72
GENERAL CONCLUSIONS.....	75
6. SANTRAUKA .....	76
REFERENCES .....	106
CURRICULUM VITAE .....	113
LIST OF PUBLICATIONS.....	114
ACKNOWLEDGMENTS .....	116

## List of figures

<b>Fig. 1.1.</b> Theoretical (green lines) and experimental (red line) Lassen's curves: green circles show theoretical reactions of hydrodynamic resistances of cerebral blood vessels to changes of CPP, red circles show averaged reactions of hydrodynamic resistances of cerebral blood vessels to changes of CPP taken from prospective clinical study of 77 TBI patients (adapted from [17]), where PbtO <sub>2</sub> – brain tissue oxygen tension, which is directly related to CBF, LLCA – lower limit of CA, ULCA – upper limit of CA.....	21
<b>Fig. 1.2.</b> Complex system of cerebral autoregulation (adapted from [18]) .....	22
<b>Fig. 1.3.</b> Different form slow ICP waves: a) absence of slow waves, b) symmetrical slow waves, c) asymmetrical slow waves, d) asymmetrical shape with plateau phase (adapted from [22]).....	23
<b>Fig. 1.4.</b> Structure mechanism of dynamic cerebral blood flow autoregulation (adapted from [27]).....	24
<b>Fig. 1.5.</b> ARI index, 10 different vMCA responses to ABP step function: a) positive front (adapted from [31]), b) different vMCA reactions to negative front (adapted from [29]) .....	25
<b>Fig. 1.6.</b> The carotid artery compression test (adapted from [32]).....	25
<b>Fig. 1.7.</b> Example of Valsalva maneuver: on the left side – Valsalva maneuver of the control group, the change in the heart rhythm and CBFV restoration are clearly shown; on a right side, low changes of heart rhythm are shown due to ganglionic blockade and no restoration of CBFV during Valsalva maneuver (adapted from [35]) .....	26
<b>Fig. 1.8.</b> Example of transfer function computation from spontaneous pulsations (adapted from [39]).....	27
<b>Fig. 1.9.</b> Squat-stand maneuver with squatting for 5 s and standing for 5 s (adapted from [40]) .....	28
<b>Fig. 2.1.</b> Example of PRx monitoring with external ventricular drainage and invasive ABP sensor (adapted from [45]).....	31
<b>Fig. 2.2.</b> Schematic representation of non-invasive intracranial pressure (ICP) monitoring equipment (adapted from [47]): (a) relevant orbit and brain anatomy in contact with the ICP measurement device, (b) block diagram of the system control unit: ICA – internal carotid artery, IOA – intracranial part of the ophthalmic artery, EOA – extracranial part of the ophthalmic artery, TCD – transcranial Doppler, Pe – external pressure applied to the ocular globe .....	32
<b>Fig. 2.3.</b> Example of Mx monitoring with ultrasonic transcranial Doppler transducer and invasive ABP sensor (adapted from [57]).....	33
<b>Fig. 2.4.</b> Example of monitoring volumetric reactivity index with Vittamed device and non-invasive Finnappress device.....	35
<b>Fig. 2.5.</b> Optimal ABP value identification according to optCPP concept: red – impaired CA, yellow – uncertain CA, green – intact CA .....	36



**Fig. 2.6.** Lassen’s curve of patient and optimal ABP curve; the plateau of approximated Lassen’s curve is below  $Prx < 0$  ..... 37

**Fig. 2.7.** ROC curves of different classifiers of CA impairment duration of the longest CA impairment event (blue solid line): sensitivity 76%, specificity 82%, AUC 0.81; dose of longest CA impairment events (brown dashed line): sensitivity 76%, specificity 76%, AUC 0.76; total duration of all CA impairment events (green dashed line): sensitivity 90%, specificity 50%, AUC 0.74; dose of all CA impairment events (violet dotted line): sensitivity 90%, specificity 61%, AUC 0.74 (adapted from [8]) ..... 37

**Fig. 3.1.** Stockert S5 heart and lung machine (adapted from [71]) ..... 39

**Fig. 3.2.** Example of constant flow mode generated by 3–3.5 Hz sinusoidal fluctuations generated by a heart and lung machine: a) ABP(t) pump vibrations, b) vMCA(t) pump vibrations ..... 40

**Fig. 3.3.** Example of pulsatile flow mode of a heart and lung machine: a) ABP(t) pulsatile flow mode, b) vCMA(t) pulsatile flow mode..... 40

**Fig. 3.4.** Sinus flow mode generated by a heart and lung machine: a) ABP(t) sinus flow mode, b) cerebral volumetric changes (t) to ABP(t) changes ..... 41

**Fig. 3.5.** The rectangular wave sequence generated with heart and lung machine by changing blood flow: a) ABP rectangular waves, b) transient vMCA response to ABP changes, which associates to intact CA ..... 42

**Fig. 3.6.** The rectangular wave sequence generated with heart and lung machine by changing blood flow: A) ABP rectangular waves, b) no transient vMCA response to the ABP changes, which corresponds to the impaired CA ..... 42

**Fig. 3.7.** Patent pending device which modulates square waves on a heart and lung machine ..... 43

**Fig. 4.1.** A structural diagram of transcranial Doppler blood flow velocity in middle cerebral artery (vMCA (t)) monitoring and invasive ABP(t) monitoring during CPB ..... 44

**Fig. 4.2.** Cardiac-pulmonary bypass surgery and its spectrum: a) ABP(t) signal over time, at the moment 150–210 min, heart and lung machine is used, b) cardiac bypass surgery spectrum used by MUSIC algorithm ..... 46

**Fig. 4.3.** Signal decomposition: a) raw ABP(t) signal, b) noradrenaline induced waves, c) rectangular wave modulation, d) 3 Hz pump motor frequency ..... 47

**Fig. 4.4.** Different filters are used to filter ABP noise: a) raw data of ABP signal, b) ABP signal filtered with 1 Hz lowpass filter, c) ABP signal filtered with 1 Hz lowpass filter, d) ABP signal filtered with 0.2 Hz lowpass filter, e) ABP signal filtered with 0.1 Hz lowpass filter..... 48

**Fig. 4.5.** Different filters used to filter vMCA noise: a) raw data of vMCA signal, b) vMCA signal filtered with 1 Hz lowpass filter, c) vMCA signal filtered with 0.5 Hz lowpass filter, d) vMCA signal filtered with 0.2 Hz lowpass filter, e) vMCA signal filtered with 0.1 Hz lowpass filter ..... 49

**Fig. 4.6.** Aliasing between noradrenaline induced waves and rectangular waves.... 50

**Fig. 4.7.** Aliasing between heart pulsations and rectangular waves: a) pulsation aliasing during ABP pulse (red line) and filtered ABP signal (black line), b) the vMCA reaction due to pulsations is distorted; however, it is visible in positive and negative fronts (blue line); black color shows filtered vMCA signal ..... 50

**Fig. 4.8.** Transient function response (blue color) to negative front ABP challenge (red color): a) lost CA correlation coefficient between challenge and response is  $R = 0.89$ , b) intact CA correlation coefficient between challenge and response is  $R = 0.16$  ..... 51

**Fig. 4.9.** Transient function response (blue color) to positive front ABP challenge (red color): a) lost CA correlation coefficient between challenge and response is  $R = 0.91$ , b) intact CA correlation coefficient between challenge and response is  $R = 0.64$  ... 51

**Fig. 4.10.** Distributions of Tfx intact and impaired values: a) estimated intact CA, b) estimated impaired CA; black line shows the median of a group ..... 52

**Fig. 4.11.** Tfx evaluation over time: a) ABP(t) signal, b) vMCA(t) signal, c) Tfx(t) ..... 52

**Fig. 4.12.** Example of Mx calculation: a) ABP(t) signal, b) vMCA(t) signal, c) Mx(t) data ..... 53

**Fig. 4.13.** Algorithm of Ex calculation..... 54

**Fig. 4.14.** Pump envelope decomposition: a) ABP(t) pump modulated envelope, b) vMCA(t) pump modulated envelope, c) comparison between ABP(t) and vMCA (t) pump modulated envelopes, d) Ex(t) data ..... **Error! Bookmark not defined.**

**Fig. 4.15.** Rectangular wave amplitude changes during noradrenaline injected wave: a) rectangular wave sequence during noradrenaline wave, b) detrended rectangular wave sequence ..... 56

**Fig. 4.16.** Pulse amplitude dependency from mean ABP; correlation coefficient  $R = 0.22$  ( $p = 0.063$ ) shows no significant associations between pulse amplitude and mean ABP; the orange color shows linear approximation ..... 56

**Fig. 4.17.** The algorithm of Ex2 calculation..... 57

**Fig. 4.18.** Rectangular wave envelope decomposition: a) ABP rectangular wave modulated envelope, b) vMCA wave modulated envelope, c) comparison between ABP and vMCA rectangular wave modulated envelopes, d) Ex2 reactivity index.. 58

**Fig. 4.19.** Noradrenaline induced waves; a) red color is ABP signal, blue color is vMCA; when ABP exceeds 110 mmHg, vMCA wave is sharp, in other cases, it is rounded, b) Mx2 calculation according to induced noradrenaline waves ..... 59

**Fig. 4.20.** Comparison of 3 ABP signals during cardiac bypass surgery with pump-on: a) filtered ABP signal, b) pump induced ABP envelope waves, c) rectangular modulated envelope waves ..... 60

**Fig. 4.21.** Comparison of three different ABP slow wave spectrum components using FFT transformation..... 61

<b>Fig. 4.22.</b> Comparison of 3 vMCA signals during cardiac bypass surgery with pump-on: a) filtered ABP signal, b) pump induced ABP envelope waves, c) rectangular modulated envelope waves.....	61
<b>Fig. 4.23.</b> Comparison of three different ABP slow wave spectrum components using FFT transformation.....	62
<b>Fig. 5.1.</b> Association between the duration of single longest cerebral autoregulation impairment (LCAI) event and POCD for two groups of patients using CA status identification index TF; there is no statistically significant difference ( $p = 0.047$ ) between two groups.....	63
<b>Fig. 5.2.</b> The distribution of mean ABP during LCAI event with CA identification index TFx; green color shows cases of no deterioration, and red color shows cases of POCD.....	64
<b>Fig. 5.3.</b> Association between duration of single longest cerebral autoregulation impairment event and POCD for two groups of patients using CA status identification index Mx; no statistically significant difference (Mann–Whitney U test, $p = 0.84$ ) between the two groups has been found.....	65
<b>Fig. 5.4.</b> The distribution of mean ABP during LCAI event with CA identification index Mx; green color shows cases of no deterioration, and red color shows cases of POCD.....	66
<b>Fig. 5.5.</b> Association between duration of single longest cerebral autoregulation impairment event and POCD for two groups of patients using CA status identification index Ex; no statistically significant difference ( $p = 0.10$ ) has been found between two groups; blue line shows the threshold separating 2 groups $LCAI = 160$ , ( $\chi^2 = 5.20$ , $p = 0.022$ ).....	67
<b>Fig. 5.6.</b> The distribution of mean ABP during LCAI event with CA identification index Ex; green color shows cases of no deterioration, and red color shows cases of POCD.....	68
<b>Fig. 5.7.</b> Association between the duration of single longest cerebral autoregulation impairment event and POCD for two groups of patients using CA status identification index Ex2; there is a statistically significant difference ( $p = 0.015$ ) between two groups; blue line shows the threshold separating 2 groups $LCAI = 220$ s, ( $\chi^2 = 11.54$ , $p = 0.001$ ).....	69
<b>Fig. 5.9.</b> Association between duration of single longest cerebral autoregulation impairment event and POCD for two groups of patients using CA status identification index Mx; statistically not significant difference (Mann–Whitney U test, $p = 0.12$ ) between two groups.....	71
<b>Fig. 5.10.</b> The distribution of mean ABP during LCAI event with CA identification index Mx2; green color shows cases of no deterioration, and red color shows cases of POCD.....	72
<b>6.1.1 pav.</b> Teorinė (žalia linija) ir eksperimentinė (raudona linija) Laseno kreivė. Žali skirtuliai rodo teorines reakcijas į hidrodinaminis varžos pokyčius smegenų	

kraujagyslėse kintant SPS. Raudoni skrituliai rodo reakcijas į kintančias hidrodinamines varžas kintant SPS ankstesnio perspektyviojo tyrimo su 77 sunkią galvos traumą patyrusiais pacientais metu (pritaikyta iš [17]). Čia PbtO <sub>2</sub> – smegenų audinio deguonies įtempis, kuris yra tiesiogiai susijęs su smegenų kraujo tekėjimu, LLCA – apatinė SKAR riba, ULCA – viršutinė SKAR riba.....	82
<b>6.2.1 pav.</b> Stocker S5 širdies ir plaučių mašina (pritaikyta iš [71]) .....	83
<b>6.2.2 pav.</b> Stačiakampio formos seka, sugeneruota naudojant širdies ir plaučių mašiną: a) AKS stačiakampio formos bangos, b) pereinamųjų vMCA bangų atsakai į AKS pokyčius, kurie yra siejami su veikiančia SKAR .....	84
<b>6.2.3 pav.</b> Stačiakampio formos seka, sugeneruota naudojant širdies ir plaučių mašiną: a) AKS stačiakampio formos bangos, b) pereinamųjų vMCA bangų atsakai į AKS pokyčius, kurie yra siejami su sutrikusia SKAR. ....	84
<b>6.2.4 pav.</b> Patentuojamas prietaisas moduluoti stačiakampes bangas Stocker S5 širdies ir plaučių mašinai, keičiant kraujo srautą.....	85
<b>6.3.1 pav.</b> Pereinamosios funkcijos atsakas (mėlyna spalva) į krentantį AKS frontą (raudona spalva): a) sutrikusios SKAR koreliacija tarp pokyčio ir atsako yra $R = 0,89$ , b) veikiančios SKAR koreliacija tarp pokyčio ir atsako yra $R = 0,16$ .....	86
<b>6.3.2 pav.</b> Pereinamosios funkcijos (mėlyna spalva) atsakas į kylantį AKS frontą (raudona spalva): a) sutrikusios SKAR koreliacija tarp pokyčio ir atsako yra $R = 0,91$ , b) veikiančios SKAR koreliacija tarp pokyčio ir atsako yra $R = 0,64$ .....	86
<b>6.3.3 pav.</b> TFX įvertinimas realiu laiku: a) AKS(t) signalas, b) vCMA(t) signalas, c) TFX įvertinimas. Juoda spalva rodo ilgiausią SKAR sutrikimo epizodą.....	87
<b>6.3.4 pav.</b> Mx koeficiento skaičiavimas. a) AKS(t) signalas, b) vMCA(t) signalas, c) Mx(t) duomenys.....	88
<b>6.3.5 pav.</b> Ex indekso įvertinimo algoritmas.....	89
<b>6.3.6 pav.</b> DKA mašinos moduluotų bangų dekompozicija: a) pompos AKS(t) moduluota gaubtinė, b) vMCA(t) pompos moduluota gaubtinė, c) palyginimas tarp ABP(t) ir vMCA(t) pompos moduluotų gaubtinių, d) Ex(t) duomenys .....	90
<b>6.3.7 pav.</b> Stačiakampio formos bangos amplitudės pokyčiai suleidžiant noradrenalino: a) stačiakampių bangų seka suleidus noradrenalino, b) stačiakampių seka pašalinus žemo dažnio komponentę .....	91
<b>6.3.9 pav.</b> Ex <sub>2</sub> skaičiavimo algoritmas.....	92
<b>6.3.10 pav.</b> Stačiakampio formos bangos gaubtinės: a) AKS(t) stačiakampio formos bangos moduluota gaubtinė, b) vMCA(t) stačiakampio formos bangos moduluota gaubtinė, c) palyginimas tarp AKS(t) ir vMCA(t) stačiakampių gaubtinių, d) Ex <sub>2</sub> (t) reaktyvumo indeksas .....	93
<b>6.3.11 pav.</b> Noradrenalino sukeltos bangos: a) raudona spalva yra AKS(t), mėlyna vMCA(t). Kai AKS viršija 110 mmHg, vMCA banga tampa aštri. Kitais atvejais vMCA banga yra suapvalinta, b) Mx <sub>2</sub> skaičiavimas iš lėtųjų noradrenalino bangų.	94

<b>6.4.1.</b> Asociacija tarp ilgiausio SKAR sutrikimo epizodo trukmės tarp POCD ir neturinčių kognityvinio sutrikimo grupių, naudojant SKAR būsenos indeksą <i>TFx</i> . Statistiškai reikšmingas skirtumas yra rastas ( $p = 0,047$ ) tarp dviejų grupių.....	95
<b>6.4.2 pav.</b> Pasiskirstymas tarp vidutinio AKS ilgiausio SKAR sutrikimo epizode naudojant SKAR būsenos identifikavimo indeksą <i>TFx</i> . Žalia spalva rodo atvejus, kai nebuvo kognityvinio sutrikimo, raudona spalva rodo atvejus įvykus POCD.....	96
<b>6.4.3 pav.</b> Asociacija tarp ilgiausio SKAR sutrikimo epizodo trukmės tarp POCD ir neturinčių kognityvinio sutrikimo grupių, naudojant SKAR būsenos indeksą <i>Mx</i> . Statistiškai reikšmingo skirtumo nerasta ( $p = 0,84$ ) tarp dviejų grupių.....	97
<b>6.4.4 pav.</b> Pasiskirstymas tarp vidutinio AKS ilgiausio SKAR sutrikimo epizode naudojant SKAR būsenos identifikavimo indeksą <i>TFx</i> . Žalia spalva rodo atvejus, kai nebuvo kognityvinio sutrikimo, raudona spalva rodo atvejus įvykus POCD.....	98
<b>6.4.5 pav.</b> Asociacija tarp ilgiausio SKAR sutrikimo epizodo trukmės tarp POCD ir neturinčių kognityvinio sutrikimo grupių, naudojant SKAR būsenos indeksą <i>Ex</i> . Statistiškai reikšmingo skirtumo nerasta ( $p = 0,10$ ) tarp dviejų grupių. Mėlyna linija yra slenkstis, skiriantis 2 grupes, jis yra lygus 160 s ( $\chi^2 = 8,50$ , $p = 0,004$ ). .....	99
<b>6.4.6 pav.</b> Pasiskirstymas tarp vidutinio AKS ilgiausio SKAR sutrikimo epizode naudojant SKAR būsenos identifikavimo indeksą <i>Ex</i> . Žalia spalva rodo atvejus, kai nebuvo kognityvinio sutrikimo, raudona spalva rodo atvejus įvykus POCD.....	100
<b>6.4.7 pav.</b> Asociacija tarp ilgiausio SKAR sutrikimo epizodo trukmės tarp POCD ir neturinčių kognityvinio sutrikimo grupių, naudojant SKAR būsenos identifikavimo indeksą <i>Ex2</i> . Statistiškai reikšmingas skirtumas yra rastas ( $p = 0,015$ ) tarp dviejų grupių. Mėlyna linija yra slenkstis, skiriantis 2 grupes, jis yra lygus 220 s ( $\chi^2 = 11,54$ , $p = 0,001$ ) .....	101
<b>6.4.8 pav.</b> Pasiskirstymas tarp vidutinio AKS ilgiausio SKAR sutrikimo epizode naudojant SKAR būsenos identifikavimo indeksą <i>Ex2</i> . Žalia spalva rodo atvejus, kai nebuvo kognityvinio sutrikimo, raudona spalva rodo atvejus įvykus POCD.....	102
<b>6.4.9 pav.</b> Asociacija tarp ilgiausio SKAR sutrikimo epizodo trukmės tarp POCD ir neturinčių kognityvinio sutrikimo grupių, naudojant SKAR būsenos identifikavimo indeksą <i>Mx2</i> . Statistiškai reikšmingas skirtumas yra rastas ( $p = 0,12$ ) tarp dviejų grupių.....	103
<b>6.4.10 pav.</b> Pasiskirstymas tarp vidutinio AKS ilgiausio SKAR sutrikimo epizode naudojant SKAR būsenos identifikavimo indeksą <i>Mx2</i> . Žalia spalva rodo atvejus, kai nebuvo kognityvinio sutrikimo, raudona spalva rodo atvejus įvykus POCD.....	104

## List of tables

<b>Table 1.1.</b> Comparison of different CA evaluation methods .....	29
<b>Table 2.1.</b> Comparison of different CA monitoring technologies .....	38
<b>Table 3.1.</b> Comparison of flow modes.....	43
<b>Table 4.1.</b> Demographic patient data .....	45
<b>Table 6.1.</b> Comparison of durations of the longest CA impairment episodes .....	73

## **LIST OF ABBREVIATIONS AND TERMS**

### **Abbreviations**

ABP – arterial blood pressure  
ARI – autoregulatory index  
CA – cerebral autoregulation  
CBF – cerebral blood flow  
CBFV – cerebral blood flow velocity  
Cox – cerebral oximetry index  
CPB – cardiac bypass  
CPP – cerebral perfusion pressure  
Ex – pump vibration envelope based envelop reactivity index  
Ex2 – rectangular modulation envelope based envelop reactivity index  
FFT – fast Fourier transformation  
FV – flow velocity  
IBV – intracranial blood volume  
ICP – intracranial pressure  
ICU – intensive care unit  
LCAI – longest cerebral autoregulation impairment  
LLCA – lower limit of cerebral autoregulation  
MABP – mean arterial blood pressure  
MUSIC – multiple signal classification  
Mx – mean flow index  
nICP – non-invasive intracranial pressure  
NIRS – near infrared spectroscopy  
optCPP – optimal cerebral perfusion pressure  
POCD – postoperative cognitive decline  
PRx – pressure reactivity index  
TBI – traumatic brain injury  
TCD – transcranial Doppler  
TFx – transient function index  
TOF – time of flight  
ULCA – upper limit of cerebral autoregulation  
vMCA – blood flow velocity in middle cerebral artery  
VRx – volumetric reactivity index

### **Terms**

Delirium – acute confusion state, a medical condition characterized by a sudden and severe disturbance in mental abilities.  
Postoperative cognitive dysfunction (POCD) – a decline in cognitive function (especially in memory and executive functions).

## INTRODUCTION

### Relevance of the research

One of the modern world health issues is coronary artery disease. Each year worldwide, due to this problem, around 7 million people's lives are lost, and 129 million people cannot continue the life that they were adjusted to [1]. In order to prevent such consequence, cardiac-pulmonary bypass (CPB) surgery is used to restore previous vascular blood flow by adding shunt for carotid arteries. According to 2020-year data, in European Union, such type of surgery was performed 139,000 times, and in Lithuania, there were performed 39.6 surgeries per 100,000 people [2]. Due to such demand, the number of CPB surgeries will increase in the future.

The complications of CPB surgery are that around 50% of patients develop neurocognitive dysfunctions, such as postoperative delirium, postoperative cognitive dysfunction (POCD), and stroke [3]. POCD is a state with impaired cognition, awareness, attention, and perception compared to the preoperative state. Besides neurocognitive dysfunctions, the complications can be acute kidney injury and arterial fibrillation [4]. Using heart and lung machine surgery is safe because blood flow is controlled by machine operator. However, there is no scientific evidence that surgery without heart and lung machine cause less cases of postoperative cognitive complications [5].

The cause of brain damage is that instead of natural blood flow, artificial blood flow produced by heart and lung machine does not always allow to maintain adequate arterial blood pressure (ABP). Cerebral autoregulation is brain function that ensures appropriate nutrition of brain cells with nutrients and oxygen demands. This function is implemented by maintaining constant cerebral blood flow within wide ABP range. This function is disturbed if ABP is outside of these limits of cerebral autoregulation. The CBF is controlled by vasodilation or vasoconstriction. Due to the autoregulatory mechanism, the constant CBF of 50 ml/100 g/min is maintained in changing the CPP conditions [6].

In medical literature, the process called "static" autoregulation means the stabilization of cerebral blood flow within some physiological limits of cerebral perfusion pressure (CPP). Stabilization, according to system control theory, means negative feedback and active dynamic autoregulatory process. "Static" autoregulation is impossible. A more correct term in slow autoregulatory process situation is "quasistatic". Intact quasistatic cerebral autoregulation can be identified in different ways. One of the simplest ways is to identify the phase shift between slow ICP(t) waves and ABP(t) waves.

Theoretically, if phase difference between these waves is close to  $180^\circ$ , it shows that CA is active and intact, because in the case of ABP(t) increment, the arterial blood vessels (including arterioles) constrict to decrease cerebral blood volume and make CBF stable. In an opposite case, the decrement of ABP(t) causes dilatation of arterioles, increment of cerebral blood volume, and as a consequence, the stabilization of CBF. If ABP(t) and ICP(t) slow waves are synphase, it is considered as impaired CA [7].



In a previous clinical study, the artificial slow waves with fixed period were generated during CBP surgery for continuous noninvasive monitoring of CA status using ultrasonic Vitamed time of flight device. The results have shown that longer than 5-minute cerebral blood flow autoregulation impairment event is associated with POCD [8]. Independent study was performed in Denmark during cardiac bypass surgery by using higher mean arterial blood pressure (above 70–80 mmHg) and comparing patient group where lower (40–50 mmHg) mean ABP was used. The comparison of two groups showed no association with POCD ( $p = 0.12$ ) [9]. This is the evidence that personal cerebral autoregulation impairment events are more important factors than mean ABP thresholds for ABP management during the surgery.

In order to determine optimal ABP or optimal CPP values in clinical practice of severe TBI patients intensive care, it takes usually minutes or hours to average the needed amount of monitoring data in order to achieve the needed uncertainty of CA impairment identification. However, author's new study on TBI patients provided evidence that it is possible to determine optimal ABP/ CPP value in 24 minutes on studied population when intermittent slow physiological ABP and ICP waves exist [10]. However, "static" CA estimation has a flaw: due to the noise, it requires averaging, which causes a delay in decision making.

A faster method to evaluate cerebral autoregulation status is to measure a transient function of CA system. Generally, CA is a non-linear system. In order to measure CA transient response, a linearization of CA system is needed. Thus, for that purpose, a small ( $\Delta ABP \text{ step} \leq 10 \text{ mmHg}$ , which is much less than mean ABP) ABP(t) challenge in the input of CA system is needed. Such step function challenge can be implemented by thigh-cuff release, cerebral artery compression in the neck, or squat-stand maneuver. In medical literature, a transient function of CA system identification is called "dynamic" cerebral autoregulation status evaluation [11, 12]. In an ABP step challenge, the normal physiological CA transient function duration (settling time) time is around 7–12 seconds or even more. If cerebral autoregulation is impaired, transient function follows step shape ABP(t) pattern [13].

In the current global market of medical devices and technologies, there is no equipment, which would allow to determine optimal ABP (or optimal CPP) faster than in 5–20 minutes. The idea was to modulate a blood flow of heart and lung machine by rectangular pulses (period of the pulses one minute or less) in order to continuously monitor CA transient functions. Such mode of heart and lung machine is novel and has never been clinically tested. Current heart and lung machines have constant flow working mode and pulsatile flow mode in order to imitate physiological heart pulsation. Pulsatile blood flow mode cannot be used for CA status monitoring because pulses are too short compared with intact CA settling time [28]. The prospective clinical study has been performed in order to clinically validate proposed novel heart and lung machine operation mode and evaluate an added value of CA transient function continuous real-time monitoring in the development of methodology and technology for human brain protection against functional brain damage during cardiac bypass surgery.

## **Scientific-technological problem and research hypothesis**

The scientific-technological problems:

1. In which way and by which means is it possible to protect a human brain from ischemic and hyperemic events by monitoring cerebral autoregulation non-invasively in the real time?

2. Is it possible to identify cerebral blood flow autoregulation within sub-minute delay and how to restore intact cerebral autoregulation before irreversible damage and death of neurons?

The research hypotheses: it is possible to identify intact or impaired cerebral autoregulation status with sub-minute time resolution by monitoring of transient responses of cerebral autoregulation system to rectangular shape blood flow sequences generated by a heart and lung machine; it is possible to protect an individual patient's brain from functional injuries during cardiac bypass surgery by identification of CA impairment start moment using sub-minute time resolution of CA transient function monitoring and using feedback from CA status monitor to a surgery and anesthesiology teams in order to stop CA impairment and restore intact CA in minutes before irreversible neurons damage.

### **Aim and tasks of the research**

The aim of the research is following the concept of precise and personalized medicine, to propose technology for non-invasive identification of the start moments of ischemic or hyperemic events inside individual patient's brain in order to restore a patient-specific optimal brain perfusion within time interval, which is shorter than the critical time of irreversible neuron damage.

The following tasks are formulated to achieve the aim of the research:

1. To analyze and review the existing literature on cerebral blood flow autoregulation and its estimation methods.
2. To propose safe electronic technology for patient in order to continuously modulate arterial blood flow, which would allow to identify cerebral blood flow autoregulation status with needed temporal resolution.
3. To identify factors allowing timely detection of CA impairment episodes according to the proposed arterial blood flow modulation technology.
4. To explore associations of proposed CA-related factors (CA-indexes) and other influential factors with the outcome of cardiac surgery patients.

### **Scientific novelty**

For the first time, there was proposed and tested a rectangular wave sequence generating method, which was implemented in heart and lung machine during cardiac bypass surgery. The generated sequence is monitored by transcranial Doppler technology (Viasonix Dolphin 4D, Raanna, Israel) in the middle cerebral artery to detect response to the ABP challenge. If cerebral flow velocity in the MCA is returning to mean velocity value, it is considered as the intact CA status. If cerebral blood flow velocity in the MCA is following ABP challenge, in this case, it is considered impaired CA status. It was shown for the first time that the proposed square

wave generation method allows to achieve necessary time delay for detecting CA impairment events. Such delay is a critical time associated with POCD during cardiac surgery and, therefore, could be used for the implementation in real time neuroprotection.

There were proposed new CA status indexes: pump vibration modulated envelope index (Ex), rectangular wave modulated envelope index (Ex2), and noradrenaline induced wave index (Mx2). These indexes have been explored for the first time.

### **Research methods and tools**

Cardiac pulmonary bypass patients were monitored with Viasonix 4D transcranial Doppler monitoring technology in the Hospital of Lithuanian University of Health Science, Kaunas Clinics. The protocol of the prospective study was approved by the Kaunas Regional Bioethics Committee (Permission No: BE-2-64, 2021-06-08). The patients' written consent was obtained in accordance with the Declaration of Helsinki (BMJ 1991; 302:1194). The performed clinical study of proposed methodology and technology was registered in ClinicalTrials.gov Identifier: NCT04943458.

Neuromonitoring data collection software ICM+ (Cambridge, UK) was used to collect the data.

The electronic device that can modulate square wave sequence was developed in the Health Telematics Science Institute, Kaunas University of Technology.

MATLAB 2016 software was used to process clinical monitoring data and make statistical analysis of the data.

### **Dissemination of findings**

The findings were published in two Q1 journals, in one Q2 journal and were presented in 6 international conferences (2 award winning) and EU and the USA patent applications.

### **Structure of the dissertation**

Dissertation consists of an introduction, eight chapters, conclusion, a list of references, a list of scientific publications, a list of conferences, and a list of patents.

In chapter one of the dissertation, the mechanism of cerebral autoregulation is described by dividing into static and dynamic cerebral autoregulation.

In chapter two, the different neuroprotection monitoring technologies, optimal CPP guided therapy, and a previously conducted clinical study are described.

In chapter three, arterial blood flow wave induction using heart and lung machine is explained.

In chapter four, the materials of study, signal processing and challenges of rectangular waves, transient function estimation, described moving correlations coefficient-based indexes are described.

In chapter five, the results of the study are provided.

The thesis is composed of 117 pages, 56 figures, 5 tables, and 77 references.

## **Funding of the research**

Project is funded by the European Regional Development Fund. Grant No. 01.2.2-CPVA-K-703-03-0025 Innovative non-invasive neuroprotection technology for cardiac-surgery, neurosurgery and ophthalmology.

## **Statements presented for the defense**

1. The rectangular blood flow modulation technology was developed, which is capable of generation of physiological arterial blood pressure waves that are necessary for CA status continuous monitoring.
2. The proposed rectangular manipulating blood flow modulation technology allows to estimate CA status as well as to detect CA impairment events with 1–2 min delay.
3. The duration of impaired cerebral autoregulation events estimated according to the methodology based on the proposed rectangular manipulating blood flow modulation is associated with POCD during cardiac surgery with cardiopulmonary bypass.
4. Notably, it has been observed for the first time that the interaction between blood flow and vascular resistance impacts the sequence of square waves and high-frequency pump-induced blood flow, which modulates slower cerebral blood flow oscillations.

# 1. THE CONCEPT OF CEREBRAL AUTOREGULATION

## 1.1. Introduction

The Monro–Kelly doctrine [14] postulates that volume in skull is constant and consists of blood, brain, and cerebrospinal fluid volumes. The changes of one component's volume results in changes of other component volumes to remain constant cerebral volume [14]. In 1959, Niel Lassen illustrated the relationship between cerebral blood flow (CBF) and cerebral perfusion pressure (CPP) [15]. Cerebral perfusion pressure is the difference between the mean arterial pressure (ABP) and mean intracranial pressure (ICP) (1):

$$CPP = ABP - ICP. \quad (1)$$

The Lassen's cerebral autoregulation curve (Fig. 1.1) has a range where CBF is constant in some patient specific interval of CPP [6]. CA autoregulation is a complicated process of cerebral arterial blood vessel (including arterioles) diameter control [16]. The singularity points of CA curve (Fig. 1.1) are called lower limit and upper limit of cerebral autoregulation. CBF stays almost constant between the singularity points. CA is intact between these points. In case of impaired CA, the ability of cerebral arterial blood vessel diameter control is lost. CA is lost when CPP is below LLCA or above ULCA. In TBI cases, CA impairments have been observed, which are expressed by linear dependence (no plateau interval) of CBF versus CPP. In individual patients, plateau can be narrowed, moved up or down, or moved to the left or right comparing with the theoretical Lassen's curve [77].

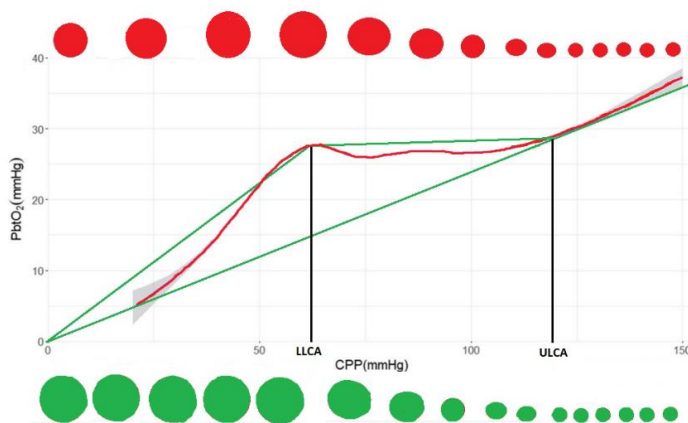


**Fig. 1.1.** Theoretical (green lines) and experimental (red line) Lassen's curves: green circles show theoretical reactions of hydrodynamic resistances of cerebral blood vessels to changes of CPP, red circles show averaged reactions of hydrodynamic resistances of cerebral blood vessels to changes of CPP taken from prospective clinical study of 77 TBI patients (adapted from [17]), where PbtO<sub>2</sub> – brain tissue oxygen tension, which is directly related to CBF, LLCA – lower limit of CA, ULCA – upper limit of CA

A lot of controversy exists in the medical literature [77] regarding the identification of LLCA and ULCA. LLCA is more clearly expressed in the experimental Lassen curve (Fig. 1.1). ULCA even theoretically is less clearly expressed (Fig. 1.1). The conducted clinical studies of CPB patients confirm that the speculation proposed in the paper [77] on quadriphasic experimental Lassen's curve has no clinical evidences.

Cerebral autoregulation is a complex process where cerebral blood flow is controlled by metabolic (CO<sub>2</sub>, glucose), myogenic (baroreflex), endothelium, and neurogenic changes [18]. During cardiac surgery, these processes are disturbed by the general anesthesia, which consists of three main components: sleep medication, painkillers, and muscle relaxants. Muscle relaxants decrease muscle tension, impacts autonomic and cardiovascular responses (increasing blood pressure and heart rate) [19]. During cardiac surgery with heart and lung machine, due to the absence of cardiac pulse waves, baroreflex is lost, and it is impossible to respond to the sudden changes of ABP in response by increasing or decreasing the heart rate. Additionally, the pulmonary ventilation does not provide adequate reaction to CO<sub>2</sub> changes by changing the frequency of respiration. All these factors during general anesthesia changes the CA responses to ABP changes. ICP starts to increase at higher dose of inhaled anesthetics, and in this way, it changes the shape of Lassen's curve. The plateau zone of Lassen's curve starts to narrow and getting steeper with higher dose of anesthetics [20]. Due to such problem, it is important to find the plateau zone where CA is intact and maintain during the surgery, prevent damage ischemic and hyperemic strokes and provide adequate nutrient and oxygen amount to the brain. The complex CA system is shown in Fig. 1.2.

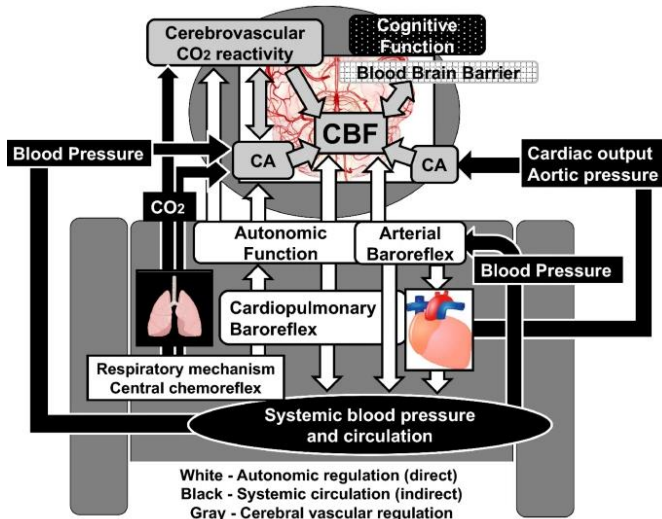


**Fig. 1.2.** Complex system of cerebral autoregulation (adapted from [18])

## 1.2. Slow waves of static CA

Slow ICP waves (as well called B waves) were introduced by Nils Lundberg in 1959. These waves are sinus shaped and have 0.5 to 2 cycles per minute. The origin of such waves is rhythmic changes of arterial CO<sub>2</sub> concentration due to the respiration, which cause oscillations in blood volume [21]. ICP slow waves can be absent, symmetrical shape, asymmetrical shape, and with plateau phase (Fig. 1.3) [22]. If ascending phase is longer, it creates asymmetrical wave shape, which is common at higher ICP [23]. The plateau waves can be described with sudden ICP elevations from normal or moderate ICP. They occur for brain injury, tumor, and acute hydrocephalus patients [24]. There is evidence that lower ICP slow wave magnitude associates with poor outcome with traumatic brain injury (TBI) patients [25].

If slow waves are absent, it is possible to generate it artificially by using pharmacological interventions, changing positive lower body pressure or changing concentration of CO<sub>2</sub> [26]. The manipulations are safe and change both ABP and CBF, which can allow to evaluate the status of CA.

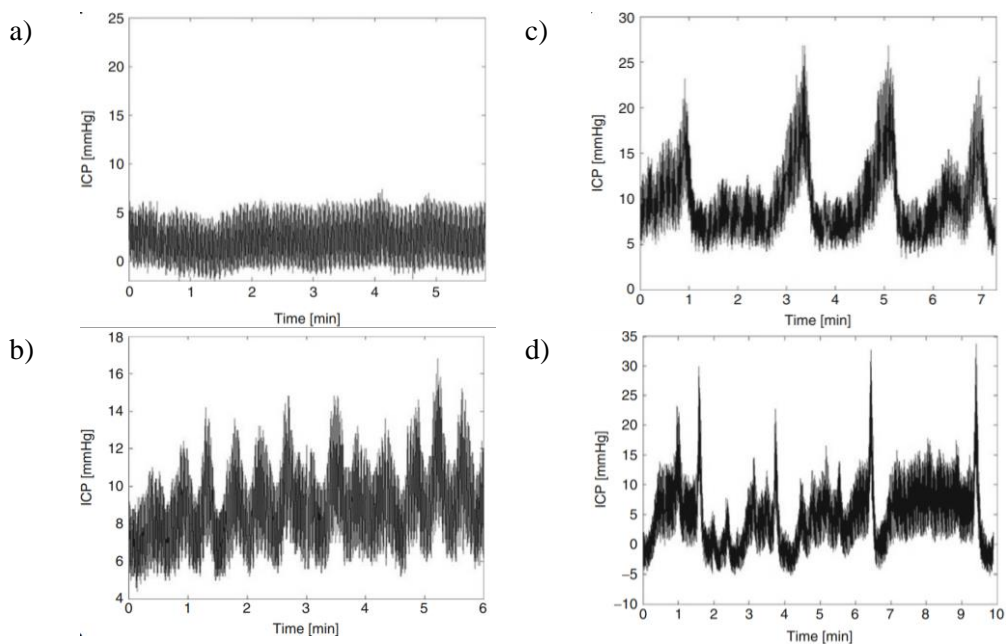


**Fig. 1.3.** Different form slow ICP waves: a) absence of slow waves, b) symmetrical slow waves, c) asymmetrical slow waves, d) asymmetrical shape with plateau phase (adapted from [22])

## 1.3. Concept of dynamic cerebral autoregulation

In medical literature, the term of dynamic cerebral autoregulation is an autoregulatory mechanism with a feedback loop. The CBFV is influenced by the changes of ABP. The CBFV reacts to the ABP changes by changing ICP and in such

a way changing CPP to maintain constant blood flow [27]. The time constant of such processes is around 5–7 seconds; thus, it is required to generate a challenge of duration longer or equal to 7 seconds. In case of such a system test, there is given an ABP challenge by creating step function (thigh cuff, carotid artery compression, squat–stand maneuver). In case of intact CA, the feedback control loop can restore the previous blood flow, and in case of impaired CA, the mechanism cannot restore, and CBFV follows ABP changes (Fig. 1.4). The created challenge as well provides better signal to the noise ratio [28].

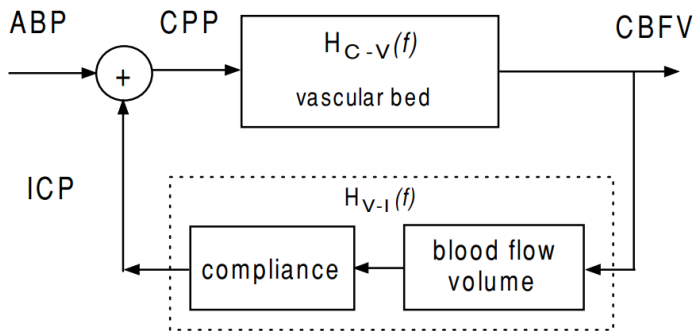


**Fig. 1.4.** Structure mechanism of dynamic cerebral blood flow autoregulation (adapted from [27])

### 1.3.1. Thigh cuff method

In order to determine dynamic CA functionality, thigh cuff method can be used, which increases ABP by 20 mmHg and then suddenly releases. After such impact, there was seen 10 different response reaction in MCA velocity. These different reactions differ by brain’s ability to restore previous blood flow. Such reaction introduced by Frank P. Tiecks and autoregulatory index (ARI) shows if  $ARI < 5$ , then CA is impaired (poor to non-ability to restore previous blood flow) and if  $ARI > 5$ , CA is intact (good ability to restore previous blood flow) (Fig. 1.5) [29]. The ARI responses are made with theoretical mathematical model, and the real response is compared with least square method to the nearest theoretical ARI responses. Recent studies have shown that dynamic autoregulation CA response decreases with age in men, but not for women [13]. Additionally, the decreased ARI value of patients after 7 days of cardiac surgery had postoperative delirium [30]. The settling time of CA response is around 5–7 seconds, and because of this reason, the duration of step function should be longer than 7 seconds. However, such method can be unsafe if a patient has peripheral artery disease, and due to the sudden cuff release, the stenosis can migrate to the brain and cause ischemia.



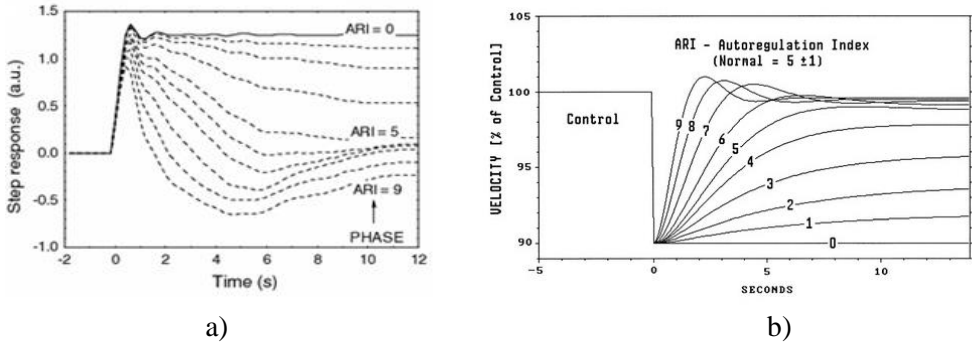


**Fig. 1.5.** ARI index, 10 different vMCA responses to ABP step function: a) positive front (adapted from [31]), b) different vMCA reactions to negative front (adapted from [29])

### 1.3.2. Carotid artery compression

The alternative dynamic CA evaluation test is carotid artery compression. Pressing the carotid artery in the neck, the blood flow is blocked to the brain, and the restoration of cerebral blood flow is observed with transcranial Doppler sonography (Fig. 1.6) [32]. However, such method requires that a patient does not have carotid artery stenosis because stenosis can migrate to the brain and cause ischemia, and it is required that a professional doctor could press carotid arteries.

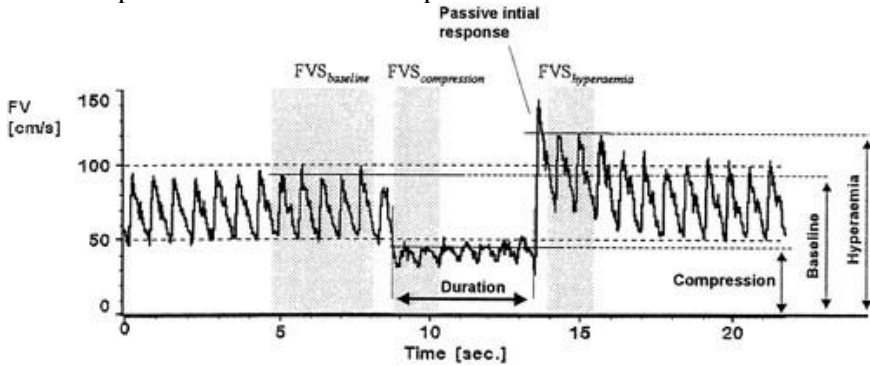


**Fig. 1.6.** The carotid artery compression test (adapted from [32])

### 1.3.3. Valsalva maneuver

Valsalva maneuver is commonly used for testing baroreflex by forcefully exhaling against a closed glottis. It elevates the intrathoracic pressure and affects venous blood flow, myocardial contractility, and vasomotor tone [33]. This test is simple and cheap and widely used. Valsalva maneuver has IV phases: I – sudden increase intrathoracic pressure, IIa – sudden ABP drop, IIb – ABP restoration by sympathetic system, III – ABP drop due to the rapid intrathoracic pressure drop, IV – overshoot of ABP [34]. It is possible to evaluate CA status by measuring the TCD

reactions of CBFV. The study used ganglionic blockade, which affects neural activity and shows no CBFV restoration after ABP fall during phase II (Fig. 1.7) [35].

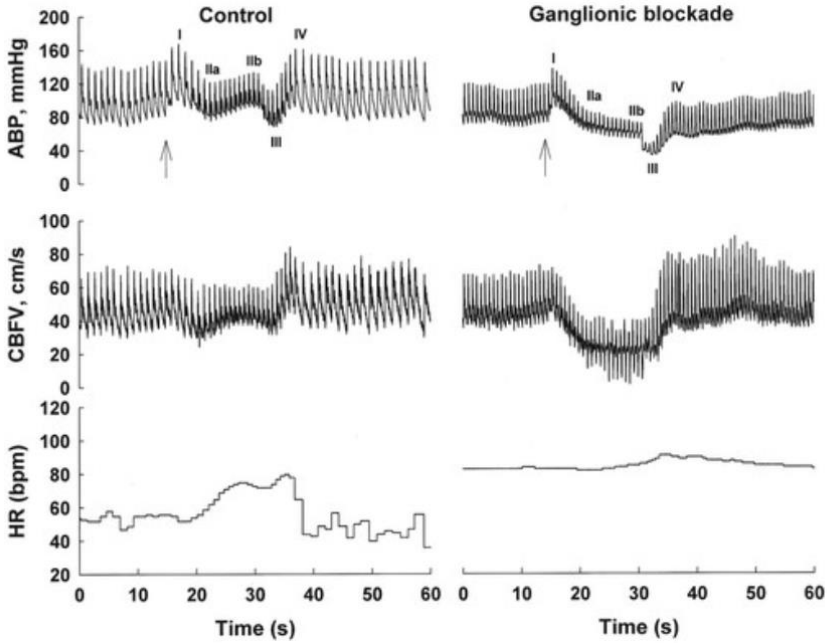


**Fig. 1.7.** Example of Valsalva maneuver: on the left side – Valsalva maneuver of the control group, the change in the heart rhythm and CBFV restoration are clearly shown; on a right side, low changes of heart rhythm are shown due to ganglionic blockade and no restoration of CBFV during Valsalva maneuver (adapted from [35])

### 1.3.4. Spontaneous pulsations evaluation

Professor Roney B. Panerai introduced a method for calculating transfer function from spontaneous pulse wave fluctuations. The ABP pulse waves are considered as system’s input, and cerebral blood flow velocity is considered as system’s output. The transfer function (2) is calculated with Fast Fourier transformation (FFT), and it is decomposed to gain (3), coherence, and phase (4) analysis [36]. The shift in frequency domain of phase and gain shows the CA condition. The transfer function is analyzed in very low frequency (0.003–0.04 Hz) of non-periodical components, low frequency (0.04–0.15 Hz) of Mayer waves, which is around 0.1 Hz together with slow waves and high frequency (>0.15 Hz) of respiratory waves [37]. Such method has an advantage: it does not require additional ABP manipulation and is safe for all patients.

$$H(f) = \frac{G_{pv}(f)}{G_{pp}(f)}; \tag{2}$$

where  $H(f)$  – transfer function,  $G_{pv}(f)$  – Fourier transformation of flow velocity(t) signal,  $G_{pp}$  – Fourier transformation of ABP(t) signal.

$$|H(f)| = \sqrt{H_r(f)^2 + H_i(f)^2}; \quad (3)$$

where  $|H(f)|$  – transfer functions gain,  $H_r(f)$  – real transfer functions part,  $H_i(f)$  – imaginary transfer functions part.

$$\Phi(f) = \tan^{-1} \left( \frac{H_i(f)}{H_r(f)} \right); \quad (4)$$

where  $\Phi(f)$  – transfer functions phase,  $H_r(f)$  – real transfer functions part,  $H_i(f)$  – imaginary transfer functions part

However, these parameters have a low reproducibility in 75 healthy volunteers' study. This could be caused due to the physiological variability or non-stationarity [38]. The physiological variability or non-stationarity can be caused due to the room temperature or food, drinks, or medication taken before the tests. Moreover, the different signal processing methods, such as spectral smoothing, low or high pass filtering, detrending give different results, and there is no standard for TFA analysis, just recommendations [39]. The transfer function calculations are shown in Fig. 1.8.

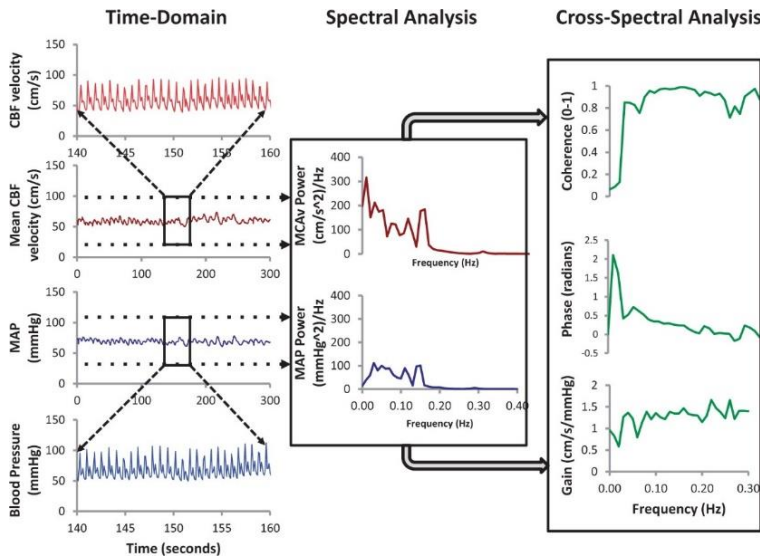


**Fig. 1.8.** Example of transfer function computation from spontaneous pulsations (adapted from [39])

### 1.3.5. Squat–stand maneuver

The doing of squat–stand maneuver changes the ABP, CBFV, and CO<sub>2</sub> due to the changes in different body positions. When doing such a maneuver, there is generated a similar to rectangular shape oscillations due to the fast transition between standing and squatting. The oscillations can be controlled by changing standing or squatting duration (Fig. 1.9) [40]. Such a test is very unpractical because not every patient can do squat due to the physiological condition, and it cannot be performed during anesthesia.

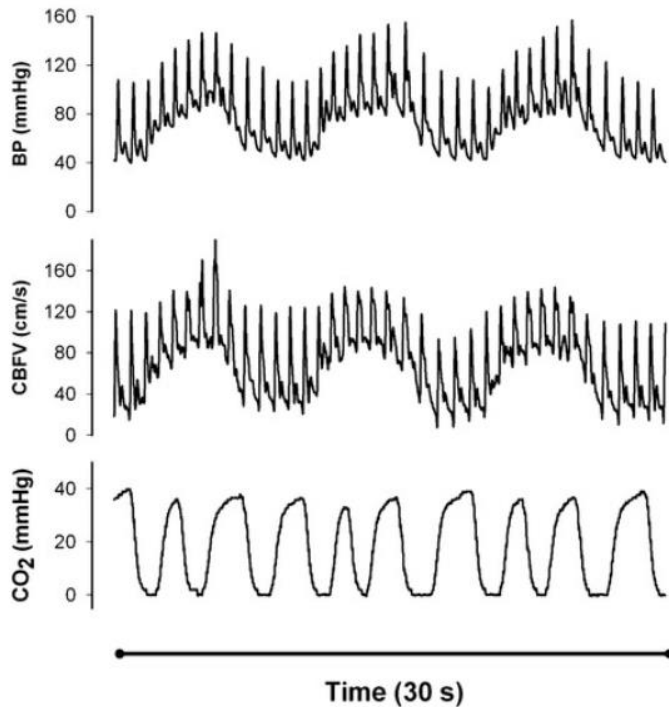


**Fig. 1.9.** Squat-stand maneuver with squatting for 5 s and standing for 5 s (adapted from [40])

## Conclusions

1. Cerebral blood flow autoregulation is responsible for maintaining constant cerebral blood flow. It is a complex system which is controlled by myogenic, metabolic, endothelin, and neurogenic mechanisms. Due to the anesthetics or brain damage, these mechanisms are impaired, and the cerebral blood flow cannot be maintained constant in the physiological range.
2. Static cerebral autoregulation monitoring consists of slow arterial and blood flow waves. Such methodology has disadvantages because there is no clear cerebral autoregulation impairment beginning event, and there is a few minutes delay in the cases when slow waves amplitude is low or absent. Therefore, the artificial generation of physiological slow waves could be a solution allowing to increase the reliability of CA assessment.
3. Dynamic cerebral autoregulation consists of ABP manipulation that changes CBF. If CBF has the ability to restore previous blood flow, it is considered as intact, if it loses such ability, it is considered as impaired. It has an advantage to determine the beginning of CA impairment; however, this test cannot be applied on all patients who have arterial stenosis in neck or peripheral artery disease, which can cause brain ischemia. The comparison of CA evaluation methods is shown in Table 1.1.

**Table 1.1.** Comparison of different CA evaluation methods

Method	Safe for all patients	Can be performed during surgery	CA Evaluation time
Slow wave generation (pharmacological interventions, changing positive lower body pressure or changing concentration of CO <sub>2</sub> )	Yes	Yes	Slow
Thigh cuff	No	Yes	Fast
Carotid artery compression	No	Yes	Fast
Valsalva maneuver	Yes	No	Moderate
Spontaneous waves	Yes	No	Moderate
Squat–stand maneuver	No	No	Moderate

## 2. NEUROPROTECTION BY MONITORING CEREBRAL BLOOD FLOW AUTOREGULATION

### 2.1. Introduction

The monitoring of CA consists of arterial blood pressure and cerebral blood flow in real time. Arterial blood pressure usually is taken from a carotid artery of arm invasively or blood pressure monitoring with finger cuff non-invasively. Cerebral blood flow can be estimated invasively by measuring intracranial pressure (ICP), or it can be taken non-invasively (blood flow velocity, volumetric changes, brain tissue oxygenation, etc.). The selection of cerebral blood parameter is dependent on monitoring time, cost, and patient's ability to accept the technology (e.g., cannot be inserted invasive sensor, temporal window cannot be found, etc.).

The evaluation of CA is usually taken by the correlation coefficient between slow waves of arterial blood pressure and slow waves of cerebral blood flow slow waves. Currently, there exist various CA indexes, which have different ranges of sensitivity to distinguish impaired or intact CA. Optimal CPP or ABP therapy could be applied by choosing a zone where CA is intact. However, optimal CPP therapy is controversial due to the lack of evidence and too long a delay for the treatment due to the data accumulation.

### 2.2. CA evaluation methods

#### 2.2.1. Invasive CA evaluation by using pressure reactivity index (PR<sub>x</sub>)

In intensive care unit (ICU), there are widely used invasive intracranial pressure monitoring sensors. The reason of such usage is simplicity and reliability by inserting micro pressure transducer into ventricles through a burr hole in the skull [41]. Normal ICP value ranges from 5 to 15 mmHg for healthy adults. Increased ICP of over 15 mmHg is considered as impairment of CA, because it lowers CPP and can cause brain ischemia [42]. However, invasive micro pressure transducer or external ventricular drainage can cause infection, damage the brain in an inserted area, and require an experienced surgeon for transducer insertion.

The pressure reactivity index (PR<sub>x</sub>) was introduced by Professor Marek Czosnyka in 1995. This index is calculated as moving Pearson correlation coefficient window between the ABP and ICP slow waves (5) over 5–10-time window or more. Pr<sub>x</sub> varies from -1 to 1. Positive index (PR<sub>x</sub> > 0) shows impaired CA, because ABP and ICP slow waves are in synphase. Negative index (PR<sub>x</sub> < 0) shows intact CA because ABP and ICP waves are in opposite phase. This index is a golden standard for evaluating CA [43].

$$PR_x = r\{ABP_{sw}(t), ICP_{sw}(t)\}; \quad (5)$$

where PR<sub>x</sub> – pressure reactivity index, ABP<sub>sw</sub>(t) – arterial blood pressure slow waves, mmHg, ICP<sub>sw</sub> – intracranial pressure slow waves, mmHg.

However, such methodology requires the presence of physiological slow waves; otherwise, the noisy signals or low slow wave amplitude will result in correlation coefficient close to zero. Due to such reason, in practice, PRx threshold 0.2–0.4 is used to classify CA status into intact and impaired. The uncertainty area is  $PRx > 0$  and  $Prx < 0.2$ . The studies have shown that averaged  $PRx > 0.57$  is associated with unfavorable outcome, and  $PRx > 0.65$  is associated with the mortality of TBI patients [44]. The PRx monitoring is shown in Fig. 2.1.

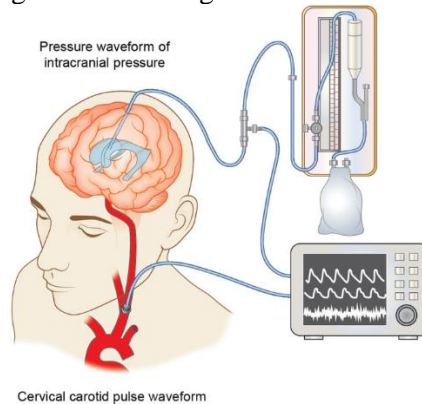


**Fig. 2.1.** Example of PRx monitoring with external ventricular drainage and invasive ABP sensor (adapted from [45])

## 2.2.2. Non-invasive CA evaluation methods

It is not possible to measure ICP invasively for non-traumatic brain injury patients because of required burr hole for a pressure sensor. However, it is necessary to estimate CPP for individual patients. There are 2 alternatives to measure ICP value non-invasively: using a model by Arminas Ragauskas [46, 48, 48] that is based on ocular and external pressure measuring with ultrasound and a model by Bernard Schmidt [49] that is based on ABP and vCMA pulse wave relationship.

### 2.2.2.1. Non-invasive ICP assessment by Arminas Ragauskas model

The possibility to measure absolute ICP was introduced by Professor Arminas Ragauskas [46, 48, 48]. The operator must manually determine the proper depths of the intracranial (IOA) and extracranial spaces in order to produce a trustworthy non-invasive ICP measurement using the approach that is currently being presented. Using a multi-depth TCD, the portions of the ocular artery (EOA) were identified [46]. An external pressure cuff is used to apply pressure to the tissues around the eye. Due to the incompressibility of the eye and its surrounding tissues, the progressively imposed external pressure is transferred to the EOA [47]. Clinical investigations have demonstrated the usefulness of non-invasive ICP measurement method in terms of accuracy, precision, diagnostic sensitivity, and specificity [48]. However, such method does not allow continuous measurement and takes just a snapshot in certain amount of time (Fig. 2.2).

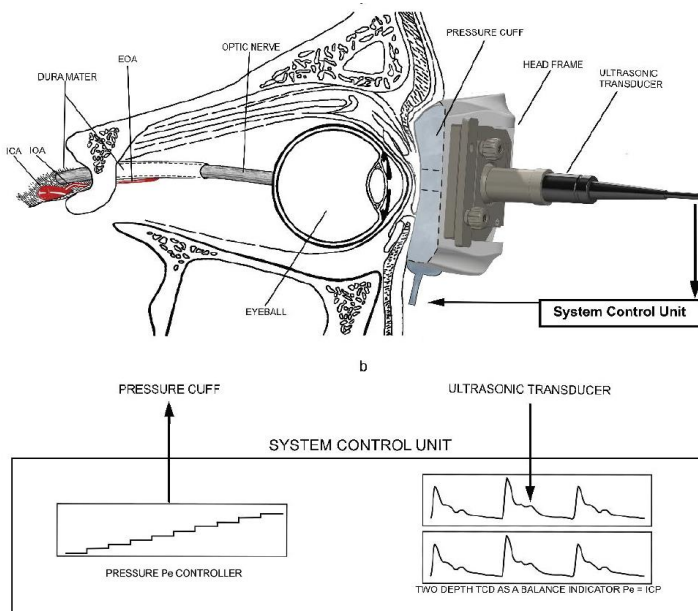


**Fig. 2.2.** Schematic representation of non-invasive intracranial pressure (ICP) monitoring equipment (adapted from [47]): (a) relevant orbit and brain anatomy in contact with the ICP measurement device, (b) block diagram of the system control unit: ICA – internal carotid artery, IOA – intracranial part of the ophthalmic artery, EOA – extracranial part of the ophthalmic artery, TCD – transcranial Doppler,  $P_e$  – external pressure applied to the ocular globe

### 2.2.2.2. Non-invasive ICP assessment by Bernard Schmidt model

Non-invasive ICP monitoring evaluation using a mathematical model was introduced by Bernard Schmidt. This model evaluates nICP (6) from ABP and flow velocity (FV) pulse waveforms. In traumatic brain injury patients, the CA status was regularly estimated by correlation coefficients between FV and nCPP (nMx) and between ABP and nICP (nPRx) in 10 second window [49]. These indexes are used to calculate nICP value by fitting coefficients to the CA status. After calibration of 39 TBI patients, the absolute systematic error between nICP and ICP was around 5–7 mmHg [50].

$$nPRx = r\{ABP_{sw}(t), nICP_{sw}(t)\}; \quad (6)$$

where, nPRx – non-invasive pressure reactivity index,  $ABP_{sw}(t)$  – arterial blood pressure slow waves,  $nICP_{sw}$  – non-invasive ICP slow waves.

### 2.2.2.3. Mean flow autoregulation index (Mx)

Transcranial Doppler sonography (TCD) is a widely used measurement technology in neurocritical care to measure the blood flow velocity in middle cerebral artery (MCA). The 2 MHz transducers are placed on the temporal window of human skull, and the ultrasound wave reflects from red blood cells in 50–60 mm depth where



MCA is located [51]. This method is based on Doppler law where the velocity reflects from red blood cells with a changed frequency (7). However, the uncertainty of angle  $\theta$  does not show the true velocity in blood vessel. If the angle between transducer and a vessel approaches 90 degrees, the signal will be lost. It is recommended to keep the angle  $\theta < 60^\circ$  [52]. Moreover, bone structure (density) and thickness of temporal bone affects the ultrasound propagation. By decreasing the density of bone, more air pockets occur, and due to the ultrasound reflection and scattering, more energy is lost [53]. The tendency of osteoporosis affects women sooner and faster comparing to men [54], which could be harder for elderly female patients to find ultrasonic temporal window. However, this system has an advantage, because it is not sensitive to the movement and allows to measure velocity in both hemispheres.

$$v_b = \frac{c_s}{2f \cos(\theta)} \Delta f; \quad (7)$$

where,  $V_b$  – velocity of brain flow,  $c_s$  – ultrasonic velocity in medium,  $f$  – frequency,  $\theta$  – angle.

In 1996, Professor Marek Czozyka introduced mean flow index (Mx). This method is widely used in neuroprotection because it is a non-invasive way for estimating CA. It uses moving Pearson correlation coefficient between the flow velocity (Fv) from transcranial Doppler and the arterial blood pressure (ABP) calculated over 5–10 min moving time window (8). It varies from -1 and 1. The considered CA impairment varies in studies and yet is unknown. The classificatory varies from 0.00 to 0.44, and the threshold of 0.30 would be considered that healthy have impaired CA [55]. The comparative study of Mx and PRx indexes showed a correlation coefficient between the indexes –  $R = 0.58$  [56].

$$Mx = r\{ABP_{sw}, FV_{sw}\}; \quad (8)$$

where Mx – mean flow index,  $ABP_{sw}(t)$  – arterial blood pressure slow waves, mmHg,  $FV_{sw}$  – flow velocity slow waves, cm/s.



**Fig. 2.3.** Example of Mx monitoring with ultrasonic transcranial Doppler transducer and invasive ABP sensor (adapted from [57])

#### 2.2.2.4. Cerebral oximetry index (COx)

Near-infrared spectroscopy (NIRS) is a non-invasive optical technique, which measures brain tissue oxygenation and hemodynamics in real time. This technology uses near-infrared light that ranges from 600 to 1,000 nm. NIRS technology gains its popularity because of cheapness and simplicity to use [58]. This technology is used to evaluate cerebral oximetry index (Cox), which is moving Person correlation coefficient between the regional oxygen saturation (rSO<sub>2</sub>) slow waves and ABP slow waves (9). The COx threshold above 0.3 is considered impaired and below, is considered intact. Additionally, higher COx is associated with higher stroke rates, acute kidney injury, and mortality [59]. However, the Cox index is controversial because the correlation coefficient between COx and PRx is  $R = 0.16$  and between Mx and Cox,  $R = 0.15$  [60].

$$\text{Cox} = \text{corr}\{\text{ABPsw}, \text{rSO}_2\text{sw}\}; \quad (9)$$

where Cox – cerebral oximetry index, ABPsw – arterial blood pressure slow waves, rSO<sub>2</sub>sw – regional oxygen saturation slow waves.

#### 2.2.2.5. Volumetric reactivity index (VRx)

Volumetric changes in cerebral blood flow were introduced by Professor Arminas Ragauskas in 1994 [61]. This technology is made from 2 ultrasonic transducers placed to each other perpendicularly on a temporal window. The changes in time of flight (TOF) is proportional to the changes to intracranial blood volume (IBV), brain tissue, and cerebrospinal fluid. The decreasing TOF is associated with increasing blood volume, and increasing TOF is associated with increasing cerebrospinal spinal fluid (10) [62].

$$\text{IBV}(t) \approx \frac{1}{\text{TOF}(t)}; \quad (10)$$

where IBV(t) intracranial blood volume , TOF(t) – time of flight

Volumetric reactivity index (VRx) is moving Pearson correlation coefficient between the arterial blood pressure slow waves and intracranial blood volume slow waves (11). Time window for the data accumulation is 2–5 minutes. The coefficient varies from -1 to 1. If VRx < 0, CA is considered intact, and if VRx > 0, CA is considered impaired. The correlation between VRx and PRx is  $r = 0.843$  [63]. The monitoring of CA is shown in Fig. 2.4.

$$\text{VRx} = r\{\text{ABPsw}(t), \text{TOFsw}(t)\}; \quad (11)$$

where VRx – volumetric reactivity index, ABPsw – arterial blood pressure slow waves, TOFsw – time of flight slow waves.



**Fig. 2.4.** Example of monitoring volumetric reactivity index with Vittamed device and non-invasive Finnapress device

#### 2.2.2.6. The concept of optimal cerebral perfusion pressure

The concept is based on the U shape curve approximation of CPP and pressure reactivity index, such as PRx, Mx, Cox, etc. The minimum value shows where CA is optimal. The area below threshold shows intact CA and above threshold, shows impaired CA. The left side of U shape curve shows too low CPP (hypoperfusion), and the right side of U shape shows too high CPP (hyperperfusion) [64]. By knowing optimal CPP, the clinician can reduce or increase ABP or ICP value. The time to identify optimal CPP in clinical practice requires 4–6-hour monitoring window [65]. This time window is chosen due to the noise, artefacts, low CPP physiological changes, and absence of slow waves.

Instead of PRx value for non-traumatic brain injury patients, other reactivity index are used, such as Mx, Cox, VRx, and it measured optimal ABP. However, this therapy is controversial between clinicians due to the lack of evidence [66]; 4 hour window is too long delay to treat a patient because his/her physiological condition changes during such time. New proposed algorithm with machine learning can identify optCPP threshold in 24 minutes [10]. Moreover, our previously conducted study found that patients who experienced TBI and were treated with optCPP therapy had better outcomes if they were younger than 45 years old [67].

However, there is an uncertain area, because noise to noise gives PRx value 0, and then, the index has to be raised up to 0.2 where the uncertainty zone is. If optCPP threshold is moved up, the boundaries of LLCA and ULCA are widened where CA is intact. Due to this reason, optCPP therapy could be harmful for a patient (Fig. 2.5).

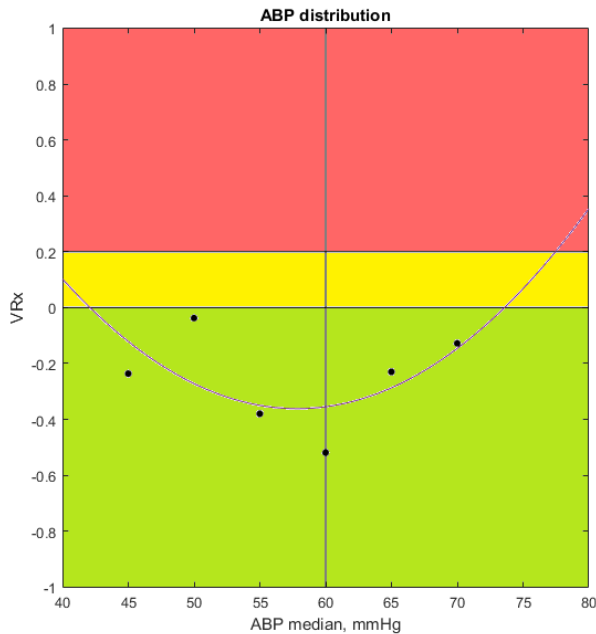


**Fig. 2.5.** Optimal ABP value identification according to optCPP concept: red – impaired CA, yellow – uncertain CA, green – intact CA

### 2.2.2.7. Previous clinical study findings

Lithuanian University of Health Sciences' hospital, Kaunas Klinikos, hosted a prospective observational study. Kaunas Regional Ethics Committee of LUHS approved the study (protocol No BE-2- 49, 2014-10-08). The patients' written consents were obtained in accordance with the Declaration of Helsinki (BMJ 1991; 302:1194). Without having any neurological conditions before surgery, patients were included for coronary artery bypass grafting (CABG). In addition to routine monitoring, a "Vittamed" non-invasive monitor was used to monitor CA. The approach is based on tracking variations in intracranial blood volume (IBV), which affect ICP. The volumetric reactivity index  $VRx(t)$ , which is closely related to the invasive  $PRx$ , is monitored by using a non-invasive technique (t). Intensive care units for neurosurgery frequently use invasive  $PRx(t)$  monitoring. Due to the requirement of implanting a pressure sensor into the heart during cardiac surgery, such monitoring is not practical. Recent studies have shown that the lower and upper limits of cerebrovascular autoregulation (LLCA and ULCA) are patient-specific and individual values of LLCA and ULCA can differ from the CPP values of 50 mmHg and 150 mmHg, established in historical Lassen's curve (Fig. 2.6) [68, 8].

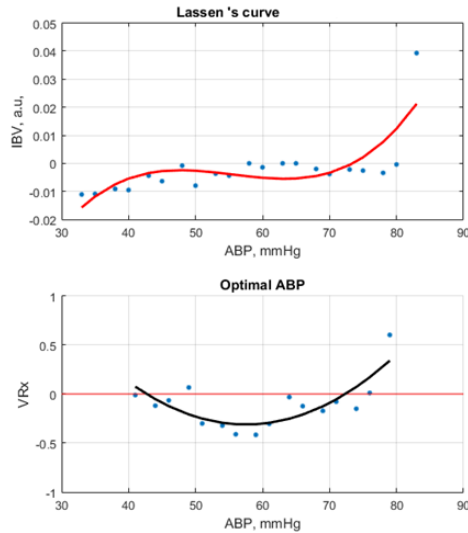


**Fig. 2.6.** Lassen's curve of patient and optimal ABP curve; the plateau of approximated Lassen's curve is below  $Prx < 0$

The previous study has shown that most sensitive factor using receiver operating characteristic curve (ROC) is LCAI with sensitivity 76%, specificity 82%, area under curve (AUC) 0.81; dose of LCAI sensitivity 76%, specificity 76%, AUC 0.76; total duration of all CA impairment events sensitivity 90%, specificity 50%, AUC 0.74; dose of all CA impairment events sensitivity 90%, specificity 61%, AUC 0.74 (Fig. 2.7) [8].

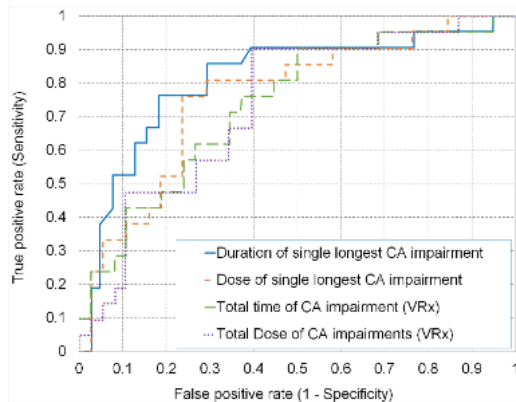


**Fig. 2.7.** ROC curves of different classifiers: duration of the LCAI event (blue solid line): sensitivity 76%, specificity 82%, AUC 0.81; dose of LCAI events (brown dashed line): sensitivity 76%, specificity 76%, AUC 0.76; total duration of all CA impairment events (green dashed line): sensitivity 90%, specificity 50%, AUC 0.74; dose of all CA impairment events (violet dotted line): sensitivity 90%, specificity 61%, AUC 0.74 (adapted from [8])

## Conclusions

1. There are existing invasive and non-invasive CA estimation methods. Invasive require an intervention and experienced surgeon. Non-invasive methods require skills to find an ultrasonic signal except for NIRS technology. The golden standard is considered to be invasive PRx. The non-invasive technology has a good correlation with PRx, except with NIRS technology, which it is still widely used in studies due to the cheapness and simplicity. The comparison is shown in Table 2.1. In addition, all these correlation coefficient calculation-based methods require the presence of physiological slow waves to provide reliable CA assessment.

**Table 2.1.** Comparison of different CA monitoring technologies

CA parameter	Invasive	Accuracy	Cost of technology	Skill for transducer placement
PRx	Yes	High	Moderate	Expert
nPrx	No	Low	Moderate	Moderate
Mx	No	Moderate	Moderate	Moderate
Cox	No	Low	Low	Low
VRx	No	High	Moderate	Moderate

2. Optimal CPP therapy is controversial due to the lack of evidence and too long delay for a treatment. The studies have shown that is possible to determine optCPP in 24 minutes instead of in clinical practice used 4-hour window using machine learning algorithms. Moreover, it has been found that traumatic brain injury (TBI) patients that are younger than 45 years old have better outcomes with optCPP therapy compared to the elderly patients. Additionally, there is uncertainty zone where to keep CA impairment threshold.

3. Previous clinical study has shown that during cardiac surgery, the optimal MABP range is narrowed to 45–75 mmHg. The LCAI is the factor who associates best with the outcome in the ROC curve, and the 5-minute duration of LCAI associates with POCD. There is an issue how to determine optimal CPP value faster than 5 minutes and maintain adequate pressure.

## 2. HEART AND LUNG MACHINE OPERATIONAL MODES

### 3.1. Introduction

In 1953, there was first performed a successful cardiac surgery using a heart and lung machine by Dr. Gibbon for an 18-year-old woman [69]. During cardiac bypass surgery, it is necessary to stop a heart for surgeons in order to operate. While the heart cannot produce blood flow, a heart and lung machine is used to produce oxygenated blood for a human body artificially. Currently, there exist 25 vendors of such type of machine in the global market, and it is forecasting to grow by \$195.04 mn during 2022–2027 [70]. In this study, Stockert S5 heart and lung machine was used, which has pulsatile mode (Fig. 4.1). Such a machine produces 3–3.5 Hz frequency vibrations for constant blood flow mode. During surgery, there is a possibility to use 4 operating modes: constant flow mode, pulsatile mode, which imitates heart pulsation, and professor Arminas Ragauskas introduced sinus flow mode [8] and a new rectangular flow mode. Such manipulations can be achieved by changing the arterial blood flow with a heart and lung machine.



**Fig. 3.1.** Stockert S5 heart and lung machine (adapted from [71])

### 3.2. Constant flow mode

The blood flow rate [l/min] is set by a perfusionist who evaluates patient's weight, height, and age. Constant flow mode is produced by a pump of 3–3.5 Hz sinusoidal fluctuations. Such fluctuations are not used to evaluate cerebral autoregulation because cerebral autoregulation processes are longer than 5 seconds (Fig. 3.2) Due to such reason, it is required to generate changes by using

pharmacological interventions or external factors, such as thigh cuff test or carotid artery compression, to make slow or dynamic ABP changes for CA estimation.

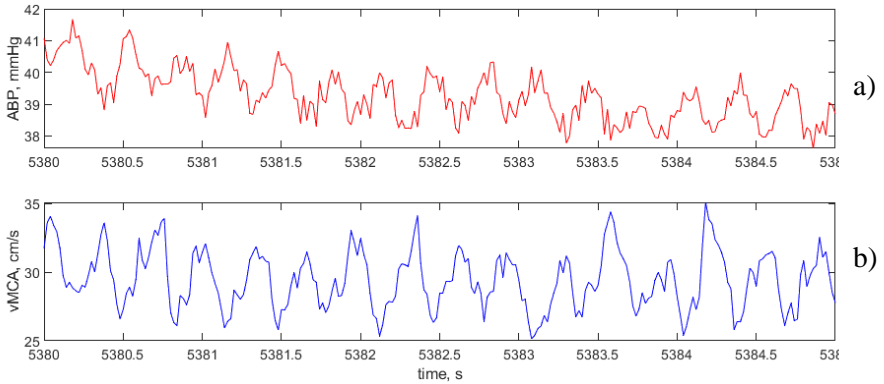


**Fig. 3.2.** Example of constant flow mode generated by 3–3.5 Hz sinusoidal fluctuations generated by a heart and lung machine: a) ABP(t) pump vibrations, b) vMCA(t) pump vibrations

### 3.3. Pulsatile mode

Pulsatile mode of heart and lung machine imitates heart pulsation. There is an existing debate that pulsatile mode is better compared to constant flow because it is more physiological for a human body. There is no clear benefit of pulsatile flow causing less cases of POCD [72]; otherwise, a study contradicts that it causes less cases of POCD [73]. The pulsatile mode has the same problem as a constant flow, because it requires an external factor to estimate CA status (Fig. 3.3).

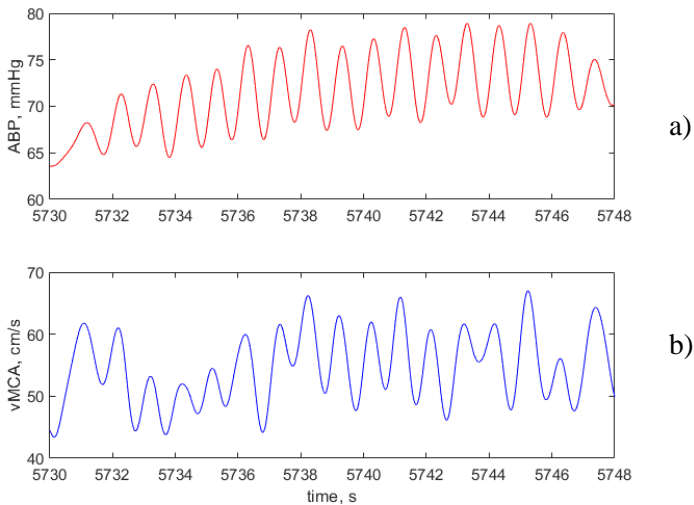


**Fig. 3.3.** Example of pulsatile flow mode of a heart and lung machine: a) ABP(t) pulsatile flow mode, b) vCMA(t) pulsatile flow mode



### 3.4. Sinus flow mode

Sinus flow mode was used in a previous clinical study. The sinus flow mode was introduced by Health Telematics Science Institute, Kaunas University of Technology, and applied in the previous clinical study [8]. The constant flow mode was controlled by the gradually increasing and decreasing flow rate. Due to such changes, a physiological sinusoidal slow wave with a period of 60 s was imitated. The cerebral blood cerebral blood flow reaction was monitored with Vittamed intracranial blood volume monitor (Fig. 3.4).

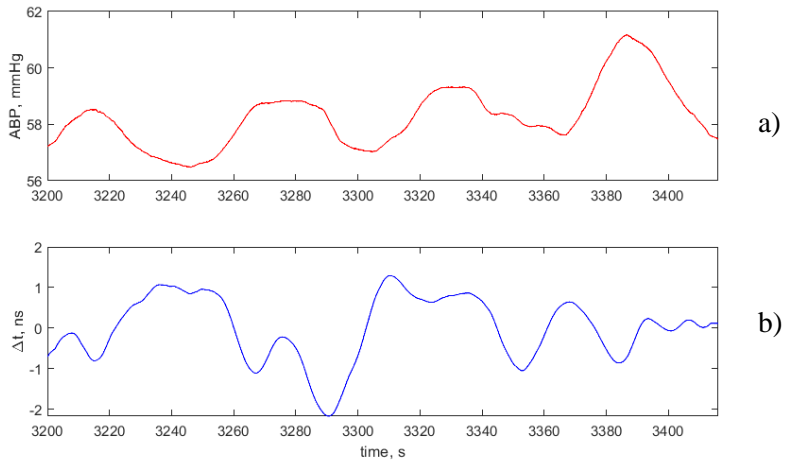


**Fig. 3.4.** Sinus flow mode generated by a heart and lung machine: a) ABP(t) sinus flow mode, b) cerebral volumetric changes (t) to ABP(t) changes

### 3.5. Rectangular sequence flow mode

The rectangular flow mode was introduced by Health Telematics Science Institute, Kaunas University of Technology, and has pending patent applications (US application No. 17/683,943 and EU patent application EP22160563). In order to make a rectangular mode, it is programmed by sudden change of blood flow by  $\pm 10\%$  of perfusionist setted value. The rising and falling time of the front is 1 second. After setted time finishes, the arterial blood flow changes again by  $\pm 10\%$  to the previous value in such way generating rectangular sequence (Fig. 3.5 and Fig. 3.6).

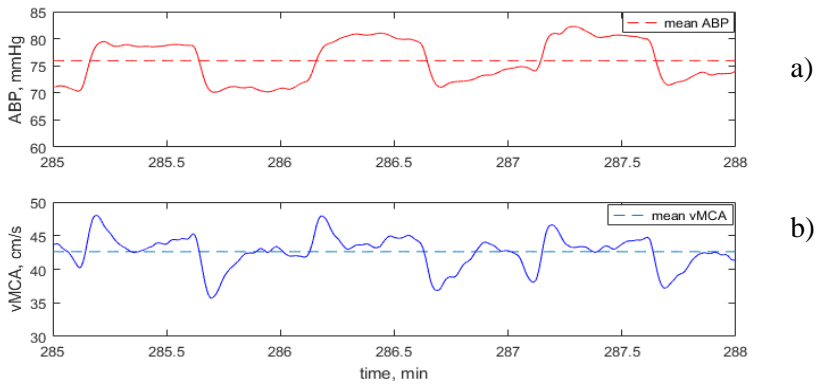


**Fig. 3.5.** The rectangular wave sequence generated with heart and lung machine by changing blood flow: a) ABP rectangular waves, b) transient vMCA response to ABP changes, which associates to intact CA

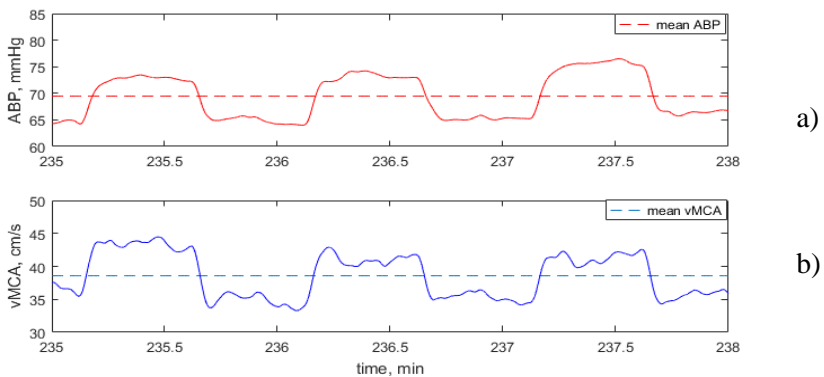


**Fig. 3.6.** The rectangular wave sequence generated with heart and lung machine by changing blood flow: A) ABP rectangular waves, b) no transient vMCA response to the ABP changes, which corresponds to the impaired CA

It is easily mountable on Stockert S5 heart and lung machine without integration to the device. Device has 2 buttons to set the main blood flow and requires setting +10% from the main blood. After selecting values, the device changes blood flow +10% from baseline by the programmable time (Fig. 3.7).



**Fig. 3.7.** Patent pending device which modulates square waves on a heart and lung machine

## Conclusions

The existing heart and lung machine modes are constant flow, pulsatile mode, sinus and rectangular flow. The constant flow and pulsatile can be integrated to the heart and lung machine. The Health Science Telematics Institute introduced flows are mountable on Stockert S5 heart and lung machine.

The constant and pulsatile mode requires external factors for the CA evaluation. The sinus flow allows to generate slow wave by itself, and it is possible to evaluate CA status in 1–2 minutes of monitoring time. The rectangular flow as well allows to estimate CA status by itself, and it could be done in 15 s of monitoring time (Table 3.1).

**Table 3.1.** Comparison of flow modes

Flow mode	Integrated to machine	Requires external factor for CA evaluation	CA estimation time
Constant	Yes	Yes	External factor dependent
Pulsatile	Not all	Yes	External factor dependent
Sinus	No	No	1–2 min
Rectangular	No	No	~15 s

## 4. METHODS AND MATERIALS

### 4.1. Data collection

The Lithuanian University of Health Sciences hospital, Kaunas Klinikos, hosted the prospective observational study. The protocol of the prospective study was approved by the Kaunas Regional Bioethics Committee (Registration No. BE – 2 – 64). The patients’ written consents were obtained in accordance with the Declaration of Helsinki (BMJ 1991; 302:1194).

The TCD data was conducted with Viasonix Dolphin 4D ultrasonic device with 2 MHz transducers. Invasive ABP data was collected with invasive ABP sensor SP844. The data was transmitted with Draeger “Infinity Delta XL” monitor. Analog data were digitized with data acquisition module DT9803. ABP, vMCA data were collected with ICM+ software at 50 Hz sampling frequency. The data was processed retrospectively with Matlab R2016 software (Fig. 4.1).

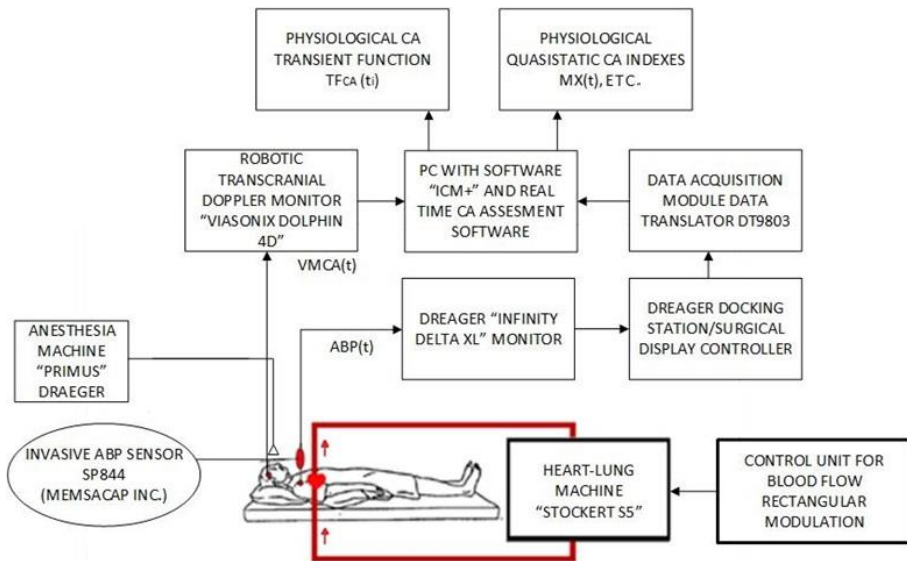


**Fig. 4.1.** A structural diagram of transcranial Doppler blood flow velocity in middle cerebral artery (vMCA (t)) monitoring and invasive ABP(t) monitoring during CPB

### 4.2. Cognitive tests

Standardized MMSE~2 cognitive tests and Adenbruck cognitive tests were used for POCD evaluation. The tests consist of orientation, attention, memory, verbal fluency, comprehension, sentence writing, reading, and drawing. If a score was below 88, it was considered as cognitive impairment. The tests are taken before and after the surgery. If a patient cannot pass the test before the surgery, then the patient is not involved in the study. Moreover, if a patient decides to stop the study, the test

is not taken. However, the test results are subjective and depend on the patient's condition (mood, daytime, fatigue). Such uncertainty distorts the validation of test.

### 4.3. Patients' demographics

The study was conducted with 108 CPB patients. Thirty-two patients were rejected due to the bad quality signal; 4 patients had not found window for transcranial Doppler signal (all females), and 16 patients refused to continue the study. 29 patients had POCD; 4 patients had delirium; 43 patients remain without cognitive deterioration. The mean age of patients involved in the study is  $66.68 \pm 8.2965$ , the mean years of education  $13.14 \pm 3.36$ , and it consists of 15 females and 61 males.

There was found a tendency that elderly patients have a bigger probability of experiencing POCD; however, due to a small population, it was not statistically significant (Mann–Whitney U test,  $p = 0.175$ ). The statistically significant threshold separating groups was found 73 years ( $\chi^2 = 6.00$ ,  $p = 0.014$ ). The years of education was a statistically significant (Mann–Whitney U test,  $p = 0.029$ ) factor with patient's outcome. The statistically significant threshold separating groups was found to be 14 years of education ( $\chi^2 = 5.51$ ,  $p = 0.019$ ). Moreover, 84.38% of patients who experienced POCD were male; however, gender was not a statistically significant factor (Fisher exact test,  $p = 0.77$ ). These factors show that the study has bias, and the longest cerebral autoregulation impairment event cannot be the main associating cause of POCD, because patients that are younger than 73 years old and have more than 14 years education can solve cognitive tests easier and in such way influence the outcome.

**Table 4.1.** Demographic patient data

Characteristics	No deterioration (40 patients)	POCD (32 patients)	p value
Mean age (years)	65.85±7.47	68.21±9.27	0.175
Men/women (%)	25.5/77.5	84.38/15.62	0.557
Education (years)	13.8±3.00	12.40±3.78	0.029

### 4.4. Signal morphology

In order to determine filter bands frequency of the filter, it is required to have knowledge about the signal's morphology. Using multiple signal classification (MUSIC) algorithm, it was determined that the cardiac bypass surgery consists of these components: pump motor vibrations (~3 Hz), pulse waves (~1 Hz), respiratory waves (~0.2 Hz), rectangular wave modulation (~1/60 s) is aliased with big and noradrenaline waves (1/120–1/180s) in the spectrum analysis (Fig. 4.2).

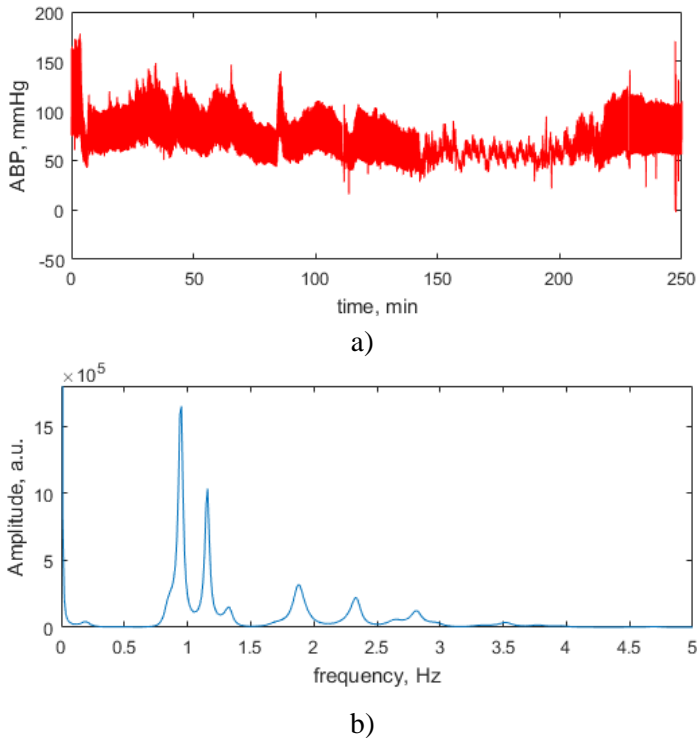


**Fig. 4.2.** Cardiac-pulmonary bypass surgery and its spectrum: a) ABP(t) signal over time, at the moment 150–210 min, heart and lung machine is used, b) cardiac bypass surgery spectrum used by MUSIC algorithm

All spectrum components of signal can carry information about the CA status. Noradrenaline waves (the injection of which is typically used during cardiac surgery with CPB to avoid hypoperfusion) are super slow waves, and the saturation of blood flow velocity can determine the ULCA and LLCA. The rectangular modulation can show transient function response. Pump modulated waves can show vascular resistivity. However, it is unknown what processes have most influence on the patient's outcome (Fig. 4.3).

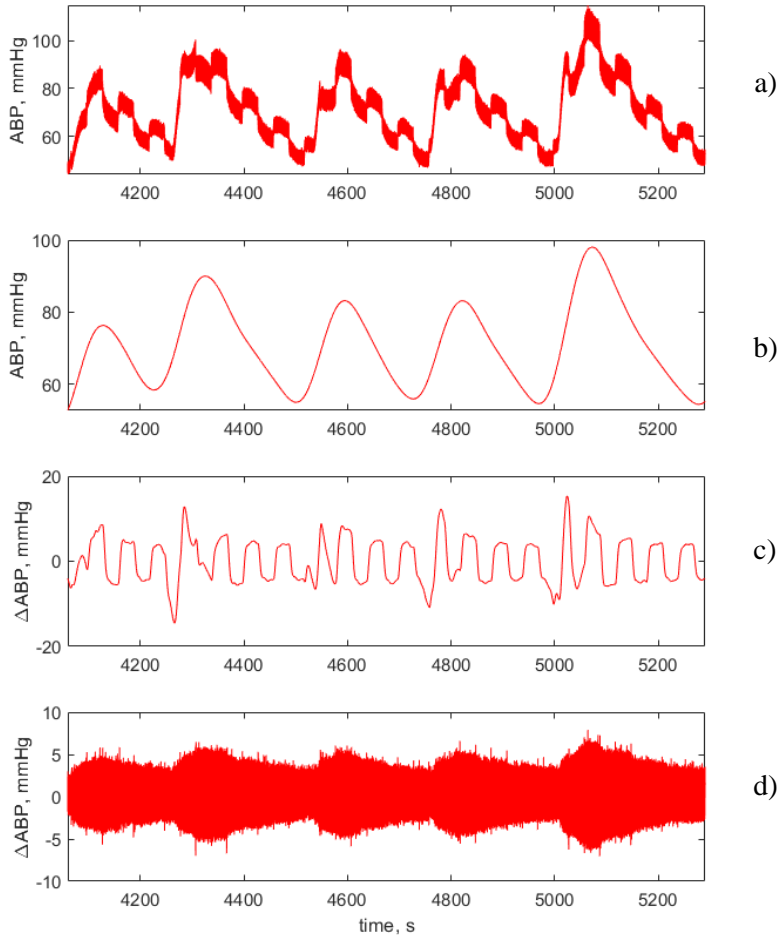


**Fig. 4.3.** Signal decomposition: a) raw ABP(t) signal, b) noradrenaline induced waves, c) rectangular wave modulation, d) 3 Hz pump motor frequency

#### 4.5. Rectangular wave filtering

Generated ABP rectangular waves have physiological crosstalk between the heart pulsations and 3 Hz pump vibrations. In rare occasions, the ABP artefact appears due to the bad connections. Due to good signal quality, it would be sufficient to use third order lowpass Butterworth filter 0.5 Hz. When using 1 Hz lowpass filter, some vibrations could be seen (Fig. 4.4).

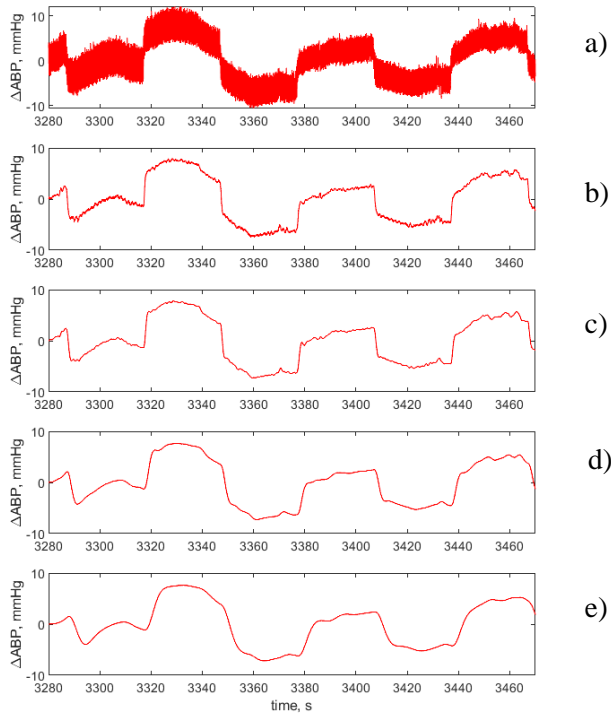


**Fig. 4.4.** Different filters are used to filter ABP noise: a) raw data of ABP signal, b) ABP signal filtered with 1 Hz lowpass filter, c) ABP signal filtered with 1 Hz lowpass filter, d) ABP signal filtered with 0.2 Hz lowpass filter, e) ABP signal filtered with 0.1 Hz lowpass filter

The vMCA signal is more affected by the external higher frequency electromagnetic noise, which comes from the environment and electromagnetic surgical knife, and additional noise comes from analog to digital data conversion. The physiological crosstalk as well occurs on the vMCA signal. During cardiac surgery, a patient's body temperature varies due to the cooling and warming processes, which can affect the ultrasound velocity. By filtering data with 3d order, cutoff frequency of 1 Hz Butterworth filter, additional noise is still seen. By filtering with cutoff frequency of 0.5 Hz, the electromagnetic and physiological crosstalk is eliminated; however, unknown lower frequency components occur, which distorts transient function reactions. By filtering with cutoff frequency 0.2 Hz, the additional low frequency noise is still present. Only by filtering data with 0.1 Hz cutoff frequency, the transient reactions are clear. Such cutoff frequency is selected for both ABP(t) and vMCA(t) filtering (Fig. 4.5).



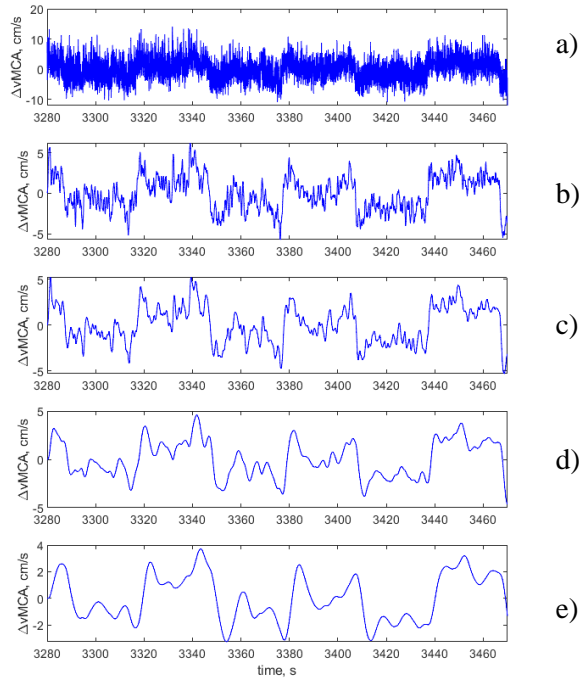


**Fig. 4.5.** Different filters used to filter vMCA noise: a) raw data of vMCA signal, b) vMCA signal filtered with 1 Hz lowpass filter, c) vMCA signal filtered with 0.5 Hz lowpass filter, d) vMCA signal filtered with 0.2 Hz lowpass filter, e) vMCA signal filtered with 0.1 Hz lowpass filter

## 4.6. Challenges of rectangular wave modulation

The previous study was made by generating slow sinus waves of 1 minute duration using heart and lung machine. However, when rapid changes were introduced, new challenges occurred. The pilot study showed that noradrenaline and heart pulsations are aliasing between rectangular waves and heart and lung machines generate abnormal pulses.

### 4.6.1. Aliasing between noradrenaline and rectangular wave modulation

In certain cases during surgery, noradrenaline is required to inject quite often, and noradrenaline waves start to alias between rectangular waves. The noradrenaline wave period can be around 1–2 minutes, and the transient time when adrenaline settles is around 30 seconds. During settling time, a sharp peak is made, which is not proper for transient function analysis. After settling time, the rectangular wave can be generated; however, there is only 1 pulse left in a noradrenaline wave. The solution for such a problem is to shorten the duration of pulse from 30 s to 15 s or less (Fig. 4.6).

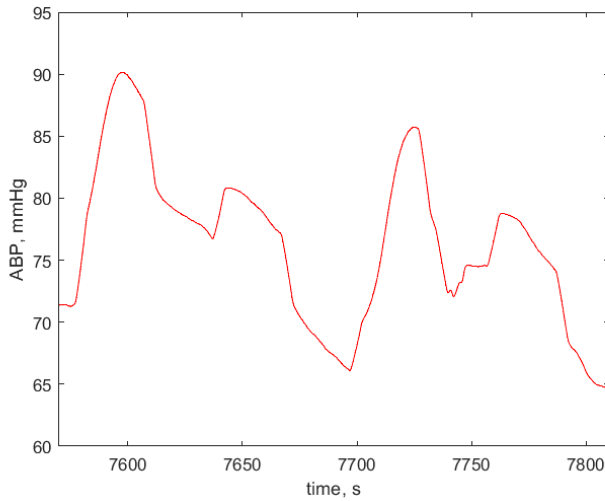


**Fig. 4.6.** Aliasing between noradrenaline induced waves and rectangular waves

#### 4.6.2. Aliasing between heart pulsation and rectangular wave modulation

During CPB surgery, there are episodes where temporal heart pulsation begins. Because autoregulatory processes are longer than 5 seconds and heart pulsation is not regular, such rectangular waves can be included. When using proper filtering, it is possible to remove the pulsation and see transient reactions (Fig. 4.7).

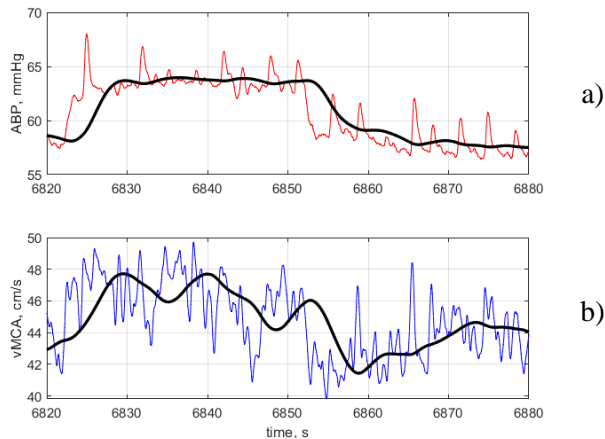


**Fig. 4.7.** Aliasing between heart pulsations and rectangular waves: a) pulsation aliasing during ABP pulse (red line) and filtered ABP signal (black line), b) the vMCA reaction due to pulsations is distorted; however, it is visible in positive and negative fronts (blue line); black color shows filtered vMCA signal

#### 4.7. Transient function index (TFx)

Transient responses occur at the beginning of 15 seconds of rising or falling front. At the beginning of first 5 or 6 seconds, the CA starts to restore previous CBF and later follows transient processes. The correlation coefficient between ABP and vMCA is a method to evaluate CA status. If CA is intact, the correlation coefficient should be lower than impaired (Fig. 4.8 and Fig. 4.9).

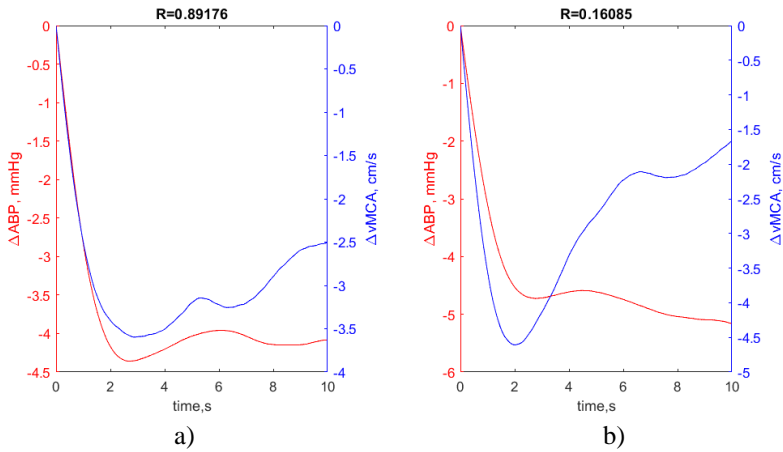


**Fig. 4.8.** Transient function response (blue color) to negative front ABP challenge (red color): a) lost CA correlation coefficient between challenge and response is  $R = 0.89$ , b) intact CA correlation coefficient between challenge and response is  $R = 0.16$

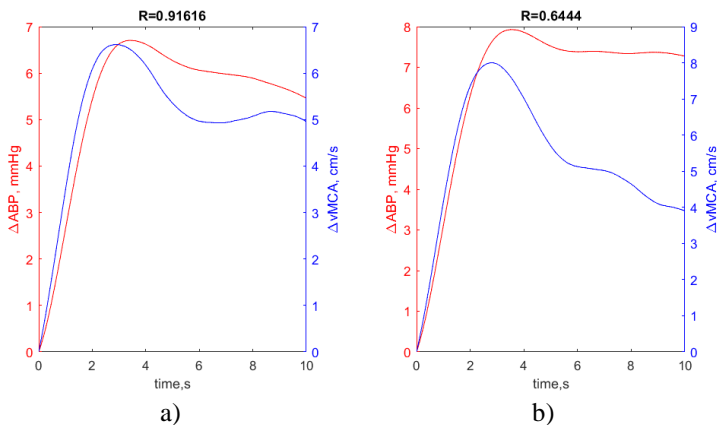


**Fig. 4.9.** Transient function response (blue color) to positive front ABP challenge (red color): a) lost CA correlation coefficient between challenge and response is  $R = 0.91$ , b) intact CA correlation coefficient between challenge and response is  $R = 0.64$

In order to determine the threshold between impaired and intact CA, 500 different reactions from 13 patients were estimated. Currently, it is hard to determine how CA is functioning properly with different TFX results. Moreover, artifacts and noise distort the reactions shape, which is hard to interpret. After subjective evaluation of each TFX sample, intact CA mean was estimated to be 0.63, and impaired CA mean 0.89. The gray zones between 0.63 and 0.89 are uncertainty area. The selected threshold was 0.7, which determines the impaired or intact CA (Fig. 4.10).

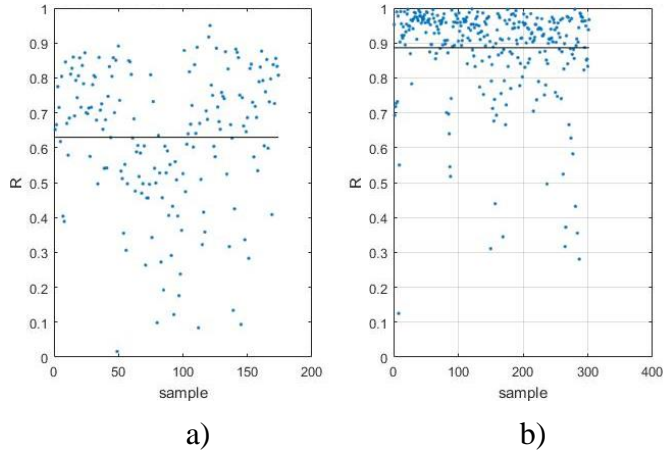


**Fig. 4.10.** Distributions of TFX intact and impaired values: a) estimated intact CA, b) estimated impaired CA; black line shows the median of a group

The detector detects rising fronts and evaluates CA status. It starts to estimate the beginning of 15 s of rising front and 15 s beginning from the falling front. In such way, it estimates CA status continuously in close to real-time (Fig. 4.11).

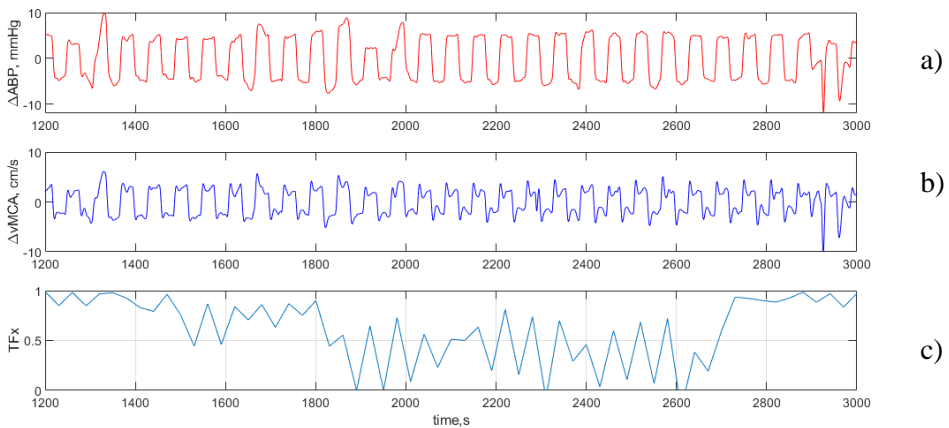


**Fig. 4.11.** TFX evaluation over time: a) ABP(t) signal, b) vMCA(t) signal, c) TFX(t)

#### 4.8. Mean flow index (Mx)

ABP and vMCA signals were filtered with 0.1 Hz cutoff frequency lowpass Butterworth filter for mean flow index (Mx) analysis. The Pearson's correlation was calculated in 30 s window due to the length of the pulse. The threshold of CA intact is  $Mx < 0.4$ , and for impaired CA, it is  $Mx > 0.4$  [74]. The main issue with this method is that it shows most of the time impaired CA (Fig. 4.12). However, the studies have shown that vasopressors have no affect or impairment for CA [75]. The delay of Mx signal calculation consists of 10 seconds of lowpass filter delay and 30 s of calculation of moving correlation coefficient window, and in total, it gives 40 s of delay.

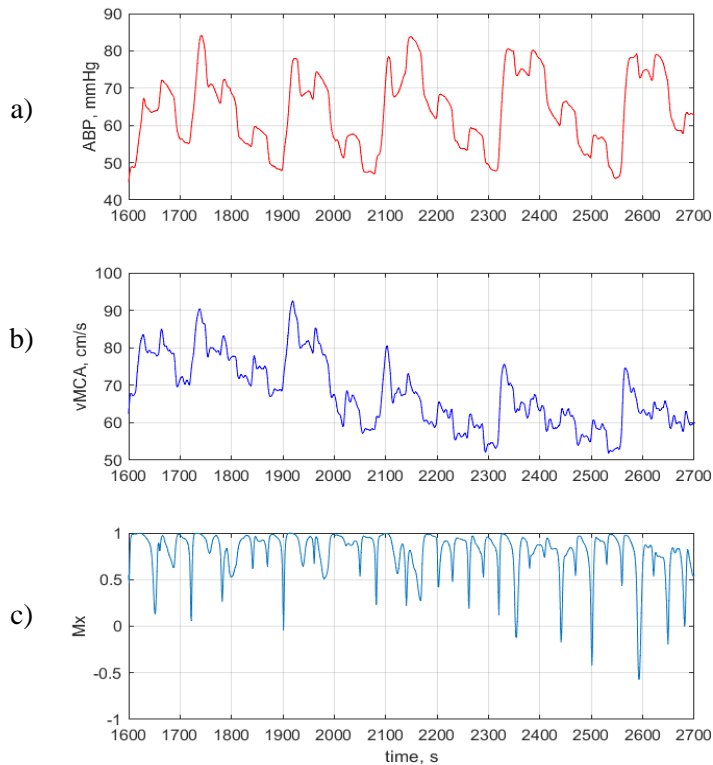


**Fig. 4.12.** Example of Mx calculation: a) ABP(t) signal, b) vMCA(t) signal, c) Mx(t) data

#### 4.9. Pump induced wave analysis (Ex)

It has been noticed that by decomposing signal, the heart and lung machine modulates slow waves during time. Fast 3 Hz motor pulsation appears due to the vascular resistance and ABP manipulation. This could be described as Ohm's law (12) [76]. The injected noradrenaline contracts blood vessels, and in such way, it increases ABP pump amplitude. The noradrenaline wave from its peak starts to lose its effect,

and after 1–5 minutes, it returns to the previous ABP pump value. During this time, the blood vessels start to dilate:

$$Q = \frac{\Delta P}{R}; \quad (12)$$

where  $Q$  – fluid flow,  $\Delta P$  – pressure gradient,  $R$  – vascular resistance.

The signal is filtered with 0.5 Hz third order Butterworth filter. The envelope of amplitude was extracted and filtered with a 3<sup>rd</sup> order lowpass Butterworth filter with 0.3 Hz cutoff frequency for envelope reactivity index (Ex) calculation. The algorithm is shown in Fig. 4.13.

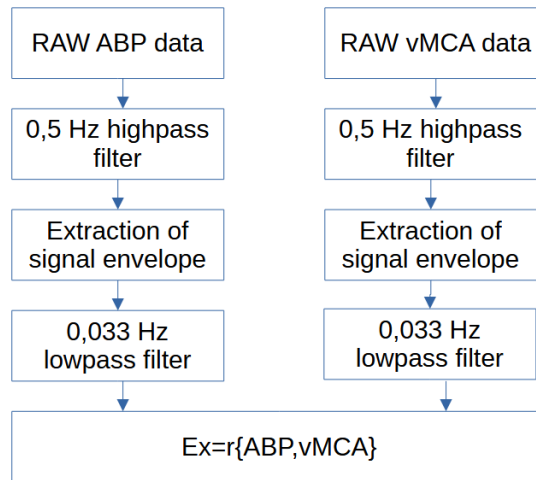


**Fig. 4.13.** Algorithm of Ex calculation

The coefficient has yet unknown properties, because it has never been studied before. It is calculated between slow ABP and Fv modulated envelope waves (13):

$$Ex = r\{eABPsw, eFVsw\}; \quad (13)$$

where  $Ex$  – envelope of pump reactivity index,  $eABPsw(t)$  – envelope of arterial blood pressure pump waves, mmHg,  $eFVsw$  – envelope of flow velocity pump slow wave, cm/s.

In order to identify diagnostic  $Ex$  threshold,  $\chi^2$  test was used within 0–1 threshold values of LCAI and patients' outcome. The most sensitive value was identified  $Ex = 0.68$  ( $\chi^2 = 7.18$ ,  $p = 0.008$ ). The classification index is considered: higher than  $Ex > 0.68$  shows impaired CA, and lower than  $Ex < 0.68$  shows intact CA.

The pump produces 10 mmHg peak to peak ABP waves and 20 cm/s peak to peak vMCA waves 3 Hz vibrations. The envelope of vMCA waves are symmetrical and around 30–50 s of period, which can be validated as slow waves. Moreover, due to noradrenaline, it has quickly ascending front and slow descending front of ABP waves. The amplitude of envelope of ABP waves is 1–2 mmHg, and vMCA is 1–2

cm/s. Such waves have a much smaller amplitude compared to big ABP and vMCA changes by calculating Mx index (Fig. 4.14). The delay of Ex consists of 0.5 seconds of highpass filter delay, the envelope extraction delay (unknown in real time), 30 s of lowpass filter delay, and 30 s of moving correlation coefficient delay, which is in total 60.5 s delay.

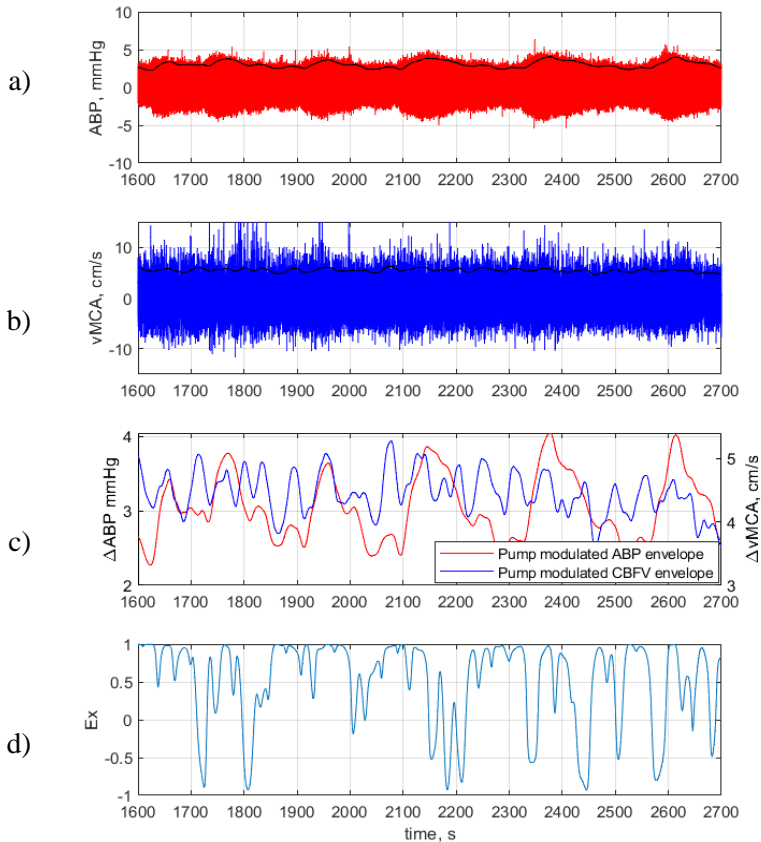


**Fig. 4.14.** Pump envelope decomposition: a) ABP(t) pump modulated envelope, b) vMCA(t) pump modulated envelope, c) comparison between ABP(t) and vMCA (t) pump modulated envelopes, d) Ex(t) data

#### 4.10. Rectangular wave envelope reactivity index (Ex2)

It has been noticed that by decomposing signal, rectangular wave amplitude varies during noradrenaline injection. This happens due to the noradrenaline change of vascular resistance and change of blood flow in the patient's body. This happens due to Ohm's law. The amplitude of rectangular waves rises with injected noradrenaline, and currently blood flow is raised up as well. This can cause front amplitude increment up to 20 mmHg. The amplitude of ABP varies over time with each noradrenaline injection (Fig. 4.15).

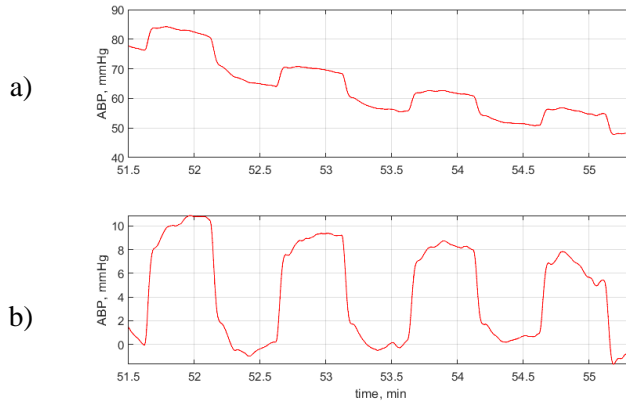


**Fig. 4.15.** Rectangular wave amplitude changes during noradrenaline injected wave: a) rectangular wave sequence during noradrenaline wave, b) detrended rectangular wave sequence

The dependency of rectangular wave amplitude is non-linear. The pulse of amplitude starts to increase with higher mean ABP. This can be the cause why noradrenaline wave is not linear. Moreover, it could be dependent on the person's weight, volume of fluids. The correlation between pulse amplitude and mean ABP is weak ( $R = 0.22$ ). The mean of pulse amplitudes is  $10 \text{ mmHg} \pm 4.2 \text{ mmHg}$  (Fig. 4.16). This shows that the amplitude is not stable and requires stabilization, in case when CA system is presented as a linear system, because a mean amplitude of  $10 \text{ mmHg}$  is less than the amplitude of physiological  $\text{ABP}(t)$  pulse waves.

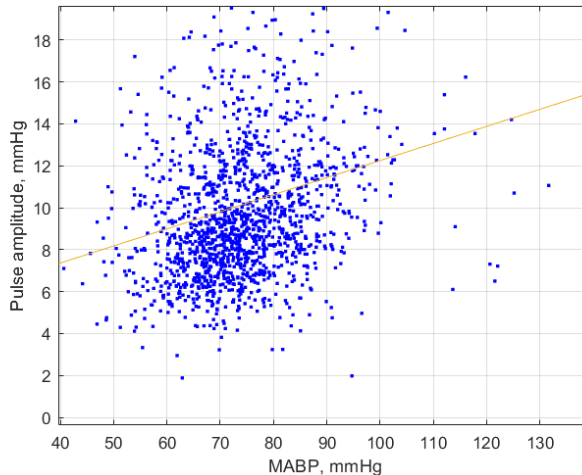


**Fig. 4.16.** Pulse amplitude dependency from mean ABP; correlation coefficient  $R = 0.22$  ( $p = 0.063$ ) shows no significant associations between pulse amplitude and mean ABP; the orange color shows linear approximation



Continuous rectangular ABP(t) pulse sequence extraction from other physiological waves is required for demodulation. The signal is filtered with 0.1 Hz third order Butterworth filter. The following step is to eliminate slow noradrenaline waves, and from filtered signal, the mean value of 60 s window is subtracted. The varying pulse amplitude allows to modulate a wave, which can be demodulated. After envelope extraction, the moving average filter of 1/30 s is used to filter out the carrier frequency of rectangular waves. The algorithm is shown in Fig. 4.17.

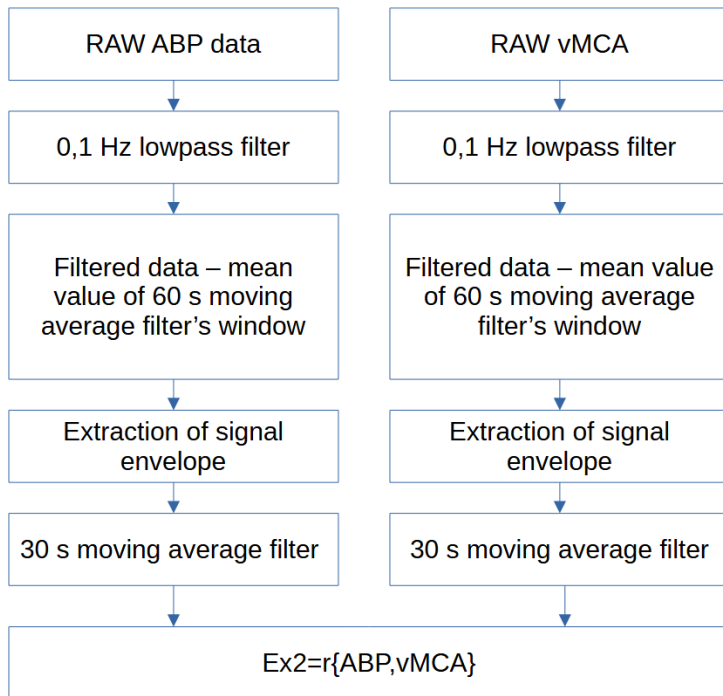


**Fig. 4.17.** The algorithm of Ex2 calculation

The coefficient has yet unknown properties as Ex2, because it has never been studied before. It is calculated between ABP and FV rectangular modulated envelope waves (14). This index is based on slow waves and Doppler, and the closest index is as well Mx. In order to identify diagnostic Ex2 threshold,  $\chi^2$  test was used within 0–1 threshold values of LCAI and patients' outcome. The most sensitive value was identified Ex2 = 0.6 ( $\chi^2 = 4.29$ ,  $p = 0.038$ ). The identified value will be used for the analysis, considering Ex2 < 0.6 as intact CA and Ex2 > 0.6 as impaired. This method is more sensitive compared to Mx and has less fluctuations compared to pump induced Ex index. The delay of Ex2 consists of 10 seconds of lowpass filter delay, 60 s of detrending, the Hilbert transformation delay (unknown in real time), 30 s of lowpass filter delay, and 30 s of moving correlation coefficient delay, which is 130 s delay in total.

$$Ex2 = r\{eABPsw, eFVsw\}; \quad (14)$$

where  $Ex2$  – envelope reactivity index,  $eABPsw(t)$  – envelope of arterial blood pressure rectangular waves, mmHg,  $eFVsw$  – envelope of flow velocity rectangular wave, cm/s.

The amplitude of rectangular modulated envelope varies around 8 mmHg of ABP and 10 cm/s of vMCA. The period of such waves is non-stationary and varies around 200 s, because it is noradrenaline dependent. Such waves have sharp peaks cause due to the noradrenaline injection and plateau phase, plateau phase with a ripple or slow descending front (Fig. 4.18).

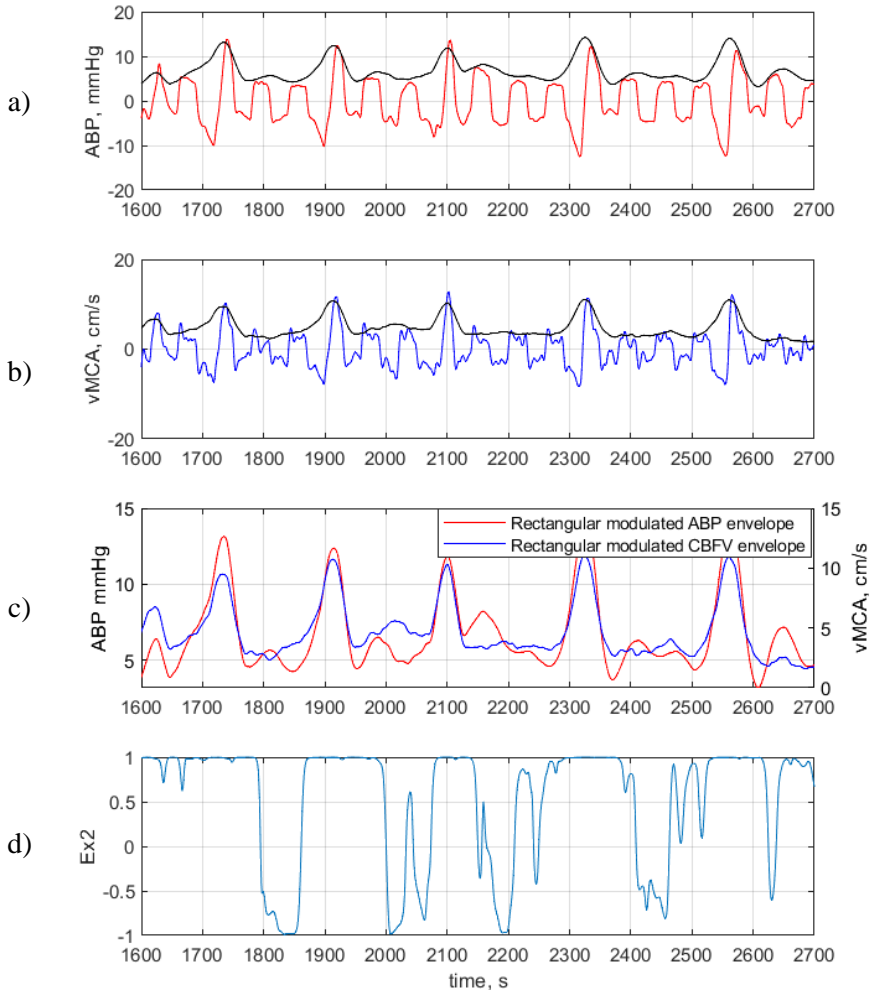


**Fig. 4.18.** Rectangular wave envelope decomposition: a) ABP rectangular wave modulated envelope, b) vMCA wave modulated envelope, c) comparison between ABP and vMCA rectangular wave modulated envelopes, d)  $Ex2$  reactivity index

#### 4.11. Noradrenaline induced wave index Mx2

During CPB surgery, noradrenaline waves are used to elevate ABP. After filtering signal with third order Butterworth filter of 6.7 mHz cut-off frequency, the noradrenaline waves were decomposed by filtering out pump vibrations and rectangular components. The duration of noradrenaline induced waves is typically 2–5 minutes. It is controlled by heart and lung machine operator who decides to inject a dose of noradrenaline. It was noticed that after reaching certain ABP value, the FV starts to saturate, and instead of sharp wave, the wave becomes dull, which could be associated with upper limit of CA. It was noticed that when ABP reaches a certain value, the FV starts to increase. This could be associated with lower limit of CA (Fig. 4.19). However, all surgeries are different, and some require frequent noradrenaline injections, while others require just a few, and in such case, the ABP is in a small variability range. Mx2 is calculated from noradrenaline slow waves of ABP and FV signals with a moving 30 s Pearson correlation window (15). The delay of Mx2 consists of lowpass filter delay and 150 s of moving correlation coefficient delay, which in total is 180 s delay.

$$Mx2 = r\{ABP_{nsw}, FV_{nsw}\}; \quad (15)$$

where Mx2 – noradrenaline induced wave index,  $ABP_{nsw}(t)$  – arterial blood pressure noradrenaline induced waves,  $FV_{nsw}$  – flow velocity of noradrenaline induced wave.

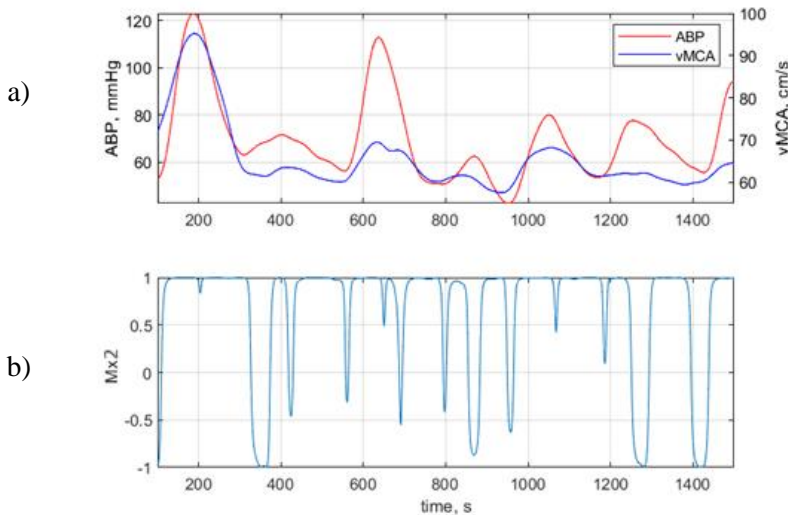


**Fig. 4.19.** Noradrenaline induced waves; a) red color is ABP signal, blue color is vMCA; when ABP exceeds 110 mmHg, vMCA wave is sharp, in other cases, it is rounded, b) Mx2 calculation according to induced noradrenaline waves

#### 4.12. Comparison of new derived envelope-based signals

The envelope amplitude modulated rectangular waves and pump waves are different as well as cerebral blood flow response to the generated changes. The rectangular wave amplitude is less noisy and has more dynamic changes due to the transient responses. However, the pump induced waves are more affected by noradrenaline injections than rectangular wave modulation. It is yet unknown what information both indexes carry, because both signals come from the same source of heart and lung machine, but they show different vascular and cerebrovascular changes. This raises new scientific question about the understanding of cerebral autoregulation during cardiac bypass surgery.

After comparing filtered ABP, pump amplitude modulated envelope, and rectangular modulated envelope waves, it was noticed that they differ in shape. The pump modulated ABP waves are similar to noradrenaline modulated waves. The rectangular modulated waves have sharper peak and slow descending front. Due to low dynamics, noradrenaline wave analysis was not included for comparison (Fig. 4.20).

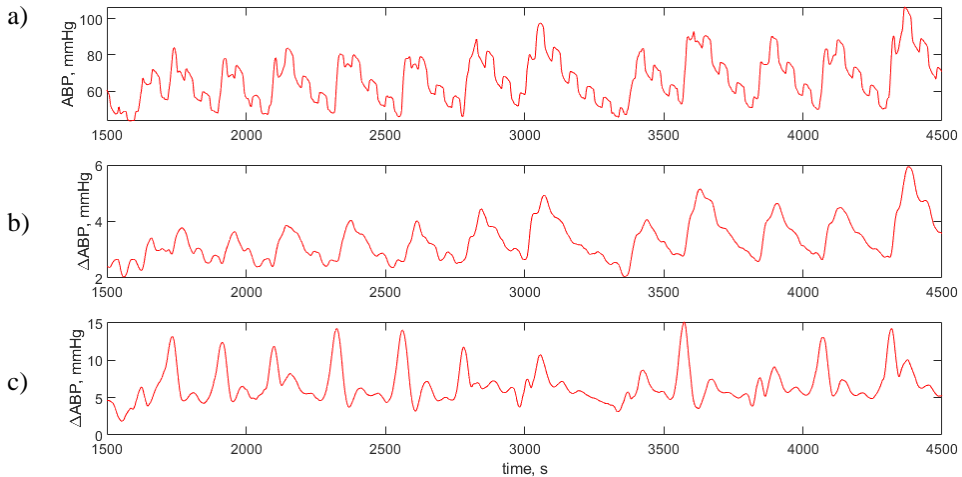


**Fig. 4.20.** Comparison of 3 ABP signals during cardiac bypass surgery with pump-on: a) filtered ABP signal, b) pump induced ABP envelope waves, c) rectangular modulated envelope waves

The rectangular modulated ABP waves have most spectra components compared to ABP and pump modulated waves. It is because of the sharp peak created by noradrenaline waves. The ABP pump modulated waves have similar spectra components compared to ABP; however, ABP modulated waves have more energy at 0.016 Hz where is the rectangular modulation (Fig. 4.21).

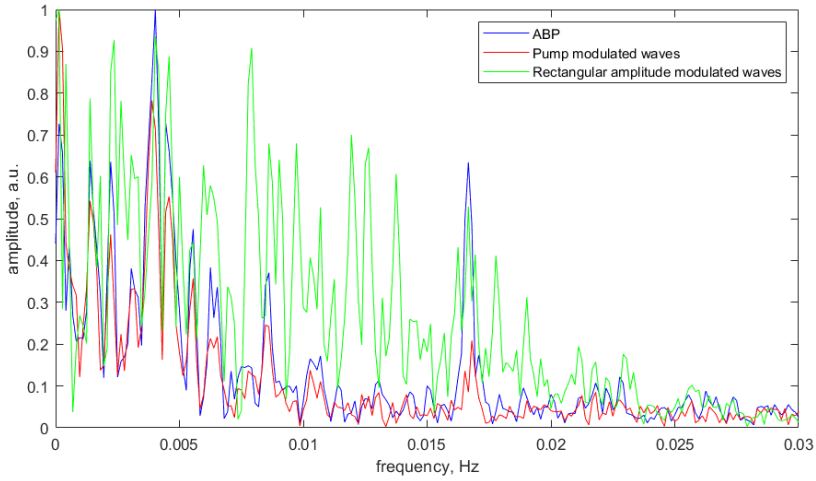


**Fig. 4.21.** Comparison of three different ABP slow wave spectrum components using FFT transformation

After comparing filtered vMCA, pump amplitude modulated envelope, and rectangular modulated envelope waves, it has been noticed that they differ in shape. The pump modulated vMCA waves show less affect to the injected noradrenaline and show symmetrical slow waves. The rectangular modulated waves have sharper peak and plateau phase (Fig. 4.22).

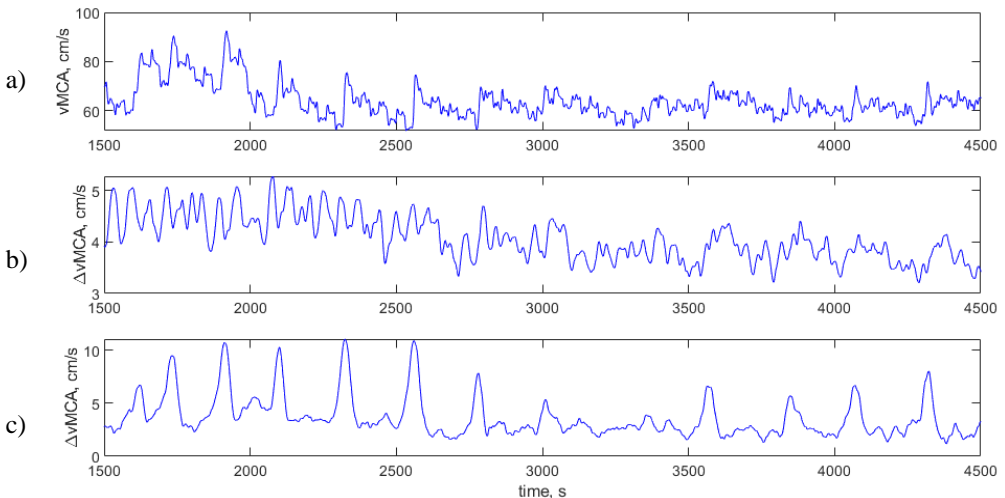


**Fig. 4.22.** Comparison of 3 vMCA signals during cardiac bypass surgery with pump-on: a) filtered ABP signal, b) pump induced ABP envelope waves, c) rectangular modulated envelope waves

The vMCA spectral components are similar to ABP. Rectangular modulated ABP waves have the most spectra components compared to vMCA and pump modulated waves. It is because sharp peaks are created by the noradrenaline waves. The ABP pump modulated waves have similar spectra components compared to vMCA; however, vMCA modulated waves have the most energy at 0.016 Hz where is the rectangular modulation and 0.005 Hz where are the noradrenaline waves. The lowest magnitude has pump modulated waves due to small pump vibrations (Fig. 4.23).

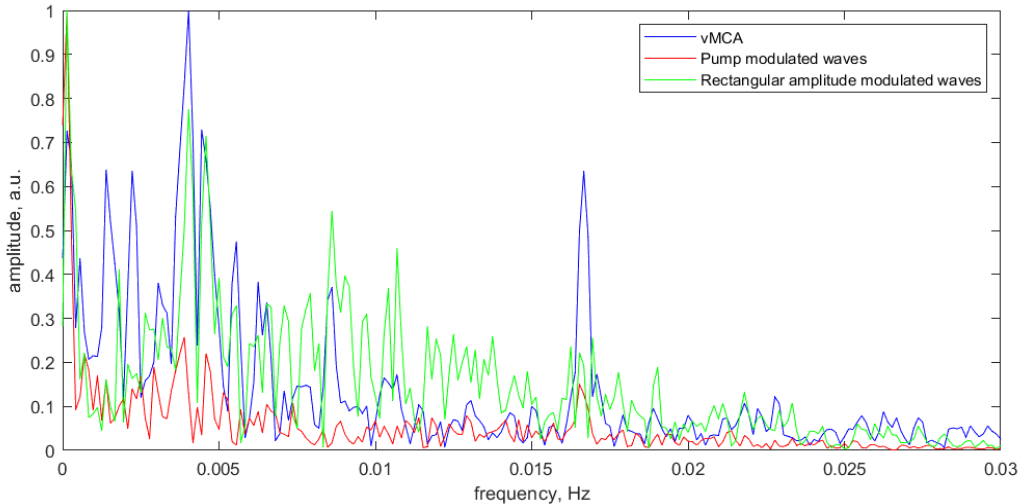


**Fig. 4.23.** Comparison of three different ABP slow wave spectrum components using FFT transformation

## Conclusions

1. The cerebral blood flow velocity signal measured in MCA requires 0.1 Hz lowpass filtering due to the presence of additional noise caused by the artifacts and ultrasound signal attenuation in skull bone structure.
2. The generated rectangular ABP waves overlap with noradrenaline induced waves and heart pulsations and therefore, sometimes have shape distortion.
3. The new indexes for CA assessment were proposed and compared to the classical TCD-based cerebral autoregulation index Mx: transient function index TFx, pump vibration envelope modulated index Ex, rectangular wave modulated envelope reactivity index Ex2, and noradrenaline wave induced reactivity index Mx2.
4. The envelope signals that derived from rectangular waves and pump vibration waves have distinguishing properties. The envelope signals that derived from rectangular waves have higher spectrum components due to the sharp peaks and plateau phase. The envelope signals that derived from the pump vibration waves have more symmetrical oscillations.

## 5. RESULTS

### 5.1. TFx

The patients in both groups experienced CA impairment episodes. The association of the longest cerebral autoregulation impairment event between no deterioration and POCD patients has been found ( $p = 0.047$ ). The median LCAI value for no deterioration group is 14.75 minutes, and for POCD group, it is 20.98 min. (Fig. 5.1).

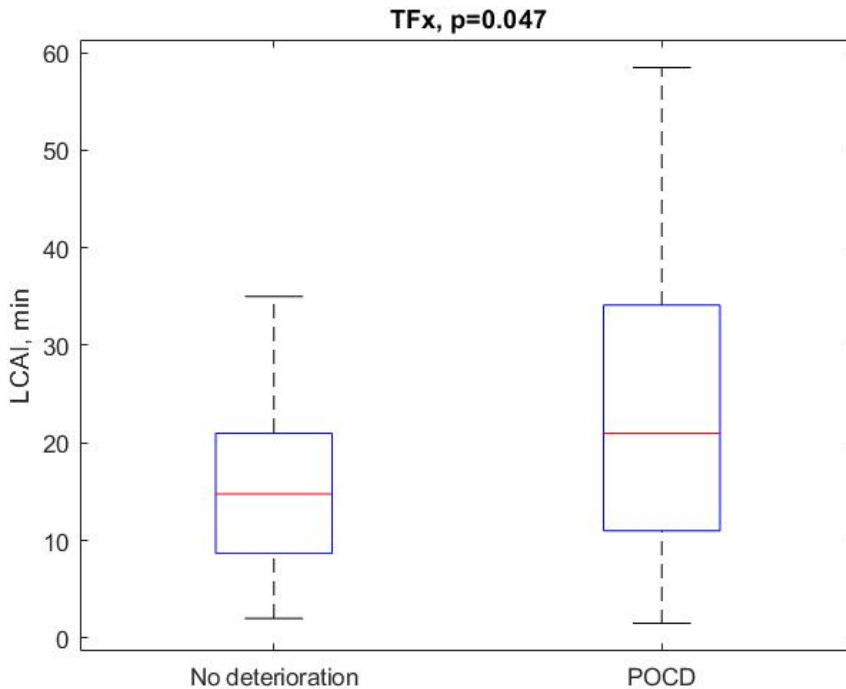


**Fig. 5.1.** Association between the duration of single longest cerebral autoregulation impairment (LCAI) event and POCD for two groups of patients using CA status identification index TF; there is no statistically significant difference ( $p = 0.047$ ) between two groups

The LCAI event happened in MABP range from 55 mmHg to 85 mmHg. Due to very long LCAI episode because of averaging, there are no clear cases of hypoperfusion or hypoperfusion causing POCD. The longest CA impairment varies up to 60 minutes (Fig. 5.2).

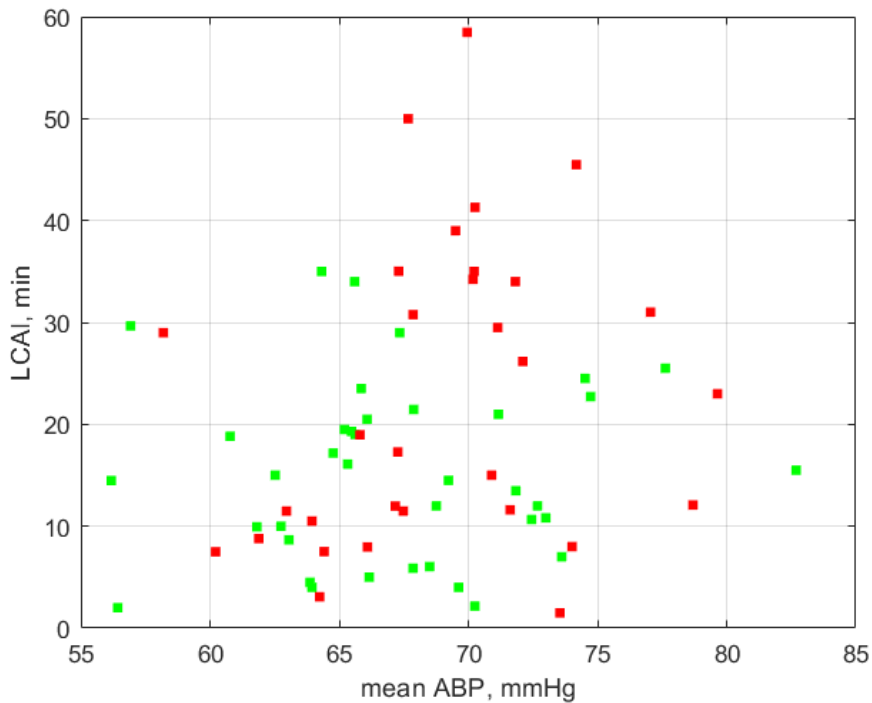


**Fig. 5.2.** The distribution of mean ABP during LCAI event with CA identification index TFX; green color shows cases of no deterioration, and red color shows cases of POCD

## 5.2. Mx

Patients in both groups experienced CA impairment episodes. The association of the longest cerebral autoregulation impairment event between no deterioration and POCD patients has not been found ( $p = 0.084$ ). The median LCAI value for no deterioration group is 8.67 minutes, and for POCD group, it is 9.20 min. Such result can be caused due to the low sensitivity of Mx signal, because lower frequency components of noradrenaline waves are covering CA status information (Fig. 5.3).



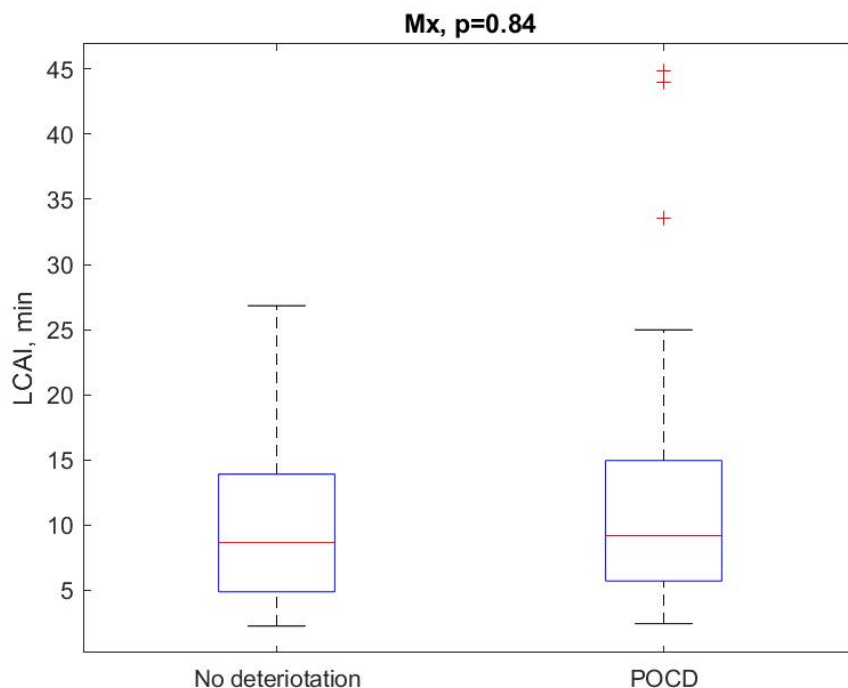


**Fig. 5.3.** Association between duration of single longest cerebral autoregulation impairment event and POCD for two groups of patients using CA status identification index Mx; no statistically significant difference (Mann–Whitney U test,  $p = 0.84$ ) between the two groups has been found

The LCAI event happened in MABP range from 50 mmHg to 100 mmHg. There are no clear cases of hypoperfusion or hypoperfusion causing POCD, and the longest CA impairment varies up to 45 minutes (Fig. 5.4).

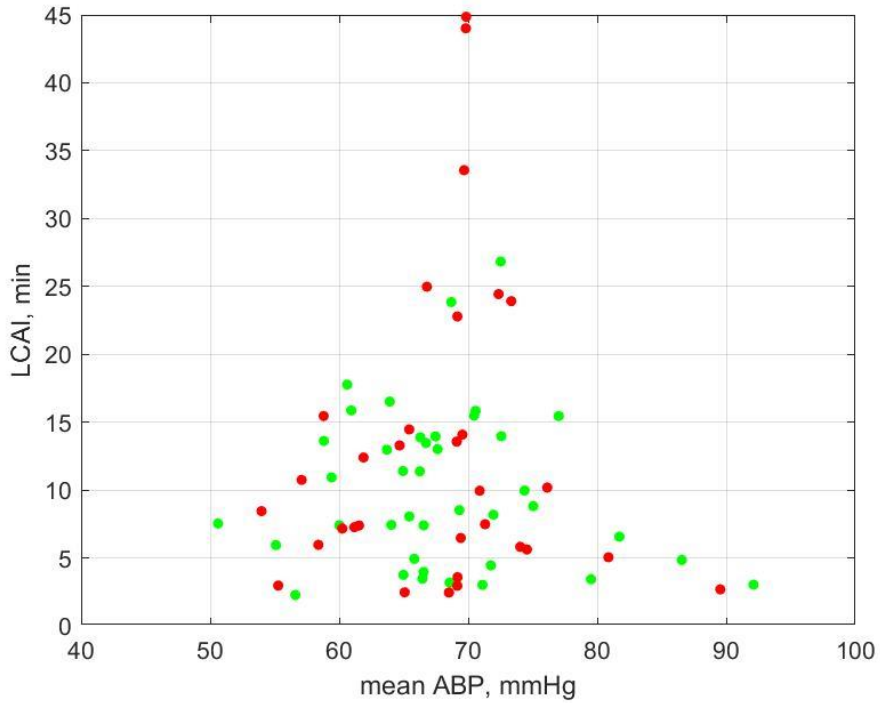


**Fig. 5.4.** The distribution of mean ABP during LCAI event with CA identification index Mx; green color shows cases of no deterioration, and red color shows cases of POCD

### 5.3. Ex

The patients in both groups experienced CA impairment episodes. The association of the longest cerebral autoregulation impairment event between no deterioration and POCD patients has not been found ( $p = 0.10$ ). The median LCAI value for no deterioration group is 2.28 minutes, and for POCD group, it is 4.32 min. The threshold separating 2 groups was found 160 s (Fig. 5.5).

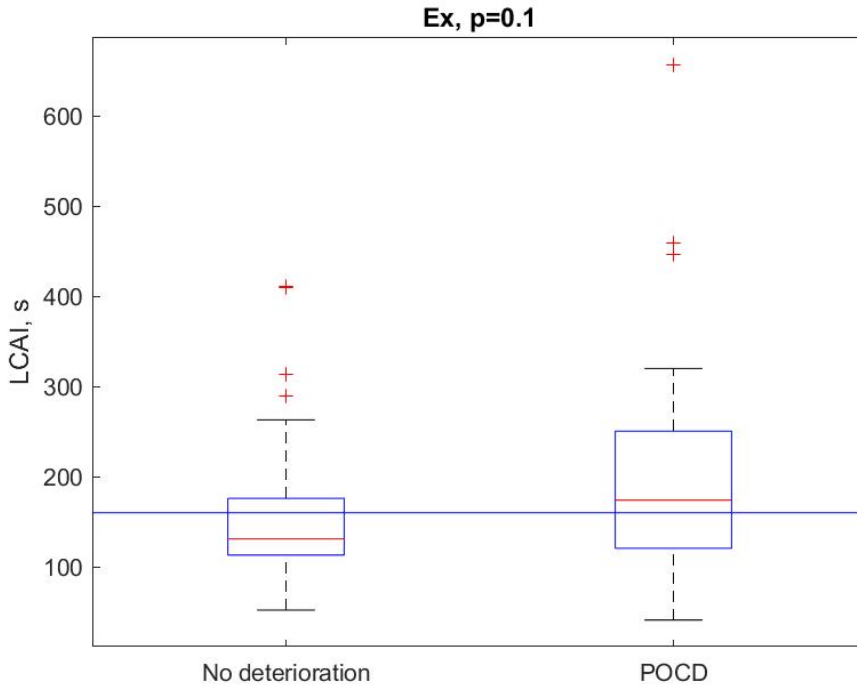


**Fig. 5.5.** Association between duration of single longest cerebral autoregulation impairment event and POCD for two groups of patients using CA status identification index Ex; no statistically significant difference ( $p = 0.10$ ) has been found between two groups; blue line shows the threshold separating 2 groups LCAI = 160, ( $\chi^2 = 5.20$ ,  $p = 0.022$ )

The LCAI event happened in ABP range from 45 mmHg to 95 mmHg. There is 1 case of POCD, which appeared below 50 mmHg of ABP that could be caused due to the hypoperfusion, and 2 cases of POCD around 90 mmHg of ABP, which could be caused due to the hyperperfusion. Other cases were in physiological limits and were caused due to too long CA impairment (Fig. 5.6).

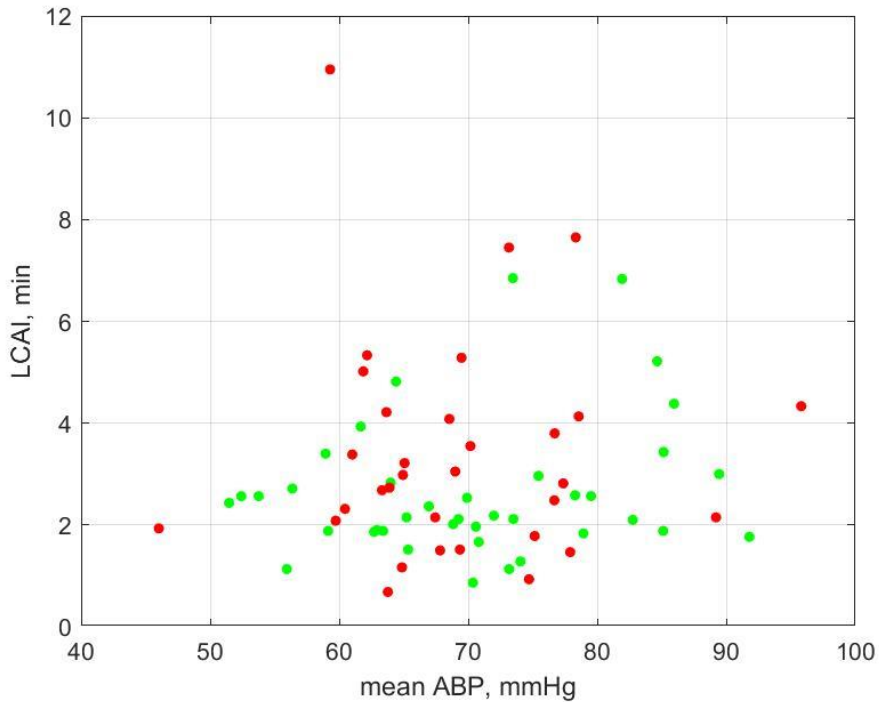


**Fig. 5.6.** The distribution of mean ABP during LCAI event with CA identification index Ex; green color shows cases of no deterioration, and red color shows cases of POCD

#### 5.4. Ex2

The patients in both groups experienced CA impairment episodes. The association of the longest cerebral autoregulation impairment event between no deterioration and POCD patients was found ( $p = 0.015$ ). The median LCAI value for no deterioration group is 3.75 minutes, and for POCD group, it is 4.33 min. Cerebral autoregulation impairment that is longer than 220 s is associated with POCD. This result is as well close to the previous study, and LCAI based on Ex index shows that LCAI that is longer than 220 s ( $\chi^2 = 11.54$ ,  $p = 0.001$ ) is associated to POCD (Fig. 5.7).

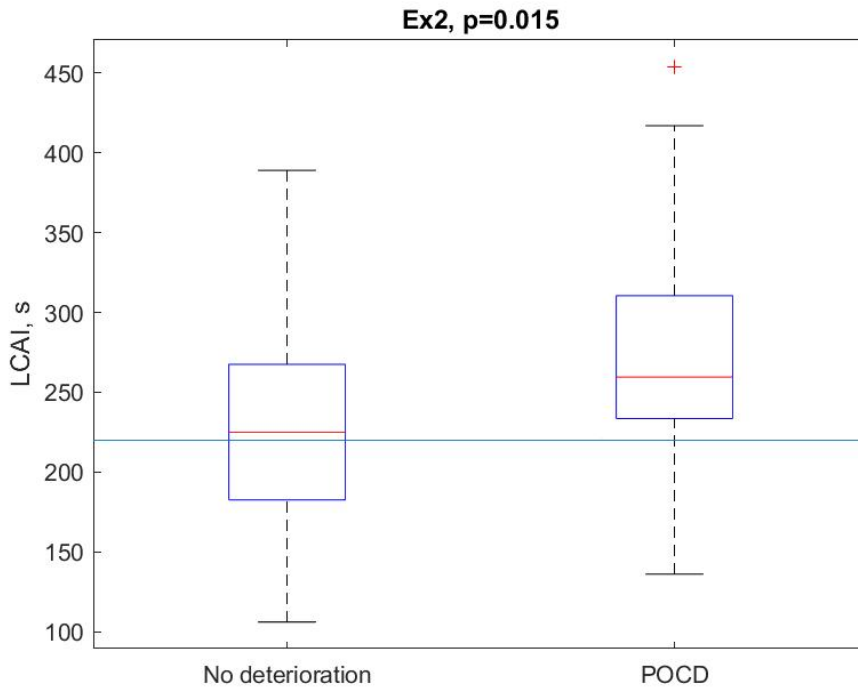


**Fig. 5.7.** Association between the duration of single longest cerebral autoregulation impairment event and POCD for two groups of patients using CA status identification index Ex2; there is a statistically significant difference ( $p = 0.015$ ) between two groups; blue line shows the threshold separating 2 groups LCAI = 220 s, ( $\chi^2 = 11.54$ ,  $p = 0.001$ )

The LCAI event happened in MABP range of 45–120 mmHg. There are no clear cases of POCD due to the hypoperfusion or hyperperfusion. However, it could be seen that the longest CA impairment event that is longer than 4 minutes is associated with POCD independently from the MABP during CA impairment event (Fig. 5.8).

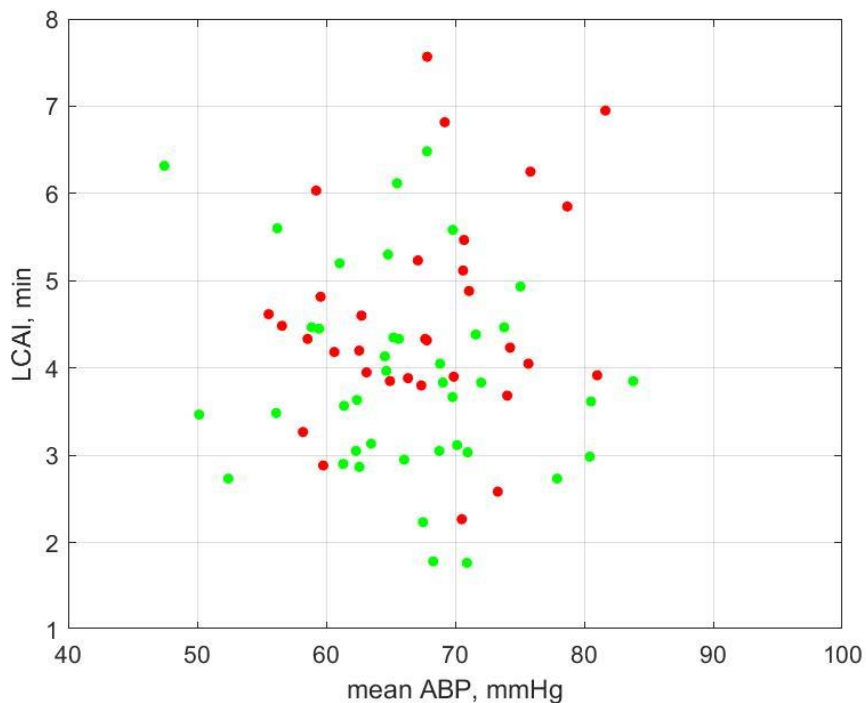


**Fig. 5.8.** The distribution of mean ABP during LCAI event with CA identification index Ex2; green color shows cases of no deterioration, and red color shows cases of POCD

### 5.5. Mx2

The patients in both groups experienced CA impairment episodes. The association of the longest cerebral autoregulation impairment event between no deterioration and POCD patients has not been found ( $p = 0.015$ ). The median LCAI value for no deterioration group is 8.74 minutes, and for POCD group, it is 6.64 min (Fig. 5.9).

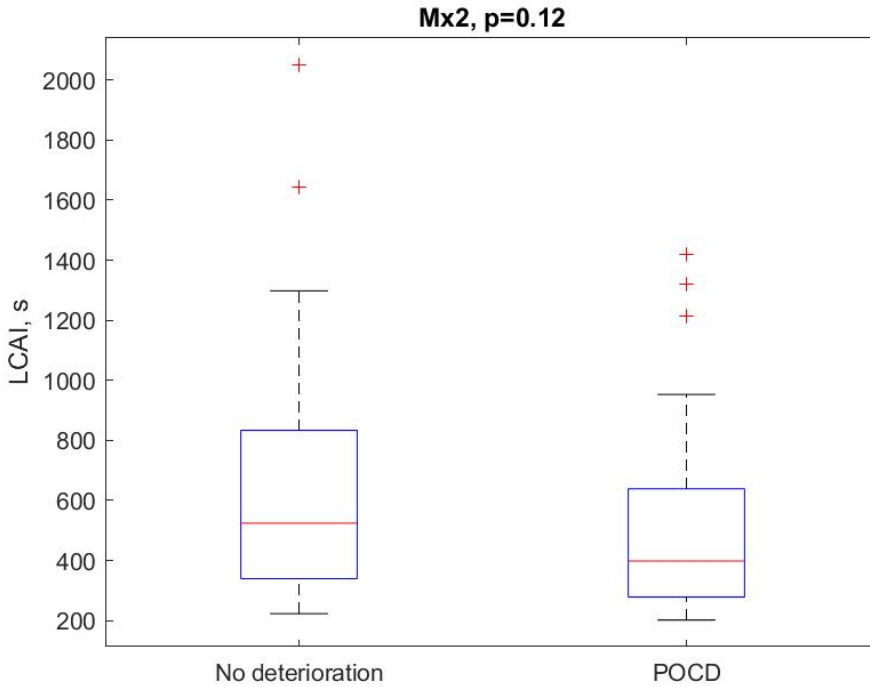


**Fig. 5.9.** Association between duration of single longest cerebral autoregulation impairment event and POCD for two groups of patients using CA status identification index Mx; statistically not significant difference (Mann–Whitney U test,  $p = 0.12$ ) between two groups

The LCAI event happened in ABP range from 55 mmHg to 85 mmHg. There are no clear cases of PCOD due to the hypoperfusion or hyperperfusion. It could be concluded that CA identification Mx2 index using noradrenaline waves is not sensitive enough for this study due to too low variability (Fig. 5.10).

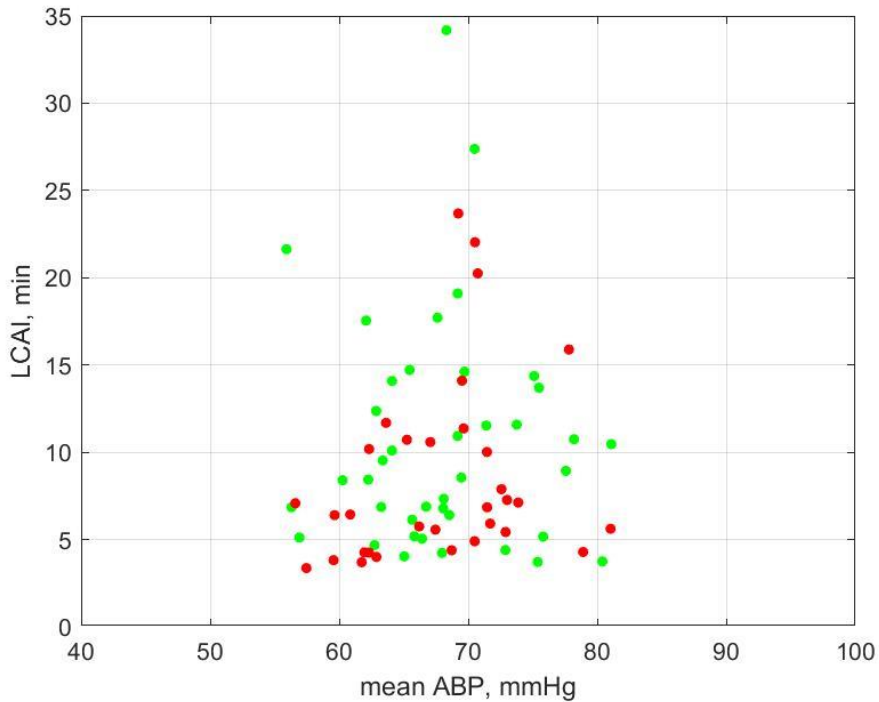


**Fig. 5.10.** The distribution of mean ABP during LCAI event with CA identification index Mx2; green color shows cases of no deterioration, and red color shows cases of POCD

### Conclusions

Different CA status estimation indexes showed different results of single longest CA impairment event duration. Correlation based method Mx shows mostly impaired CA during cardiac bypass surgery, which did not show statistically significant differences between POCD and non-POCD patients' groups. New derived indexes, such as TFx based on CA system transient responses, Ex based on envelope calculation from high frequency pump vibrations, or Ex2 based on envelope calculation from generated rectangular waves, are more sensitive for the analysis of cerebral autoregulation and used as biomarkers related with the clinical outcome of cardiac surgery patients.

The longest CA status delay has Mx2 index of 180 s, which is too long for CA due to filtering rectangular wave modulation. The shortest delay of 15 seconds has TFx index, and suboptimal delay of 60–130 s has Ex and Ex2 indexes.



**Table 6.1.** Comparison of durations of the longest CA impairment episodes

Parameter	Mx	Ex	Ex2	Mx2	TFx
Mean LCAI, s	682	183	251	581	1,000
LCAI threshold separating POCD and non-POCD groups, s	Not found	160	220	Not found	Not found
Mean sum time of CA impairment	4,531	2,402	3,475	4,259	3,275
Delay, s	40	60.5	130	180	10

## Discussion

During cardiac bypass surgery, an innovative electronic device was used to estimate the CA status for the first time. Moreover, pump and rectangular envelope induced wave analysis was analyzed for the first-time. The uncertainty of results is affected by the psychiatric test validation, lack of ability to generate stable and rectangular shape wave sequence, and lost resolution of too long pulse duration. Close to real-time transient function response and correlation-based indexes show both impaired and intact CA. However, it is unknown how much CA monitoring method of longest cerebral autoregulation impairment is contributing to the patient's outcome, because association is not equal to causation and due to biased, caused by patient's age and years of education.

Further research should be continued by applying more factors, such as magnetic resonance imagining for scanning strokes after surgery, brain oxygenation monitoring, chemical biomarkers of blood. Moreover, it could be applied to different psychological tests for the estimation of POCD.

## Limitations

1. In certain cases, the heart and lung machine generates irregularly shaped rectangular pulses. These anomalies disrupt the vMCA(t) pulsation shape. This issue could potentially be resolved by stabilizing the pulse amplitude and reducing its duration.
2. The length of the 30-second pulse is excessive, resulting in a loss of temporal resolution and introducing aliasing between noradrenaline-induced waves. Shortening the pulse to a range of 10 to 15 seconds could alleviate these problems because CA restoration time is around 7–10 seconds.
3. The amplitude of the rectangular wave fluctuates due to the noradrenaline injections. In order to get precise transient function analysis, a stable amplitude of ABP(t) rectangular pulses is needed. The amplitude value of such pulses has to

be much lesser than the mean ABP value in order to reduce non-linear CA system to linear system.

4. Transcranial Doppler signal, due to some patients' bone structure, cannot be reliably recorded. The presence of noise in the low MCA blood flow velocity signals makes the interpreting of CA status challenging.
5. Post-surgery, CA monitoring was not conducted in the intensive care unit, potentially impacting patient outcomes. Consideration could be given to monitoring CA both before and after the surgery.
6. Patient outcomes were influenced by factors, such as age and years of education, stenosis of cerebral vessels, etc. introducing bias. Utilizing unbiased tests could minimize this bias.
7. Time period of pre and post patient's general anesthesia before the start of multimodal monitoring is excluded from this study and from absolute majority of already published CPB prospective studies. It has been found only in one paper from 2004, which is related to the ABP(t) analysis before beginning of CPB patient monitoring. According to the experiences, a lot of fast mean ABP changes within the interval from 180 mmHg to 20 mmHg. Such changes can cause cerebral hyperemia or hypoemia. The associations of such ABP(t) dynamics before the beginning of multimodal CPB monitoring with POCD and delirium will be the next step in the analysis of prospectively collected data base of 195 CPB patients in Kaunas and Vilnius.

## GENERAL CONCLUSIONS

1. The literature review showed that there are no existing technologies allowing to detect CA impairment within needed time interval below one minute and implement neuroprotection before critical damage of brain cognitive functions' due to hypoperfusion or hyperperfusion events during CPB.
2. A close to real-time CA impairment identification technology has been proposed and clinically validated to identify the beginning of CA impairment. The developed technology generates a rectangular blood flow of heart and lung machine with needed modulation period. The proposed method of generation of rectangular blood flow and, as a consequence, rectangular pulses of arterial blood pressure allow to assess CA status with 30 sec or better temporal resolution by continuous monitoring of transient CA system responses to rectangular arterial blood pressure falling and rising fronts.
3. A new derived CA status identification indexes were proposed: pump vibration modulated wave index (Ex), rectangular wave modulated index (Ex2), noradrenaline induced waves Mx2, and transient function index (TFx). The reliable threshold separating intact and impaired CA status was identified for newly proposed TFx index, which is based on the real-time analysis of CBFV transient responses to rising and falling fronts of rectangular ABP pulses. Critical TFx value above 0.7 was found as a threshold associated with impaired CA status; therefore, it can be used as an indicator for detecting beginning moments of CA impairment events.
4. The identified factors that influence patient outcomes after cardiac surgery with POCD were age ( $p = 0.175$ ) and years of education ( $p = 0.029$ ). However, the duration of the longest cerebral autoregulation impairment event, as determined by the proposed CA indexes Ex2 and TFx, was found statistically significantly associated with POCD ( $p = 0.015$  for Ex2 and by  $p = 0.047$  for TFx). This underscores the conclusion that the duration of the single longest cerebral autoregulation impairment event holds the strongest association with patients' clinical outcomes.

### Confirmation of the hypotheses

It is possible to identify in close to real-time CA status by generating rectangular sequence waves. It has been observed that newly derived CA indexes based on transfer function analysis (TFx) and envelope calculation from ABP and CBFV signals (Ex2) after rectangular sequence waves generation could be used as a biomarker associated with the outcome of cardiac surgery patients.

## 6. SANTRAUKA

### Darbo svarba

Viena iš didžiausių pasaulio sveikatos problemų yra širdies arterijų ligos. Kiekvienais metais pasaulyje dėl šios problemos yra prarandama maždaug 7 milijonai žmonių ir 129 milijonai žmonių negali tęsti savo įprasto gyvenimo [1]. Norint išvengti tokių padarinių yra naudojama širdies ir plaučių šuntavimo (ŠPŠ) operacija, kuri atliekama į koronarines arterijas prijungiant šuntą, siekiant atkurti ankstesnę kraujotakos kraujagyslių būklę. 2020 m. duomenimis, Europos Sąjungoje buvo atlikta 139 000 tokių operacijų, o Lietuvoje šio tipo operacijos atliekamos 39,6 šimtui tūkstančių gyventojų [2]. Dėl tokio tendencijos ŠPŠ operacijų skaičius ateityje augs.

Po ŠPŠ operacijos apie 50 % pacientų patiria neurokognityvines disfunkcijas, tokias kaip pooperacinis delyras, pooperacinė kognityvinė disfunkcija (angl. *Post operative cognitive deterioration*, POCD) ar insultas [3]. POCD yra būklė, kai yra pažeidžiamas pažinimas, sąmonė, dėmesys ir suvokimas, lyginant su būkle prieš operaciją. Be neurokognityvinių disfunkcijų, kaip komplikacijos gali įvykti ūminis inkstų pažeidimas ar prieširdžių virpėjimas [4]. Chirurgija naudojant širdies ir plaučių mašiną yra saugesnė, nes kraujo tekėjimą valdo mašinos operatorius, tačiau nėra mokslinių įrodymų, kad operacija be širdies ir plaučių mašinos sukeltų mažiau pooperacinių kognityvinių komplikacijų atvejų [5].

Galima smegenų pažeidimo priežastis yra ta, kad vietoj natūralios kraujotakos dirbtinė kraujo apytaka (DKA), valdoma širdies ir plaučių mašina, ne visada leidžia palaikyti adekvatų arterinį kraujospūdį (AKS). Smegenų kraujotakos autoreguliacija yra smegenų funkcija, užtikrinanti pastovią smegenų ląstelių mitybą maistinėmis medžiagomis ir deguonimi. Ši funkcija leidžia palaikyti nuolatinį pastovų smegenų kraujo tekėjimą dideliame arterinio kraujo spaudimo (AKS) diapazone. Ši funkcija sutrikdoma, jei AKS yra už autoreguliacijos zonos ribų. SKAR yra kontroliuojama vazokonstrikcija ir vazodilatacija. Dėl autoreguliacinio mechanizmo yra palaikomas pastovus smegenų kraujo tekėjimas 50ml/100g/min besikeičiančiam smegenų perfuzijos slėgiui.

Medicininėje literatūroje statine smegenų kraujotakos autoreguliacija yra vadinamas procesas, kuris stabilizuoja smegenų kraujo tekėjimas tam tikrose fiziologinėse smegenų perfuzijos slėgio ribose [6]. Pagal sistemų kontrolės teoriją, stabilizacija reiškia neigiamą grįžtamąjį ryšį per aktyvų dinaminį procesą, dėl to statinė smegenų kraujotakos autoreguliacija yra neįmanoma. Labiau tinkamas terminas lėtiems autoreguliaciniams procesams apibūdinti yra kvazistatinė. Veikianti kvazistatinė autoreguliacija gali būti įvertinta įvairiais būdais. Vienas iš paprasčiausių būdų įvertinti smegenų kraujotakos būklę yra fazių matavimas tarp lėtų IKS(t) ir AKS(t) bangų.

Teoriškai, jei fazės skirtumas tarp šių bangų artimas 180°, tai rodo, kad autoreguliacija yra sveika ir aktyvi, nes AKS(t) padidėjimas sukeltų arterinių

kraujagyslių (įskaitant arterioles) susitraukimą, kad sumažintų smegenų kraujo tūrį ir padarytų smegenų kraujo tekėjimą stabilų. Priešingu atveju AKS(t) sumažėjimas sukelia arteriolių išplėtimą, kad padidintų smegenų kraujo tūrį ir stabilizuotų smegenų kraujo tekėjimą. Jei AKS(t) ir IKS(t) lėtosios bangos yra sinfaziškos, tai laikoma sutrikusia SKAR [7].

Mūsų ankstesniame klinikiniam tyrime dirbtinės lėtosios bangos su fiksuotu periodu buvo generuojamos naudojant širdies ir plaučių mašiną kardiokirurginės operacijos metu. Smegenų kraujotaka buvo stebima neinvaziniu ultragarsinio sklidimo laiko „Vittamed“ prietaisu įvertinant SKAR būklę. Rezultatai parodė, kad ilgiausias smegenų kraujotakos sutrikimas, kurio trukmė daugiau nei 5 minutės, asocijuojasi su POCD [8]. Nepriklausomų klinikinių tyrimų Danijoje metu atliekant ŠPŠ operacijas esant aukštam vidutiniam AKS (70–80 mmHg) ir žemam vidutiniam AKS (40–50 mmHg), nenustatyta jokios reikšmingos sąsajos tarp nesutrikusios ir POCD grupių ( $p = 0,12$ ) [9]. Tai gali būti įrodymas, kad individualus smegenų kraujo tekėjimo autoreguliacijos pažeidimo įvykis yra svarbesnis faktorius, palyginti su vidutiniu AKS chirurgijos metu.

Nustatyti optimalias AKS ar SPS vertes pacientams, patyrusiems sunkią galvos traumą intensyvios terapijos metu, klinikinėje praktikoje reikia minučių ar valandų vidurkinti stebėsenos duomenis norint nustatyti reikiamą SKAR sutrikimo neapibrėžtį. Mūsų nauji klinikiniai tyrimai parodė, kad galima nustatyti optimalią AKS/SPS vertę per 24 minutes sunkią galvos traumą patyrusiems pacientams, kai egzistuoja fiziologinės lėtos bangos [10]. Tačiau statinė SKAR įvertinimo problema ta, kad reikalaujamas vidurkinimas uždelsia gydymo sprendimo priėmimą.

Greitas SKAR įvertinimo metodas yra pereinamųjų SKAR sistemos funkcijų matavimas. SKAR yra netiesinė sistema. Norint įvertinti SKAR būklę pagal pereinamuosius procesus, reikia sistemą padaryti tiesinę. Tam reikia ( $\Delta$ AKS žingsnis  $\leq 10$  mmHg, kuris yra daug mažesnis nei vidutinis AKS) AKS(t) iššūkio, tokio kaip SKAR sistemos įėjimas. Tokį AKS žingsnį galima sukelti naudojant tokį metodą, kaip šlaunų manžetės atleidimas, kaklo arterinių kraujagyslių suspaudimas arba pritūpimo pratimas. Medicinos literatūroje tai yra vadinama dinamine smegenų kraujotakos autoreguliacija [11],[12]. Naudojant AKS žingsnio poveikį, normalus pereinamosios reakcijos laikas trunka apie 7–12 sekundžių ir, esant smegenų autoreguliacijos pažeidimui, smegenų kraujotaka seka AKS(t) seką [13].

Dabartinėje pasaulinėje rinkoje šiuo metu nėra įrangos, kuri leistų nustatyti optimalią AKS (arba SPS) vertę greičiau nei per 5–20 minučių. Mūsų idėja yra buvo sugeneruoti stačiakampio formos kraujo srauto bangas naudojant širdies ir plaučių mašiną (vienos minutės arba mažesnio periodo) nenutrūkstamai pereinamųjų SKAR funkcijų stebėsenai. Toks širdies ir plaučių mašinos modelis yra naujas ir niekada kliniškai netestuotas. Esantys širdies ir plaučių mašinos režimai yra pastovaus tekėjimo ir pulsinis, kuris imituoja širdies ritmą. Vis dėlto pulsinio režimo negalima naudoti SKAR būsenai stebėti, nes pulsai yra trumpesni nei veikiančios SKAR

nusistovėjimo laikas [28]. Mūsų perspektyvusis klinikinis tyrimas buvo atliktas kliniškai validuoti mūsų pasiūlytam širdies ir plaučių mašinos režimui, siekiant įvertinti pridėtinę vertę stebint realaus laiko SKAR pereinamąsias funkcijas ir vystyti technologiją ir metodologiją smegenų apsaugai nuo pažeidimo kardiochirurginės operacijos metu.

## **Mokslinės-technologinės problemos ir tyrimo hipotezė**

Mokslinės-technologinės problemos:

1. kokiais būdais ir kokiomis priemonėmis galima neinvaziniu būdu stebėti smegenų kraujotakos autoreguliaciją realiu laiku apsaugant žmogaus smegenis nuo išeminių ir hipereminių insultų?
2. ar įmanoma nustatyti smegenų kraujotakos autoreguliaciją ir atkurti nepažeistą smegenų kraujotakos autoreguliaciją prieš įvykstant smegenų neuronų mirčiai?

**Tyrimo hipotezės:** diagnozuoti sutrikusią smegenų kraujotakos autoreguliacijos būseną įmanoma naudojant smegenų kraujotakos autoreguliacinius pereinamuosius atsakus į DKA mašinos suformuotus stačiakampio formos kraujo srauto signalus. Įmanoma apsaugoti individualaus paciento smegenis nuo funkcinių pažeidimų per širdies šuntavimo operaciją, įvertinant SKAR būsenos sutrikimo pradžią su subminutine laiko skyra ir naudojant grįžtamąjį ryšį su anestezilogijos ir chirurgijos komanda siekiant atkurti veikiančią SKAR prieš negrįžtamus neuronų pažeidimus.

## **Tyrimo tikslas ir uždaviniai**

Atsižvelgiant į precizinės ir individualizuotos medicinos koncepciją, šio tyrimo tikslas yra pasiūlyti neinvazinę technologiją, leidžiančią identifikuoti kraujotakos išeminių arba hipereminių smegenų kraujotakos sutrikimų epizodus ir atkurti optimalią smegenų perfuziją individualiam pacientui prieš įvykstant negrįžtamiems neuronų pažeidimams.

Šie uždaviniai yra suformuluoti siekiant pasiekti tyrimo tikslą:

1. Išanalizuoti ir peržiūrėti esamą literatūrą apie smegenų kraujotakos autoreguliaciją ir jos įvertinimo metodus.
2. Pasiūlyti elektroninę technologiją, galinčią pastoviai moduluoti kraujo srautą, kuris galėtų įvertinti smegenų kraujotakos autoreguliacijos būklę su reikiama laikine skyra.
3. Identifikuoti laikinius faktorius, leidžiančius nustatyti SKAR sutrikimo epizodus naudojant pasiūlytą arterinio kraujo srauto moduliacijos technologiją.

4. Išanalizuoti asociacijas su paciento klinicine baigtimi naudojant pasiūlytus SKAR būsenos įvertinimo faktorius (indeksus) bei kitus darančius įtaką faktorius.

### **Mokslinis naujumas**

Pirmą kartą buvo pasiūlytas ir išbandytas stačiakampio formos bangos kraujo srauto generavimo metodas, kuris buvo įdiegtas į širdies ir plaučių mašinę kardiochirurgijos metu. Sugeneruota seka yra stebima transkranijinio Doplerio ultragarsinės technologijos prietaisu („Viasonix Dolphin 4D“, Raana, Izraelis) stebint vidurinės smegenų arterijos greičių reakcijas į arterinio kraujo slėgio (AKS) sugeneruotą pokytį. Jei smegenų kraujo srauto greitis vidurinėje smegenų arterijoje sugrįžta į vidutinį greičio vertę, tai laikoma nepažeista smegenų kraujotakos autoreguliacijos (SKAR) būseną. Jei smegenų kraujo srauto greitis vidurinėje smegenų arterijoje seka ABP poveikį, tai laikoma pažeista SKAR būseną. Pirmą kartą buvo parodyta, kad pasiūlytas stačiakampio formos generavimo metodas leidžia įvertinti SKAR sutrikimo epizodus su norimu vėlavimu. Šis vėlavimas yra mažesnis nei kritinis laikas, siejamas su POCD kardiochirurginės operacijos metu, ir gali būti įdiegtas realaus laiko neuroprotekcijai.

Buvo pasiūlyti nauji SKAR būklės įvertinimo indeksai: pompos vibracijų gaubtinės indeksas ( $Ex$ ), stačiakampių bangų moduluotos gaubtinės indeksas ( $Ex2$ ) ir noradrenalino sukeltų bangų indeksas ( $Mx2$ ). Šie indeksai yra nagrinėjami pirmą kartą.

### **Tyrimo metodai ir įrankiai**

Širdies ir plaučių mašinų pacientai buvo stebimi naudojant „Viasonix 4D“ transkranialinės Doplerio stebėsenos technologiją Lietuvos sveikatos mokslų universiteto Kauno klinikose. Perspektyviojo tyrimo protokolas buvo patvirtintas Kauno regioninio bioetikos komiteto (Leidimas Nr. : BE-2-64, 2021-06-08). Pacientų rašytinis sutikimas buvo gautas vadovaujantis Helsinkio deklaracija (BMJ 1991; 302:1194). Pasiūlytosios metodikos ir technologijos atlikto klinikinio tyrimo registracijos numeris ClinicalTrials.gov Identifikatorius: NCT04943458.

Neuromonitoringo programinė įranga ICM+ (Kembridžas, Didžioji Britanija) buvo naudojama duomenims rinkti.

Prietaisas, skirtas arterinio kraujospūdžio stačiakampio bangos sekai generuoti, buvo sukurtas, Kauno technologijos universitete, Sveikatos telematikos mokslo institute.

Duomenims apdoroti ir statistinei duomenų analizei naudota „MATLAB 2016“ programinė įranga.

## **Rezultatų sklaida**

Pasiekti rezultatai buvo publikuoti dviejuose Q1 žurnaluose, viename Q2 žurnale, pristatyti 6 tarptautinėse konferencijose (iš jų 2 pelnė apdovanojimus) ir pateiktos ES ir JAV patentinės paraiškos.

## **Disertacijos struktūra**

Ši disertacija susideda iš įvado, penkių skyrių, išvados, literatūros šaltinių sąrašo, mokslinių publikacijų sąrašo, konferencijų sąrašo ir patentų sąrašo.

Pirmajame skyriuje disertacijoje aprašomas smegenų kraujotakos autoreguliacijos mechanizmas, skiriant jį į statinę ir dinaminę smegenų kraujotakos autoreguliaciją.

Antrajame skyriuje aprašomos įvairios neuroprotekcijos ir smegenų kraujotakos autoreguliacijos stebėsenos technologijos, optimalios smegenų perfuzijos terapijos metodologija ir ankstesni klinikiniai tyrimai.

Trečiajame skyriuje aprašomas arterinio kraujo srauto bangų generavimas naudojant širdies ir plaučių mašiną.

Ketvirtame skyriuje pateikiama tyrimo medžiaga, aprašomas signalų apdorojimas ir iššūkių bei smegenų kraujotakos autoreguliacijos įvertinimo metodika.

Penktame skyriuje yra aprašomi gauti tyrimo rezultatai.

Disertacija sudaryta iš 117 puslapių, 56 paveikslų, 5 lentelių ir 77 literatūros šaltinių.

## **Mokslinių tyrimų finansavimas**

Projektas finansuojamas Europos regioninio plėtros fondo. Sutarties Nr. 01.2.2-CPVA-K-703-03-0025 „Inovatyvi neinvazinė neuroprotekcijos technologija širdies chirurgijai, neurochirurgijai ir oftalmologijai“.

## **Ginti pristatomi teiginiai**

1. Buvo sukurtas stačiakampio formos bangos kraujo srauto moduliavimo elektroninis prietaisas, kuris geba generuoti fiziologines stačiakampio formos arterinio kraujo spaudimo bangas SKAR būsenai įvertinti.

2. Pasiūlytas stačiakampio bangos manipuliacijos kraujo srauto moduliavimo metodas leidžia įvertinti SKAR būseną ir nustatyti SKAR pažeidimo įvykius su 1–2 minučių vėlavimu.



3. Ilgiausias SKAR sutrikimo epizodas yra susijęs POCD pagal naujai pasiūlytą stačiakampio kraujo srauto moduliacijos metodologiją širdies šuntavimo operacijos metu.

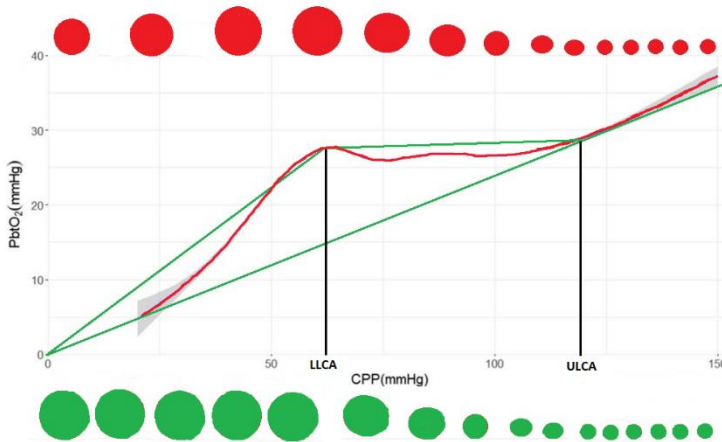
4. Pirmą kartą pastebėta sąsaja tarp kraujo tūkmės ir kraujagyslių pasipriešinimo poveikio stačiakampio formos kraujo srauto bangų sekai bei aukšto dažnio pompos vibracijų, kurios moduliuoja lėtųjų bangų osciliacijas.

## 6.1. SMEGENŲ KRAUJOTAKOS AUTOREGULIACIJOS KONCEPSIJA

Monro-Kelly doktrina teigia, kad galvos kaukolės tūris yra pastovus ir yra sudarytas iš kraujo, smegenų ir likvoro. Vienos komponentės tūrio pokyčiai sukelia kitų komponentių tūrio pokyčius, kad būtų palaikomas pastovus tūris [14]. 1959 m. Nielas Lassenas iliustravo ryšį tarp smegenų kraujo tėkmės (SKT) ir smegenų perfuzijos spaudimo (SPS) [15]. Smegenų perfuzijos spaudimas yra skirtumas tarp vidutinio arterinio spaudimo (AKS) ir vidutinio intrakranijinio spaudimo (IKS) (1):

$$\text{SPS} = \text{AKS} - \text{IKS} \quad (6.1)$$

Laseno kreivė (6.1.1 pav) turi diapazoną, kur smegenų kraujo tekėjimas yra pastovus, ir tai priklauso nuo individualaus paciento smegenų perfuzijos [6]. Ypatingi taškai LLCA – rodo apatinę SKAR ribą ir ULCA rodo viršutinę SKAR ribą. Tarp šių taškų smegenų kraujo tekėjimas išlieka beveik pastovus dėl galimybės valdyti arterinių kraujagyslių diametrą. Galvos smegenų traumą patyrusiems pacientams, sutrikus SKAR, galima pastebėti tiesinę priklausomybę (nėra plokštumos) smegenų kraujo tekėjimui kintant SPS. Taip pat individualiam pacientui plokštumos zona gali būti susiaurėjusi, pasikėlus ar nusileidusi, taip pat paslinkusi į kairę arba dešinę pusę, palyginti su teorine Laseno kreive [77].



**6.1.1 pav.** Teorinė (žalia linija) ir eksperimentinė (raudona linija) Laseno kreivė. Žali skrituliai rodo teorines reakcijas į hidrodinaminis varžos pokyčius smegenų kraujagyslėse kintant SPS. Raudoni skrituliai rodo reakcijas į kintančias hidrodinamines varžas kintant SPS ankstesnio perspektyviojo tyrimo su 77 sunkią galvos traumą patyrusiais pacientais metu (pritaikyta iš [17]). Čia PbtO<sub>2</sub> – smegenų audinio deguonies įtempis, kuris yra tiesiogiai susijęs su smegenų kraujo tekėjimu, LLCA – apatinė SKAR riba, ULCA – viršutinė SKAR riba

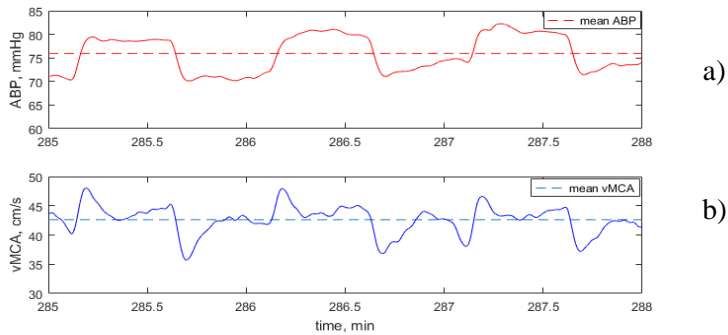
## 6.2. ŠIRDIES IR PLAUČIŲ MAŠINOS REŽIMAI

1953 m. pirmą kartą sėkmingai buvo atlikta širdies operacija naudojant širdies ir plaučių mašiną, ją atliko dr. Gibonas aštuoniolikos metų moteriai [69]. Per širdies šuntavimo operaciją būtina sustabdyti širdį, kad chirurgai galėtų atlikti operaciją. Kol širdis negali aprūpinti kraujo tėkmės, yra naudojama širdies ir plaučių mašina dirbtinai gaminti deguonies prisotintą kraują žmogaus organizmui. Šiuo metu pasaulyje yra 25 tokio tipo aparato gamintojai, ir prognozuojama, kad rinka iki 2022–2027 m. išaugs 195,04 mln. JAV dolerių [70]. Šiame tyrime buvo naudojama „Stocker S5“ širdies ir plaučių mašina, turinti pulsacinį režimą (6.2.1 pav.). Toks aparatas generuoja 3–3,5 Hz dažnio vibracijas nuolatinės kraujo tėkmės režimui palaikyti. Operacijos metu yra galimybė naudoti 4 darbo režimus: nuolatinės tėkmės režimą, pulsacinį režimą, kuris imituoja širdies pulsaciją, ir prof. Armino Ragausko anksčiau aprašytą sinusinės tėkmės režimą [8] bei naują stačiakampio tėkmės režimą. Tokias manipuliacijas galima pasiekti keičiant arterinę kraujo tėkmę širdies ir plaučių aparatu.

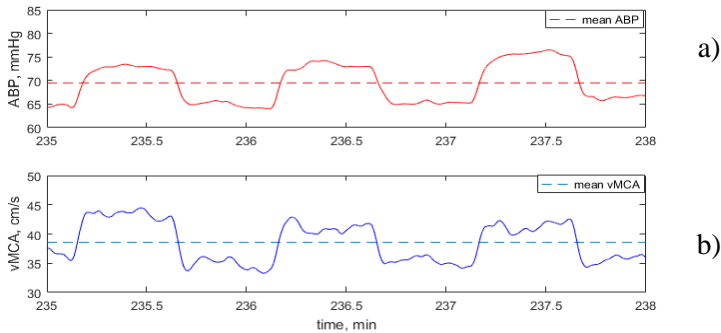


**6.2.1 pav.** Stocker S5 širdies ir plaučių mašina (pritaikyta iš [71])

Stačiakampio tėkmės režimas sukurtas Kauno technologijos universitete, Sveikatos telematikos mokslo institute. Norint sukurti stačiakampio režimą, jis yra suprogramuojamas staigiu kraujo tėkmės pokyčiu  $\pm 10\%$  nuo perfuzionisto nustatyto srauto. Kylančio ir krintančio fronto trukmė yra 1 sekundė. Pasibaigus nustatytam laikui, arterinė kraujo tėkmė vėl keičiama  $\pm 10\%$  iki ankstesnės reikšmės, tokiu būdu generuojant stačiakampę seką (6.2.2 pav. ir 6.2.3 pav.).



**6.2.2 pav.** Stačiakampio formos seka, sugeneruota naudojant širdies ir plaučių mašiną: a) AKS stačiakampio formos bangos, b) pereinamųjų vMCA bangų atsakai į AKS pokyčius, kurie yra siejami su veikiančia SKAR



**6.2.3 pav.** Stačiakampio formos seka, sugeneruota naudojant širdies ir plaučių mašiną: a) AKS stačiakampio formos bangos, b) pereinamųjų vMCA bangų atsakai į AKS pokyčius, kurie yra siejami su sutrikusia SKAR.

Šis įrenginys turi JAV (patentinės paraiškos numeris 17/683,943) ir ES (patentinės paraiškos numeris EP22160563) patentines paraiškas. Prietaisas lengvai pritvirtinamas prie Stockert S5“ širdies ir plaučių aparato be integracijos į patį įrenginį. Įrenginyje yra 2 mygtukai, skirti pagrindinei kraujo tėkmei nustatyti bei nustatyti +10 % nuo pagrindinės kraujo tėkmės. Pasirinktomis reikšmėmis nustatytoje programoje įrenginys keičia kraujo tėkmę į 10 % pokytį nuo pradinės reikšmės (6.2.4 pav.).

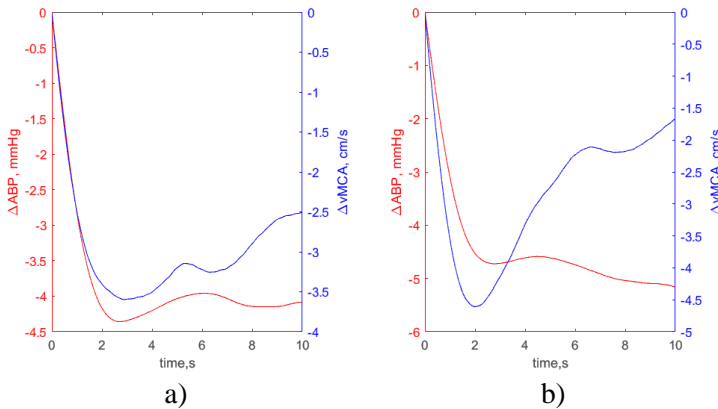


**6.2.4 pav.** Patentuojamas prietaisas moduliuoti stačiakampes bangas Stocker S5 širdies ir plaučių mašinai, keičiant kraujo srautą

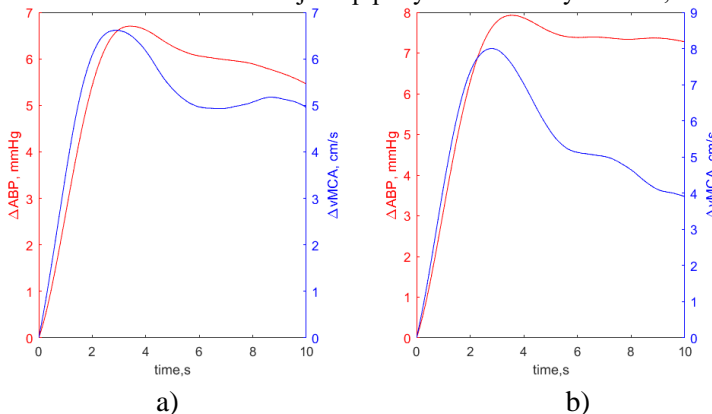
## 6.3. SMEGENŲ KRAUJOTAKOS AUTOREGULIACIJOS ĮVERTINIMAS

### 6.3.1. Pereinamųjų funkcijų indeksas (TFx)

Norint greitai nustatyti smegenų kraujotakos autoreguliacijos būklę yra vertinamos pirmos 15 sekundžių fronto pradžios. Pirmų 5 arba 6 sekundžių pradžioje SKAR pradeda atkurti ankstesnį kraujo tėkmės lygį, o vėliau vyksta pereinamieji procesai. Koreliacinis koeficientas tarp AKS ir vMCA yra metodas nustatyti SKAR būklę. Jei SKAR yra veikianti, koreliacinis koeficientas turėtų būti mažesnis nei pažeistos (6.3.1 pav. ir 6.3.2 pav.).

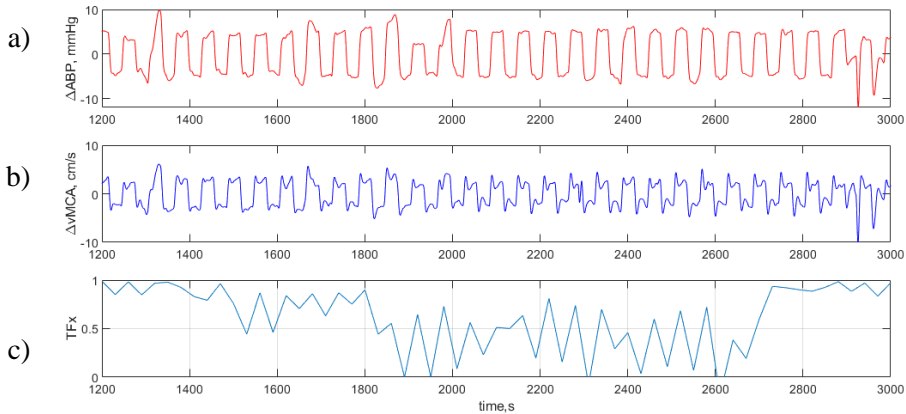


**6.3.1 pav.** Pereinamosios funkcijos atsakas (mėlyna spalva) į krentantį AKS frontą (raudona spalva): a) sutrikusios SKAR koreliacija tarp pokyčio ir atsako yra  $R = 0,89$ , b) veikiančios SKAR koreliacija tarp pokyčio ir atsako yra  $R = 0,16$



**6.3.2 pav.** Pereinamosios funkcijos (mėlyna spalva) atsakas į kylantį AKS frontą (raudona spalva): a) sutrikusios SKAR koreliacija tarp pokyčio ir atsako yra  $R = 0,91$ , b) veikiančios SKAR koreliacija tarp pokyčio ir atsako yra  $R = 0,64$

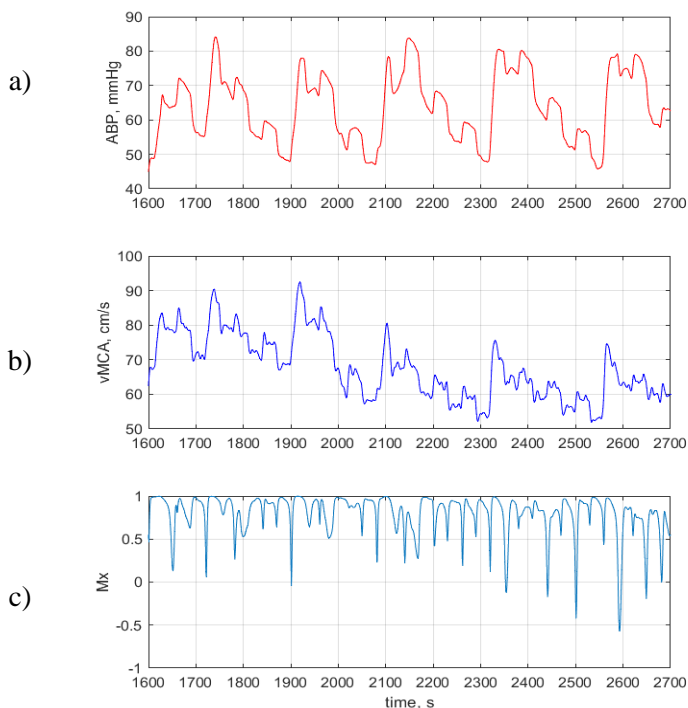
Norint nustatyti ribą tarp pažeistos ir nepažeistos SKAR, buvo įvertintos 13 pacientų 500 skirtingų reakcijų. Šiuo metu yra sunku nustatyti, kaip smegenų kraujotakos autoreguliacija tinkamai veikia su skirtingais  $TFx$  rezultatais. Be to, artefaktai ir triukšmas iškreipia reakcijų formą, kurią sunku interpretuoti. Subjektyviai įvertinus kiekvieną  $TFx$  pavyzdį, nustatyta, kad nepažeistos SKAR vidurkis yra 0,63, o pažeistos – 0,89. Tarp 0,63 ir 0,89 yra neapibrėžties zona. Šiame tyrime bus pasirinkta riba 0,7, kuri nustato, ar SKAR yra pažeista, ar nepažeista.



**6.3.3 pav.**  $TFx$  įvertinimas realiu laiku: a) AKS(t) signalas, b) vCMA(t) signalas, c)  $TFx$  įvertinimas. Juoda spalva rodo ilgiausią SKAR sutrikimo epizodą

### 6.3.2. Vidutinės tėkmės indeksas ( $Mx$ )

Vidutinės tėkmės indekso ( $Mx$ ) analizei AKS ir vMCA signalai buvo filtruojami su žemo dažnio 0,1 Hz pjūvio dažnio Batervorto filtru. Pearsono koreliacijos koeficientas buvo skaičiuojama 30 sekundžių lange dėl impulso trukmės. Nepažeistos SKAR slenkstis yra  $Mx < 0,4$ , o pažeistos SKAR slenkstis yra  $Mx > 0,4$  [74]. Pagrindinė šio metodo problema yra tai, kad jis dažniausiai rodo sutrikusią SKAR (6.3.4 pav.). Esantys tyrimai parodė, kad vazopresoriai nesukelia SKAR pažeidimo [75].  $Mx$  signalo skaičiavimo vėlavimas susideda iš 10 sekundžių žemo dažnio filtro vėlavimo ir 30 sekundžių slenkančio koreliacijos koeficiento lango skaičiavimo ir sudaro bendrą 40 sekundžių vėlavimą.

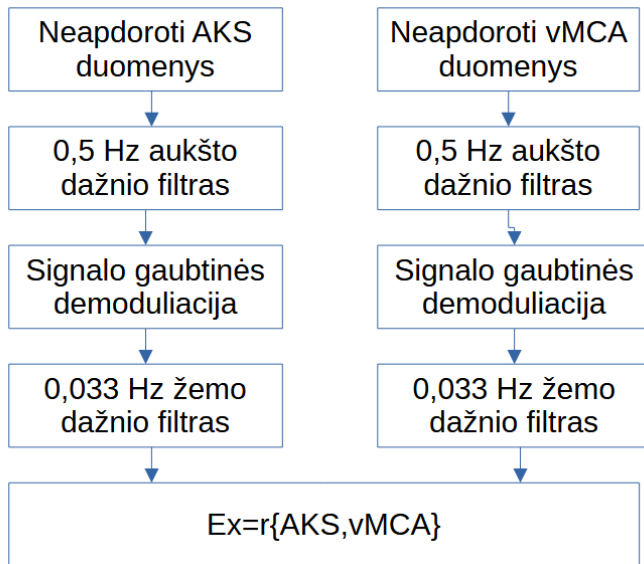


**6.3.4 pav.**  $M_x$  koeficiento skaičiavimas. a) AKS(t) signalas, b) vMCA(t) signalas, c)  $M_x(t)$  duomenys

### 6.3.3. Širdies ir plaučių mašinos vibracijų gaubtinės generuojamų lėtųjų bangų indeksas ( $E_x$ )

Signalų skaidymo metu pastebėta, kad širdies ir plaučių mašinos 3 Hz vibracijos moduliuoja lėtąsias bangas dėl kraujagyslių pasipriešinimo AKS manipuliacijų metu. Tai galima apibūdinti kaip Omo dėsnį [21]. Suleistas noradrenalinas sutraukia kraujagysles ir taip padidina AKS pompos amplitudę. Noradrenalinas pradeda prarasti savo poveikį ir po 1–5 minučių jis grįžta į ankstesnę AKS vertę. Per šį laiką kraujagyslės pradeda plėstis ir taip mažina savo amplitudę. Signalui filtruoti buvo naudojamas trečios eilės aukšto dažnio Batervorto filtras su 0,5 Hz pjūvio dažniu. Po to buvo taikoma signalo gaubtinės demoduliacija ir, naudojant trečios eilės žemo dažnio Batervorto filtrą su 0,03 Hz pjūvio dažniu, buvo apskaičiuotas tarp AKS ir vMCA vibracijų gaubtinių reaktyvumo indeksas ( $E_x$ ). Algoritmas pateiktas 6.3.5 pav.

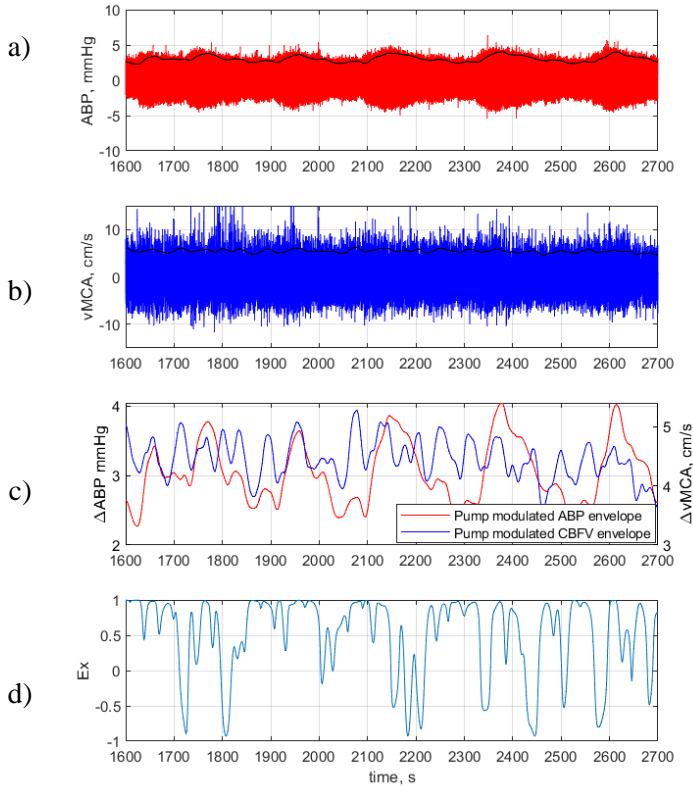




6.3.5 pav.  $Ex$  indekso įvertinimo algoritmas

Šis koeficientas turi dar nežinomas savybes, nes anksčiau jis niekada nebuvo nagrinėtas. Jis yra apskaičiuojamas tarp lėtų AKS ir vMCA moduluotų gaubtinės bangų. Norint nustatyti diagnostinę  $Ex$  ribą, buvo naudojamas  $\chi^2$  testas ribų reikšmėms tarp 0 ir 1. Jautriausia reikšmė buvo nustatyta kaip  $Ex = 0,68$  ( $\chi^2 = 7,18$ ,  $p = 0,008$ ). Nustatyta reikšmė bus naudojama analizei, laikant  $Ex < 0,68$  kaip nepažeistą SKAR ir  $Ex > 0,68$  kaip pažeistą SKAR. Dėl lėtų bangų ir kraujo tėkmės greičio artimiausias indeksas yra  $Mx$ .

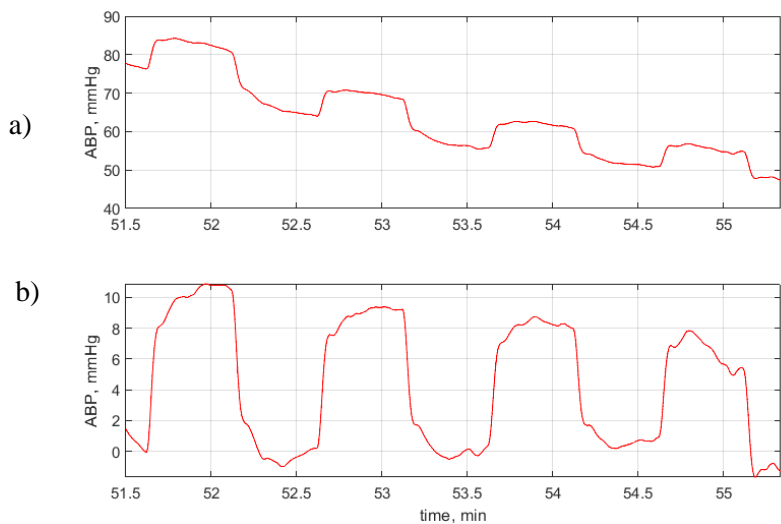
Siurblys sukuria 3 Hz ir 10 mmHg AKS amplitudės bangas ir 20 cm/s vMCA bangų amplitudes. vMCA bangų gaubtinė yra simetriška ir turi apie 30–50 sekundžių trukmės periodą, ją galima laikyti lėtą bangą. Taip pat dėl noradrenalino AKS bangos frontas sparčiai kyla ir leidžiasi lėtai. AKS bangų gaubtinės amplitudė yra 1–2 mmHg, o vMCA yra 1–2 cm/s. Tokios bangos turi daug mažesnę amplitudę, palyginti su dideliais AKS ir vMCA pokyčiais, skaičiuojant  $Mx$  indeksą (6.3.6 pav.).  $Ex$  vėlavimas sudaro 0,5 sekundės aukšto dažnio filtro vėlavimą, signalo gaubtinės demoduliacijos vėlavimą (nežinoma realiuoju laiku), 30 sekundžių žemo dažnio filtro vėlavimą ir 30 sekundžių slenkančio koreliacijos koeficiento vėlavimą, kur iš viso sudaro 60,5 sekundžių vėlavimą.



**6.3.6 pav.** DKA mašinos moduluotų bangų dekompozicija: a) pompos AKS(t) moduluota gaubtinė, b) vMCA(t) pompos moduluota gaubtinė, c) palyginimas tarp ABP(t) ir vMCA(t) pompos moduluotų gaubtinių, d)  $Ex(t)$  duomenys

### 3.4 6.3.4. Stačiakampių bangų gaubtinės indeksas ( $Ex2$ )

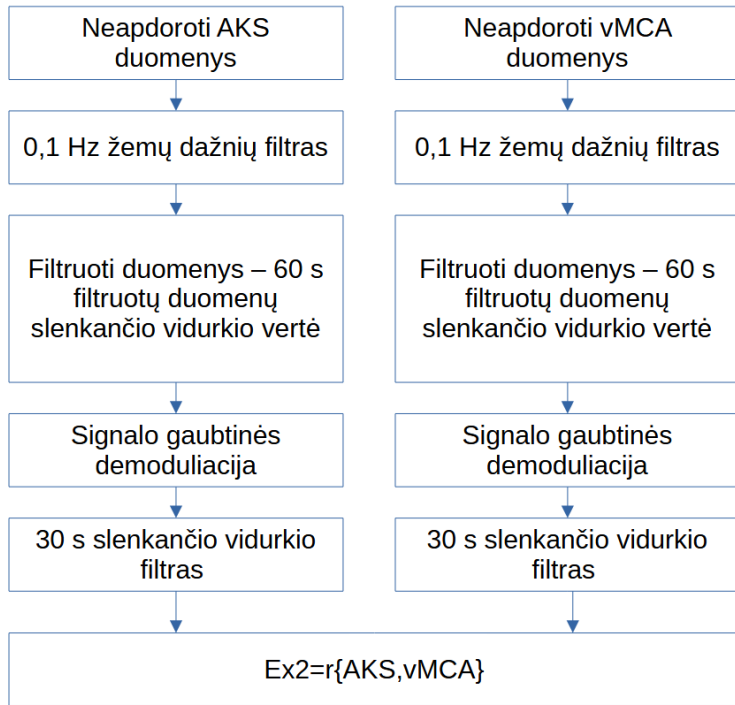
Signalų dekompozicijos metu pastebėta, kad stačiakampio signalo amplitudė kinta suleidus noradrenalino. Tai įvyksta dėl noradrenalino poveikio kraujagyslių pasipriešinimui ir kraujo srauto pokyčiams paciento kūne. Tai galima prilyginti Omo dėsnui. Stačiakampių bangų amplitudė didėja suleidus didesnę noradrenalino kiekį. Po 30 sekundžių noradrenalinas pradeda prarasti savo poveikį, dėl to kraujagyslės plečiasi, o širdies plaučių mašina mažina srautą. Tai gali lemti krantinčio fronto sumažėjimą iki daugiau nei 20 mmHg. Tokiu ciklu stačiakampio AKS amplitudė keičiasi kiekvieną kartą suleidus noradrenalino (6.3.7 pav.).



**6.3.7 pav.** Stačiakampio formos bangos amplitudės pokyčiai suleidžiant noradrenalino: a) stačiakampių bangų seka suleidus noradrenalino, b) stačiakampių seka pašalinus žemo dažnio komponentę

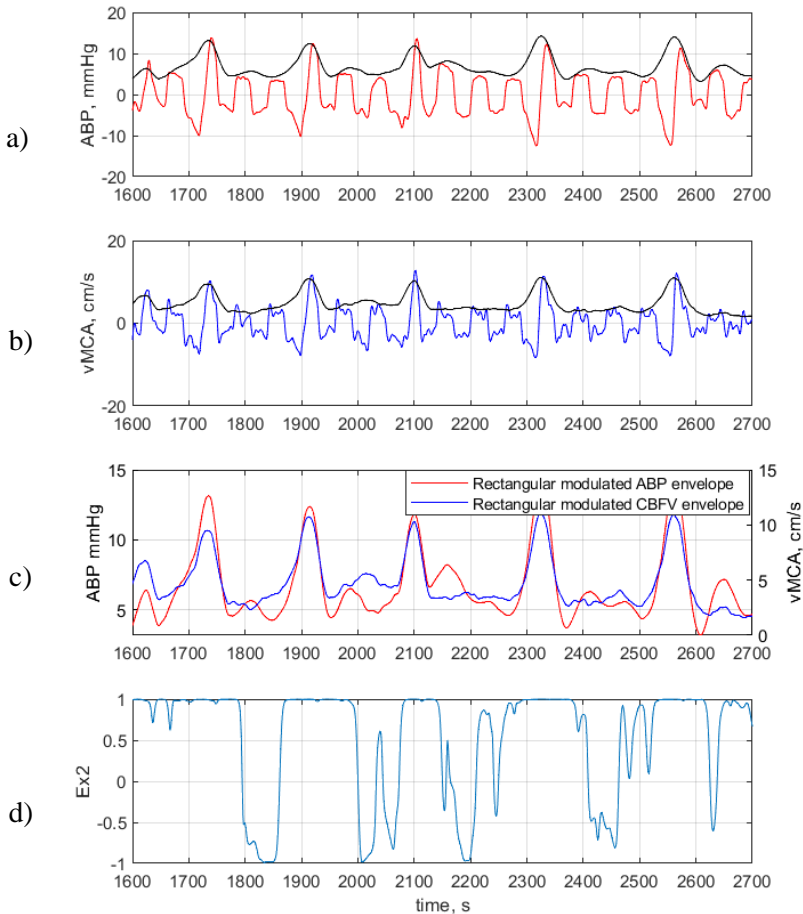
Stačiakampio kraujo srauto bangos amplitudė kinta netiesiškai. Didėjant vidutiniam AKS, amplitudės impulsas pradeda didėti. Tai gali būti priežastis, kad noradrenalino banga nėra tiesinė. Taip pat tai gali priklausyti nuo žmogaus svorio ir skysčių tūrio. Impulsų amplitudžių vidurkis yra  $10 \text{ mmHg} \pm 4,2 \text{ mmHg}$ . Koreliacija tarp impulsų amplitudės ir vidutinio ABP yra silpna ( $R = 0,22$ ). Tai rodo, kad amplitudė nėra stabili ir reikalauja stabilizavimo, nes SKAR yra apibūdinama kaip tiesinė sistema, o vidutinė  $10 \text{ mmHg}$  amplitudė yra mažesnė nei fiziologinės AKS(t) pulsinės bangos.

Šis koeficientas turi dar nežinomas savybes, panašiai kaip  $Ex$ , nes jis niekada anksčiau nebuvo tirtas. Jis skaičiuojamas tarp AKS ir vMCA stačiakampio gaubtinių moduluotų bangų. Šis indeksas taip pat pagrįstas lėtosiomis bangomis ir Doplerio signalu, tad artimiausias indeksas yra  $Mx$ . Klasifikacija grindžiama  $Mx$ , laikoma, kad jei  $Ex2 > 0,6$ , tai rodo sutrikusią SKAR, o jei  $Ex < 0,6$ , tai rodo veikiančią SKAR. Šis metodas yra jautresnis nei  $Mx$  ir turi mažiau svyravimų, palyginti su siurblio sukeltu  $Ex$  indeksu.  $Ex2$  vėlavimas susideda iš 10 sekundžių žemo dažnio filtro vėlavimo, 60 sekundžių žemų dažnio komponentių pašalinimo, signalo gaubtinės demoduliacijos vėlavimo (nežinomo realiuoju metu), 30 sekundžių žemo dažnio filtro vėlavimo ir 30 sekundžių slenkančio koreliacijos koeficiento vėlavimo. Iš viso tai sudaro 130 sekundžių vėlavimą (6.3.9 pav.).



**6.3.9 pav.** Ex2 skaičiavimo algoritmas

Stačiakampio gaubtinės amplitudė kinta apie 8 mmHg AKS ir 10 cm/s vMCA. Tokių bangų periodo yra nestacionarus ir svyruoja apie 200 sekundžių, nes jis priklauso nuo noradrenalino. Tokios bangos turi aštrias viršūnes dėl noradrenalino injekcijos ir lėtai besileidžiančio neigiamo fronto (6.3.10 pav.).

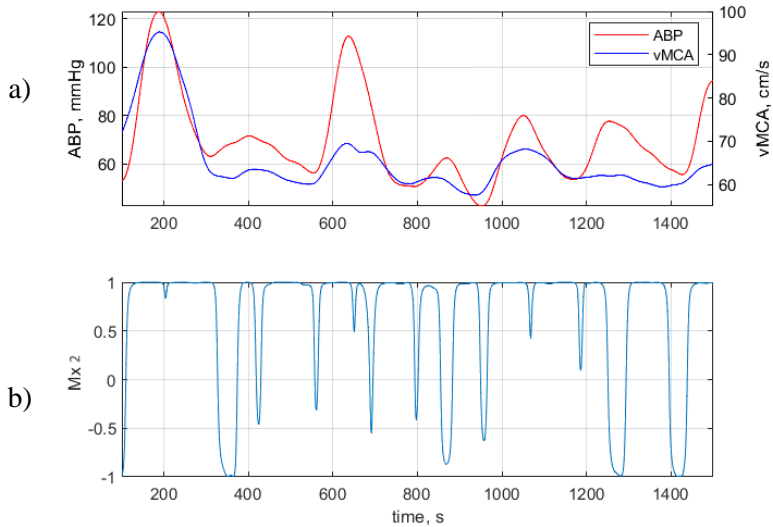


**6.3.10 pav.** Stačiakampio formos bangos gaubtinės: a) AKS(t) stačiakampio formos bangos moduluota gaubtinė, b) vMCA(t) stačiakampio formos bangos moduluota gaubtinė, c) palyginimas tarp AKS(t) ir vMCA(t) stačiakampių gaubtinių, d)  $Ex2(t)$  reaktyvumo indeksas

### 6.3.5. Noradrenalino sukeltų lėtųjų bangų indeksas ( $Mx2$ )

Per širdies šuntavimo operacijas AKS pakelti yra naudojamas noradrenalinas. Filtruojant signalą trečios eilės Buttervorto filtru, kurio pjūvio dažnis yra 6,7 mHz, buvo išskirta noradrenalino banga, išfiltruojant pompos vibracijas ir stačiakampio formos komponentus. Noradrenalino sukeltamų bangų trukmė paprastai būna 2–5 minutės. Ją valdo širdies ir plaučių mašinos operatorius, kuris nusprendžia suleisti noradrenalino dozę. Pastebėta, kad, pasiekus tam tikrą AKS reikšmę, vMCA pradeda užsiritoti ir vietoj aštraus impulso bangos ji tampa buka, kas gali būti siejama su SKAR viršutine riba. Taip pat pastebėta, kad kai AKS pasiekia tam tikrą reikšmę, FV pradeda didėti. Tai gali būti siejama su SKAR apatine riba (6.3.11 pav.). Tačiau visos operacijos yra skirtingos, kai kurios reikalauja dažnų noradrenalino suleidimo, kitos

reikalauja vos kelių, o tokiais atvejais AKS turi mažą variabilumą.  $Mx2$  vėlinimas sudaro žemo dažnio filtro 150 sekundžių vėlavimą ir slenkančio koreliacijos koeficiento vėlavimą, iš viso bendrą 180 sekundžių vėlavimą.

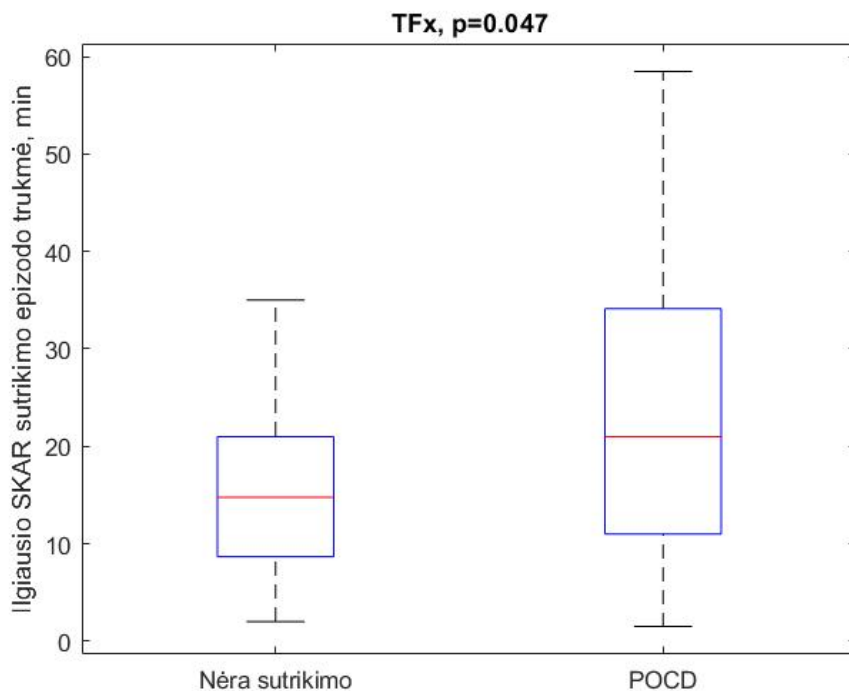


**6.3.11 pav.** Noradrenalino sukeltos bangos: a) raudona spalva yra AKS(t), mėlyna vMCA(t). Kai AKS viršija 110 mmHg, vMCA banga tampa aštri. Kitais atvejais vMCA banga yra suapvalinta, b)  $Mx2$  skaičiavimas iš lėtųjų noradrenalino bangų

## 6.4.REZULTATAI

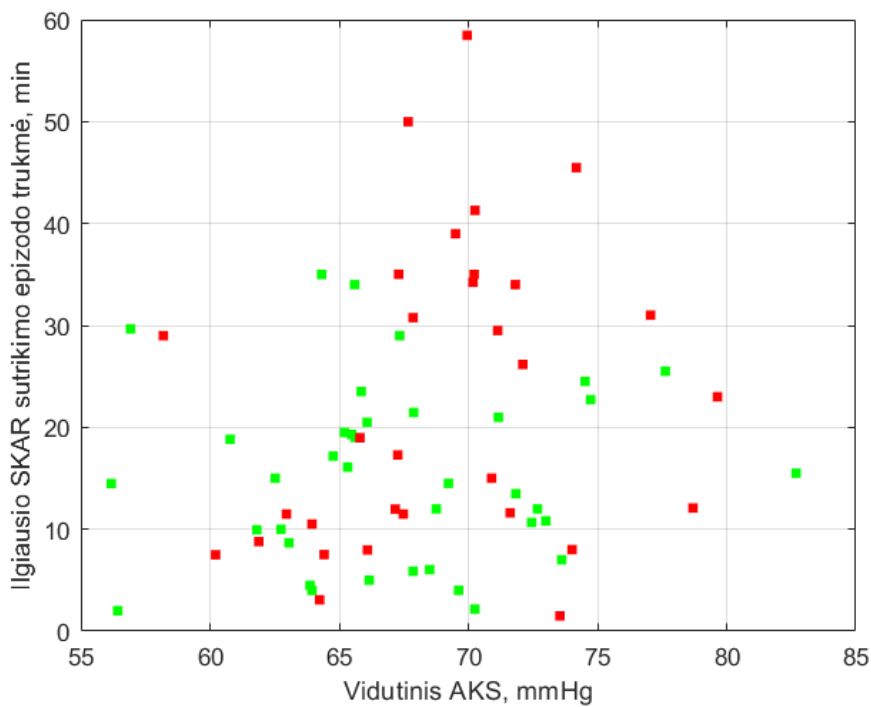
### 6.4.1 *TFx*

Pacientai abiejose grupėse patyrė SKAR sutrikimus. Ilgiausio SKAR sutrikimo epizodo trukmės asociacija tarp nepatyrusių kognityvinio sutrikimo ir POCD grupės yra statistiškai reikšminga ( $p = 0,047$ ). Medianinė ilgiausio SKAR sutrikimo trukmė nepatyrusių kognityvinių sutrikimų grupėje yra 14,75 minutės, POCD grupės medianinė vertė yra 20,98 minutės (6.4.1 pav.).



**6.4.1.** Asociacija tarp ilgiausio SKAR sutrikimo epizodo trukmės tarp POCD ir neturinčių kognityvinio sutrikimo grupių, naudojant SKAR būsenos indeksą *TFx*. Statistiškai reikšmingas skirtumas yra rastas ( $p = 0,047$ ) tarp dviejų grupių

Ilgiausias SKAR sutrikimo epizodas įvyko ties 55–85 vidutiniu AKS.. Nėra aiškių hipoperfuzijos ar hiperperfuzijos atvejų, siejamų su POCD, nes ilgiausias SKAR sutrikimo epizodas varijuoja iki 60 minučių ir dėl to labai susividurkina reikšmė (6.4.2 pav.).

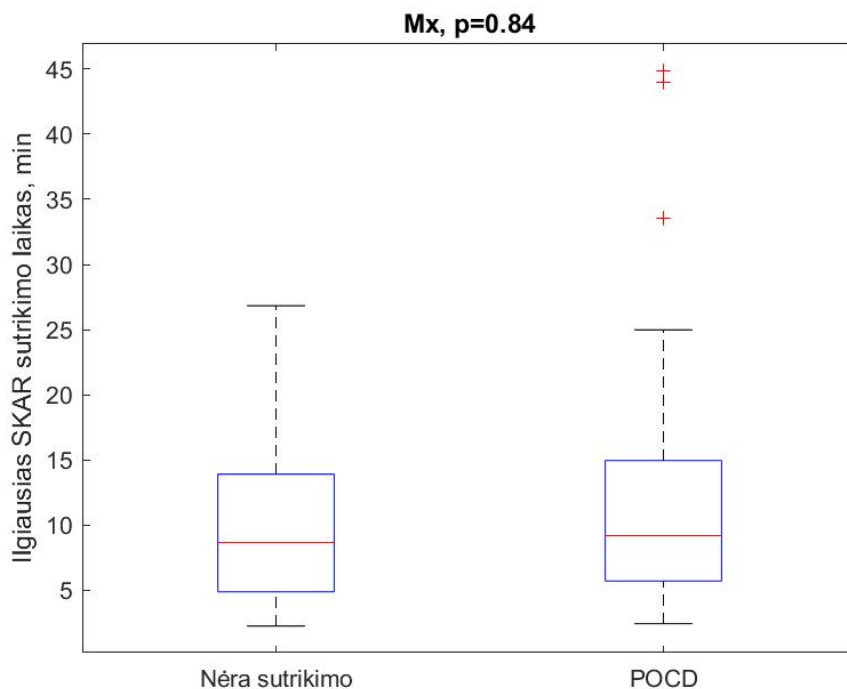


**6.4.2 pav.** Pasiskirstymas tarp vidutinio AKS ilgiausio SKAR sutrikimo epizode naudojant SKAR būsenos identifikavimo indeksą  $TFx$ . Žalia spalva rodo atvejus, kai nebuvo kognityvinio sutrikimo, raudona spalva rodo atvejus įvykus POCD

#### 6.4.2 Mx

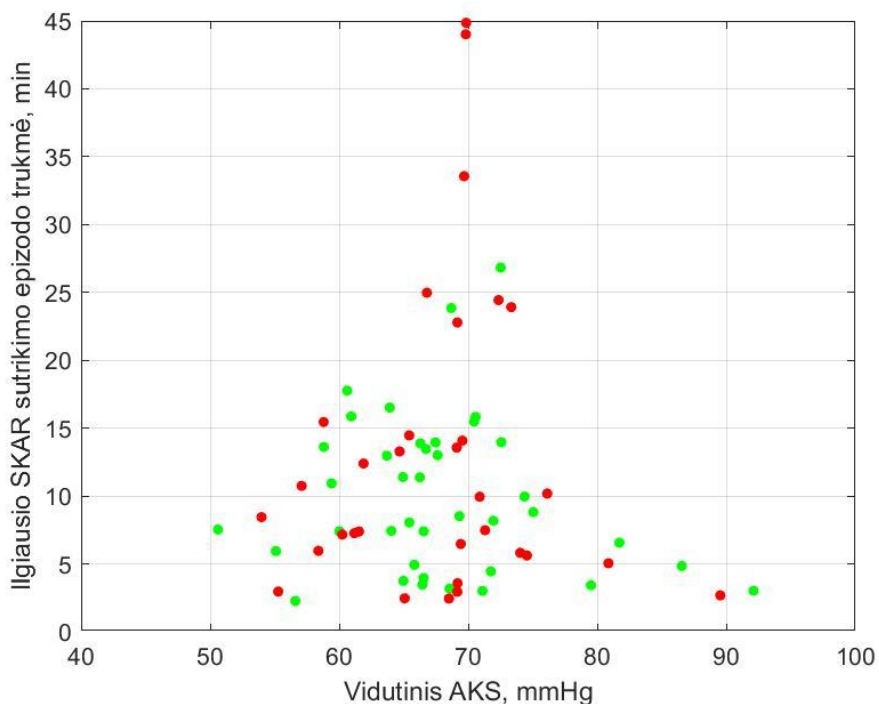
Pacientai abiejose grupėse patyrė SKAR sutrikimus. Ilgiausio SKAR sutrikimo epizodo trukmės asociacija tarp nepatyrusių kognityvinio sutrikimo ir POCD grupės yra statistiškai nereikšminga ( $p = 0,84$ ). Medianinė ilgiausio SKAR sutrikimo trukmė nepatyrusių kognityvinių sutrikimų grupėje yra 8,67 minutės, POCD grupės medianinė vertė yra 9,20 minutės (6.4.3 pav.). Grupės gali persidengti dėl žemo dažnio noradrenalino komponentės, kuri suteikia mažą jautrumą  $Mx$ .





**6.4.3 pav.** Asociacija tarp ilgiausio SKAR sutrikimo epizodo trukmės tarp POCD ir neturinčių kognityvinio sutrikimo grupių, naudojant SKAR būsenos indeksą  $Mx$ . Statistiškai reikšmingo skirtumo nerasta ( $p = 0,84$ ) tarp dviejų grupių

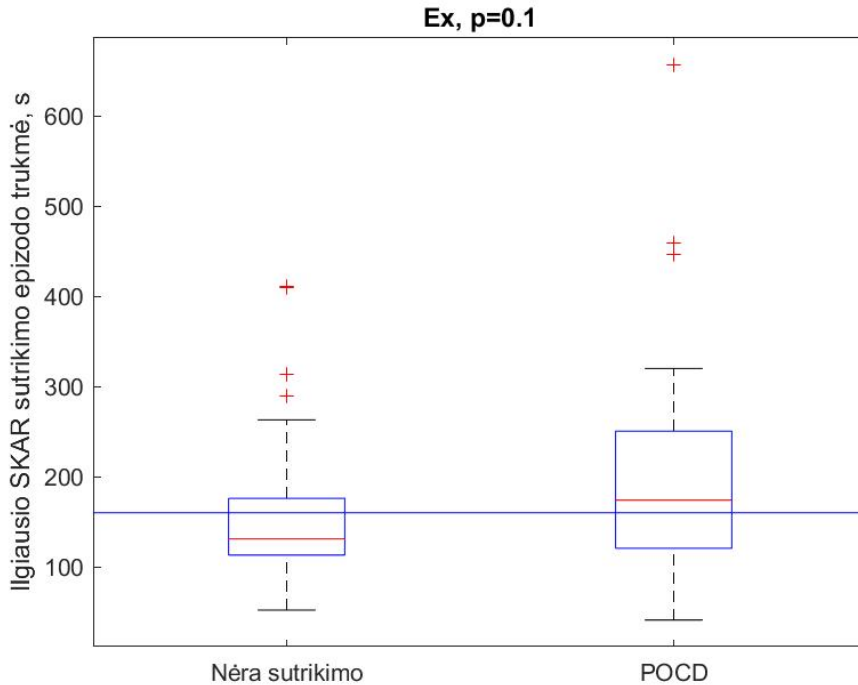
Ilgiausias SKAR sutrikimo epizodas įvyko ties 50–95 vidutinio AKS riba. Nėra aiškių hipoperfuzijos ar hiperperfuzijos atvejų, siejamų su POCD, nes ilgiausias SKAR sutrikimo epizodas varijuoja iki 60 minučių, dėl ko labai susividurkina reikšmė (6.4.4 pav.).



**6.4.4 pav.** Pasiskirstymas tarp vidutinio AKS ilgiausio SKAR sutrikimo epizode naudojant SKAR būsenos identifikavimo indeksą  $TFx$ . Žalia spalva rodo atvejus, kai nebuvo kognityvinio sutrikimo, raudona spalva rodo atvejus įvykus POCD

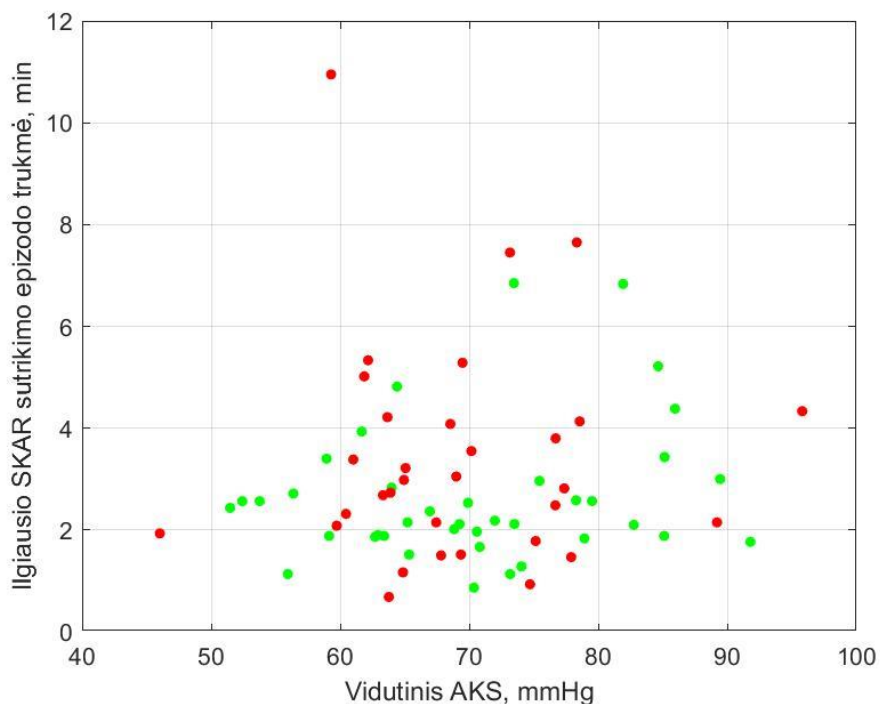
### 6.4.3 Ex

Pacientai abiejose grupėse patyrė SKAR sutrikimus. Ilgiausio SKAR sutrikimo epizodo trukmės asociacija tarp nepatyrusių kognityvinio sutrikimo ir POCD grupės yra statistškai nereikšminga ( $p = 0,10$ ). Medianinė ilgiausio SKAR sutrikimo trukmė nepatyrusių kognityvinių sutrikimų grupėje yra 2,28 minutės, POCD grupės medianinė vertė yra 2,90 minutės. Šie rezultatai siejasi su ankstesniu tyrimu (6.4.5 pav.). Slenkstis, skiriantis abi grupes, yra 160 sekundžių ( $\chi^2 = 5,20$ ,  $p = 0,022$ ).



**6.4.5 pav.** Asociacija tarp ilgiausio SKAR sutrikimo epizodo trukmės tarp POCD ir neturinčių kognityvinio sutrikimo grupių, naudojant SKAR būsenos indeksą *Ex*. Statistiškai reikšmingo skirtumo nerasta ( $p = 0,10$ ) tarp dviejų grupių. Mėlyna linija yra slenkstis, skiriantis 2 grupes, jis yra lygus 160 s ( $\chi^2 = 8,50$ ,  $p = 0,004$ ).

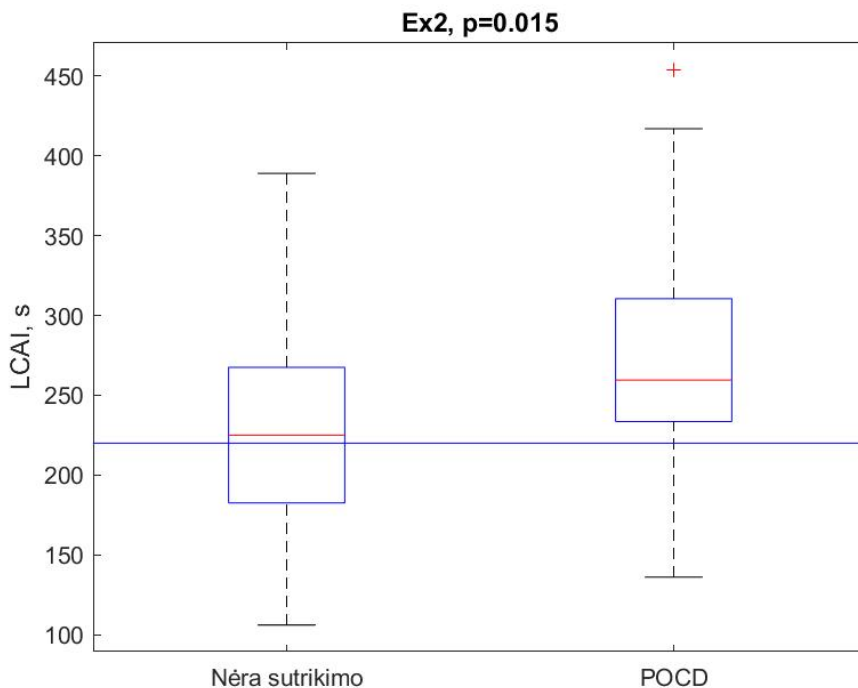
Ilgiausias SKAR sutrikimo epizodas įvyko ties 45–100 vidutinio AKS riba. Yra vienas atvejis, kai POCD galimai įvyko dėl hipoperfuzijos ties vidutiniu AKS 45 mmHg, ir 2 atvejai, kai POCD galimai įvyko ties 90 mmHg AKS dėl hiperperfuzijos. Kiti POCD atvejai gali būti siejami su per ilgu SKAR sutrikimu (6.4.6 pav.).



**6.4.6 pav.** Pasiskirstymas tarp vidutinio AKS ilgiausio SKAR sutrikimo epizode naudojant SKAR būsenos identifikavimo indeksą *Ex*. Žalia spalva rodo atvejus, kai nebuvo kognityvinio sutrikimo, raudona spalva rodo atvejus įvykus POCD

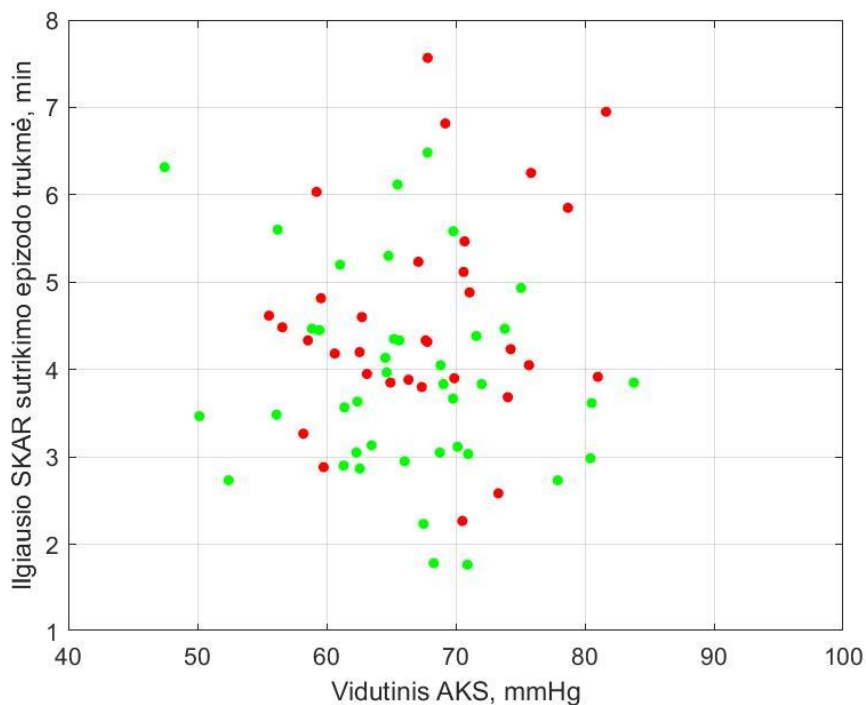
#### 6.4.4 *Ex2*

Pacientai abiejose grupėse patyrė SKAR sutrikimus. Ilgiausio SKAR sutrikimo epizodo trukmės asociacija tarp nepatyrusių kognityvinio sutrikimo ir POCD grupės yra statistiškai reikšminga ( $p = 0,015$ ). Medianinė ilgiausio SKAR sutrikimo trukmė nepatyrusių kognityvinių sutrikimų grupėje yra 3,75 minutės, POCD grupėje medianinė vertė yra 4,33 minutės, kas yra statistiškai reikšminga, tačiau šie rezultatai siejasi su ankstesniu tyrimu (6.4.7 pav.). Slenkstis, skiriantis abi grupes, yra 220 s ( $\chi^2 = 11,54$ ,  $p = 0,001$ ).



**6.4.7 pav.** Asociacija tarp ilgiausio SKAR sutrikimo epizodo trukmės tarp POCD ir neturinčių kognityvinio sutrikimo grupių, naudojant SKAR būsenos identifikavimo indeksą *Ex2*. Statistiškai reikšmingas skirtumas yra rastas ( $p = 0,015$ ) tarp dviejų grupių. Mėlyna linija yra slenkstis, skiriantis 2 grupes, jis yra lygus 220 s ( $\chi^2 = 11,54, p = 0,001$ )

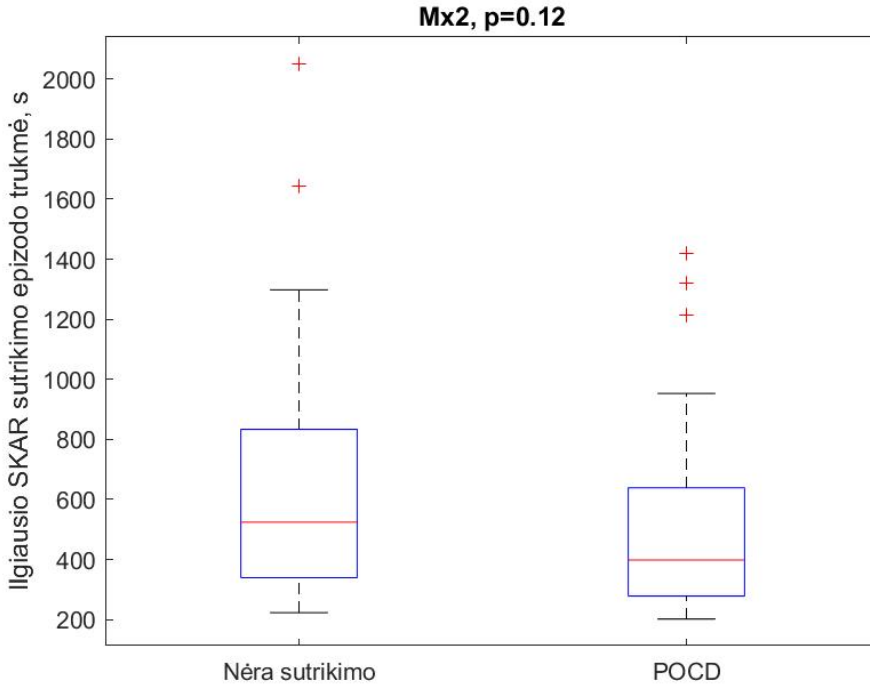
Ilgiausias SKAR sutrikimo epizodas įvyko ties 45–90 vidutinio AKS riba. Nėra hipoperfuzijos ar hiperperfuzijos atvejų, siejamų su POCD. Vis dėlto ilgesnis nei 4 minutės SKAR sutrikimo laikas yra siejamas su POCD, nepaisant vidutinio arterinio kraujospūdžio SKAR sutrikimo metu (6.4.8 pav.).



**6.4.8 pav.** Pasiskirstymas tarp vidutinio AKS ilgiausio SKAR sutrikimo epizode naudojant SKAR būsenos identifikavimo indeksą *Ex2*. Žalia spalva rodo atvejus, kai nebuvo kognityvinio sutrikimo, raudona spalva rodo atvejus įvykus POCD

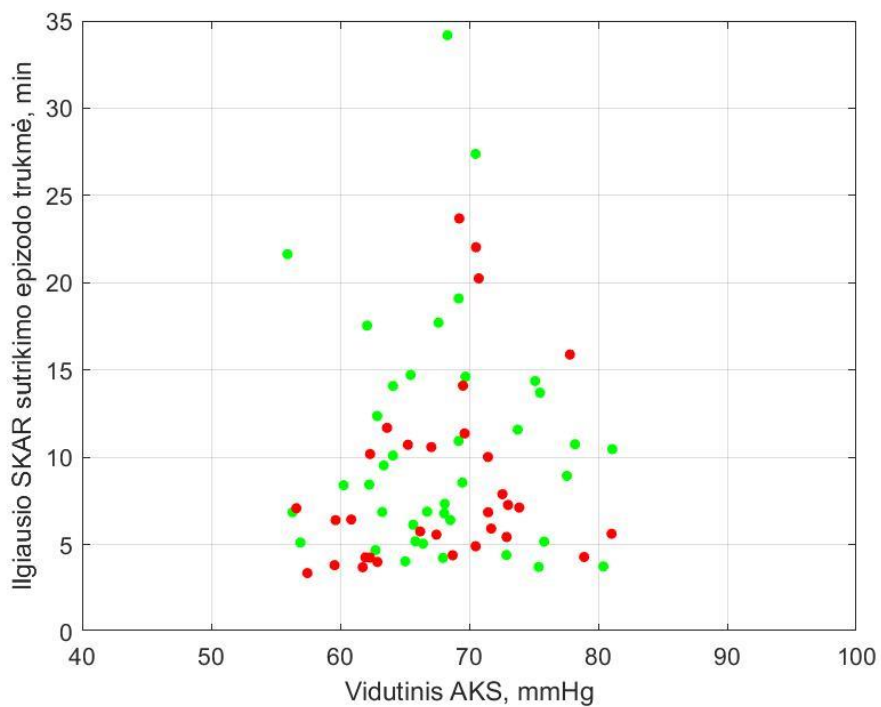
#### 6.4.5 *Mx2*

Pacientai abiejose grupėse patyrė SKAR sutrikimus. Ilgiausio SKAR sutrikimo epizodo trukmės asociacija tarp nepatyrusių kognityvinio sutrikimo ir POCD grupės yra statistiškai reikšminga ( $p = 0,12$ ). Medianinė ilgiausio SKAR sutrikimo trukmė nepatyrusių kognityvinių sutrikimų grupėje yra 8,74 minutės, POCD grupėje medianinė vertė yra 6,64 minutės (6.4.9 pav.).



**6.4.9 pav.** Asociacija tarp ilgiausio SKAR sutrikimo epizodo trukmės tarp POCD ir neturinčių kognityvinio sutrikimo grupių, naudojant SKAR būsenos identifikavimo indeksą *Mx2*. Statistiškai reikšmingas skirtumas yra rastas ( $p = 0,12$ ) tarp dviejų grupių

Ilgiausias SKAR sutrikimo epizodas įvyko ties 55–85 vidutinio AKS riba. Nėra hipoperfuzijos ar hiperperfuzijos atvejų, siejamų su POCD. Šis indeksas yra panašus į *Mx* indeksą, nes ilgiausias SKAR sutrikimas varijuoja iki 35 minučių. Tai gali būti dėl mažo variabilumo, kurį pašalina žemo dažnio filtras (6.4.8 pav.).



**6.4.10 pav.** Pasiskirstymas tarp vidutinio AKS ilgiausio SKAR sutrikimo epizode naudojant SKAR būsenos identifikavimo indeksą  $Mx2$ . Žalia spalva rodo atvejus, kai nebuvo kognityvinio sutrikimo, raudona spalva rodo atvejus įvykus POCD



## BENDROSIOS IŠVADOS

1. Literatūros apžvalga parodė, kad šiuo metu nėra technologijų, leidžiančių nustatyti SKAR pažeidimus per reikiamą laiką mažiau nei minutė ir apsaugoti smegenis nuo kognityvinių sutrikimų dėl hipoperfuzijos ar hiperperfuzijos epizodų kardiochirurgijos metu.
2. Artima realaus laiko technologija buvo pasiūlyta ir kliniškai validuota SKAR sutrikimo pradžiai nustatyti. Sukurta technologija generuoja stačiakampio formos kraujo srauto bangas naudojant širdies ir plaučių mašiną su norimu periodu. Pasiūlyta technologija, kuri generuoja arterinio kraujo srauto stačiakampio formos bangas, leidžia įvertinti SKAR sistemos būklę stebint pereinamuosius procesus į arterinio kraujospūdžio kylančius ir krintančius frontus su 30 s ar geresne laikine skyra.
3. Buvo pasiūlyti naujai išvesti SKAR būsenos indentifikavimo indeksai: pompos vibracijų gaubtinės indeksas  $Ex$ , stačiakampių bangų gaubtinės indeksas  $Ex2$  ir noradrenalino sukeltų bangų indeksas  $Mx2$  bei pereinamųjų funkcijų indeksas  $TFx$ , kuris yra paremtas realaus laiko analize į smegenų kraujotakos greičio atsaką į kylantį ar krintantį arterinio kraujospūdžio suformuotą stačiakampio frontą. Kritinis slenkstis, esantis daugiau nei  $TFx$  reikšmė 0,7, buvo nustatytas esant sutrikusiai SKAR būklei ir buvo naudojamas kaip indikatorius SKAR sutrikimo momento epizodams nustatyti.
4. Nustatyti faktoriai, darantys įtaką paciento baigčiai po kardiochirurginės operacijos, yra amžius ( $p = 0,175$ ) ir išsilavinimo metai ( $p = 0,029$ ). Vis dėlto ilgiausias SKAR sutrikimo epizodo laikas, nustatytas su mūsų pasiūlytais indeksais, yra statistiškai reikšmingai siejamas su POCD ( $Ex2$   $p = 0,015$  ir  $p = 0,047$   $TFx$ ). Tai patvirtina išvadą, jog ilgiausias SKAR sutrikimo epizodas turi stipriausią ryšį su paciento klinikiškai baigtimi.

## REFERENCES

- [1] U. Ralapanawa and R. Sivakanesan, "Epidemiology and the Magnitude of Coronary Artery Disease and Acute Coronary Syndrome: A Narrative Review," *J Epidemiol Glob Health*, vol. 11, no. 2, pp. 169–177, Jun. 2021, doi: 10.2991/JEGH.K.201217.001.
- [2] "Cardiovascular diseases statistics - Statistics Explained." Accessed: Aug. 03, 2023. [Online]. Available: [https://ec.europa.eu/eurostat/statistics-explained/index.php?title=Cardiovascular\\_diseases\\_statistics#Self-reporting\\_of\\_hypertensive\\_diseases](https://ec.europa.eu/eurostat/statistics-explained/index.php?title=Cardiovascular_diseases_statistics#Self-reporting_of_hypertensive_diseases)
- [3] B. Milne, T. Gilbey, L. Gautel, and G. Kunst, "Neuromonitoring and Neurocognitive Outcomes in Cardiac Surgery: A Narrative Review," *J Cardiothorac Vasc Anesth*, vol. 36, no. 7, pp. 2098–2113, Jul. 2022, doi: 10.1053/J.JVCA.2021.07.029.
- [4] O. M. Cole, S. Tosif, M. Shaw, and G. Y. H. Lip, "Acute Kidney Injury and Postoperative Atrial Fibrillation In Patients Undergoing Cardiac Surgery," *J Cardiothorac Vasc Anesth*, vol. 34, no. 7, pp. 1783–1790, Jul. 2020, doi: 10.1053/J.JVCA.2019.12.048.
- [5] E. Kozora *et al.*, "Cognitive Outcomes After On- Versus Off-Pump Coronary Artery Bypass Surgery," *Ann Thorac Surg*, vol. 90, no. 4, pp. 1134–1141, Oct. 2010, doi: 10.1016/J.ATHORACSUR.2010.05.076.
- [6] J. A. H. R. Claassen, D. H. J. Thijssen, R. B. Panerai, and F. M. Faraci, "Regulation of cerebral blood flow in humans: Physiology and clinical implications of autoregulation," *Physiol Rev*, vol. 101, no. 4, pp. 1487–1559, Oct. 2021, doi: 10.1152/PHYSREV.00022.2020/ASSET/IMAGES/LARGE/PHYSREV.00022.2020\_F008.JPEG.
- [7] C. J. Rhee, C. S. da Costa, T. Austin, K. M. Brady, M. Czosnyka, and J. K. Lee, "Neonatal cerebrovascular autoregulation," *Pediatr Res*, vol. 84, no. 5, p. 602, Nov. 2018, doi: 10.1038/S41390-018-0141-6.
- [8] B. Kumpaitiene *et al.*, "Cerebrovascular autoregulation impairments during cardiac surgery with cardiopulmonary bypass are related to postoperative cognitive deterioration: prospective observational study," *Minerva Anesthesiol*, vol. 85, no. 6, pp. 594–603, 2019, doi: 10.23736/S0375-9393.18.12358-3.
- [9] A. G. Vedel *et al.*, "Domain-specific cognitive dysfunction after cardiac surgery. A secondary analysis of a randomized trial," *Acta Anaesthesiol Scand*, vol. 63, no. 6, pp. 730–738, Jul. 2019, doi: 10.1111/AAS.13343.
- [10] M. Deimantavicius *et al.*, "Feasibility of the optimal cerebral perfusion pressure value identification without a delay that is too long," *Sci Rep*, vol. 12, no. 1, Dec. 2022, doi: 10.1038/S41598-022-22566-6.

- [11] S. Banik, G. P. Rath, R. Lamsal, and P. K. Bithal, "Effect of dexmedetomidine on dynamic cerebral autoregulation and carbon dioxide reactivity during sevoflurane anesthesia in healthy patients," *Korean J Anesthesiol*, vol. 73, no. 4, pp. 311–318, Aug. 2020, doi: 10.4097/KJA.19246.
- [12] D. Simpson and J. Claassen, "CrossTalk opposing view: dynamic cerebral autoregulation should be quantified using induced (rather than spontaneous) blood pressure fluctuations," *J Physiol*, vol. 596, no. 1, p. 7, Jan. 2018, doi: 10.1113/JP273900.
- [13] R. B. Panerai *et al.*, "Cerebral critical closing pressure and resistance-area product: the influence of dynamic cerebral autoregulation, age and sex," *Journal of Cerebral Blood Flow and Metabolism*, vol. 41, no. 9, pp. 2456–2469, Sep. 2021, doi: 10.1177/0271678X211004131/ASSET/IMAGES/LARGE/10.1177\_0271678X211004131-FIG5.JPEG.
- [14] J.-W. Wu *et al.*, "Brain volume changes in spontaneous intracranial hypotension: Revisiting the Monro-Kellie doctrine," *Cephalalgia*, vol. 41, no. 1, pp. 58–68, 2021, doi: 10.1177/0333102420950385.
- [15] N. A. LASSEN, "Cerebral blood flow and oxygen consumption in man," *Physiol Rev*, vol. 39, no. 2, pp. 183–238, Apr. 1959, doi: 10.1152/PHYSREV.1959.39.2.183.
- [16] S. Milanovic, K. Shaw, C. Hall, and S. Payne, "Investigating the role of pericytes in cerebral autoregulation: a modeling study," *Physiol Meas*, vol. 42, no. 5, p. 054003, Jun. 2021, doi: 10.1088/1361-6579/ABFB0A.
- [17] A. Gomez *et al.*, "Cerebrovascular pressure reactivity and brain tissue oxygen monitoring provide complementary information regarding the lower and upper limits of cerebral blood flow control in traumatic brain injury: a Canadian High Resolution-TBI (CAHR-TBI) cohort study," *Intensive Care Med Exp*, vol. 10, no. 1, Dec. 2022, doi: 10.1186/S40635-022-00482-3.
- [18] S. Ogoh and T. Tarumi, "Cerebral blood flow regulation and cognitive function: a role of arterial baroreflex function," *Journal of Physiological Sciences*, vol. 69, no. 6, pp. 813–823, Nov. 2019, doi: 10.1007/S12576-019-00704-6/FIGURES/8.
- [19] P. Bischoff and I. Rundshagen, "Awareness under general anesthesia," *Dtsch Arztebl Int*, vol. 108, no. 1–2, pp. 1–7, Jan. 2011, doi: 10.3238/ARZTEBL.2011.0001.
- [20] P. Ganjoo and I. Kapoor, "Neuropharmacology," *Essentials of Neuroanesthesia*, pp. 103–122, Jan. 2017, doi: 10.1016/B978-0-12-805299-0.00006-3.
- [21] A. Spiegelberg, M. Preuß, and V. Kurtcuoglu, "B-waves revisited," *Interdisciplinary Neurosurgery*, vol. 6, pp. 13–17, Dec. 2016, doi: 10.1016/J.INAT.2016.03.004.
- [22] M. Kasprowicz, M. Bergsneider, M. Czosnyka, and X. Hu, "Association between ICP pulse waveform morphology and ICP B waves," *Acta Neurochir Suppl*, vol. 114, pp. 29–34, 2012, doi: 10.1007/978-3-7091-0956-4\_6.

- [23] I. Martinez-Tejada, A. Arum, J. E. Wilhjelm, M. Juhler, and M. Andresen, “B waves: a systematic review of terminology, characteristics, and analysis methods,” *Fluids and Barriers of the CNS* 2019 16:1, vol. 16, no. 1, pp. 1–15, Oct. 2019, doi: 10.1186/S12987-019-0153-6.
- [24] M. Czosnyka *et al.*, “Hemodynamic characterization of intracranial pressure plateau waves in head-injured patients,” *J Neurosurg*, vol. 91, no. 1, pp. 11–19, Jul. 1999, doi: 10.3171/JNS.1999.91.1.0011.
- [25] M. Balestreri *et al.*, “Association between outcome, cerebral pressure reactivity and slow ICP waves following head injury,” *Acta Neurochir Suppl*, vol. 95, no. 95, pp. 25–28, 2005, doi: 10.1007/3-211-32318-X\_6.
- [26] B. G. Perry, S. J. E. Lucas, K. N. Thomas, D. J. Cochrane, and T. M€ Undel, “The effect of hypercapnia on static cerebral autoregulation,” *Physiol Rep*, vol. 2, no. 6, 2014, doi: 10.14814/phy2.12059.
- [27] R. B. Panerai *et al.*, “Assessment of dynamic cerebral autoregulation based on spontaneous fluctuations in arterial blood pressure and intracranial pressure,” *Physiol Meas*, vol. 23, no. 1, pp. 59–72, 2002, doi: 10.1088/0967-3334/23/1/306.
- [28] M. Czosnyka, K. Brady, M. Reinhard, P. Smielewski, and L. A. Steiner, “Monitoring of cerebrovascular autoregulation: facts, myths, and missing links,” *Neurocrit Care*, vol. 10, no. 3, pp. 373–386, Jun. 2009, doi: 10.1007/S12028-008-9175-7.
- [29] F. P. Tiecks, A. M. Lam, R. Aaslid, and D. W. Newell, “Comparison of Static and Dynamic Cerebral Autoregulation Measurements,” *Stroke*, vol. 26, no. 6, pp. 1014–1019, 1995, doi: 10.1161/01.STR.26.6.1014.
- [30] J. R. Caldas *et al.*, “Dynamic cerebral autoregulation: A marker of post-operative delirium?,” *Clin Neurophysiol*, vol. 130, no. 1, pp. 101–108, Jan. 2019, doi: 10.1016/J.CLINPH.2018.11.008.
- [31] R. B. Panerai, “Cerebral autoregulation: From models to clinical applications,” *Cardiovascular Engineering*, vol. 8, no. 1, pp. 42–59, Mar. 2008, doi: 10.1007/S10558-007-9044-6/METRICS.
- [32] P. Smielewski, M. Czosnyka, P. Kirkpatrick, H. McEroy, H. Rutkowska, and J. D. Pickard, “Assessment of Cerebral Autoregulation Using Carotid Artery Compression,” *Stroke*, vol. 27, no. 12, pp. 2197–2203, 1996, doi: 10.1161/01.STR.27.12.2197.
- [33] K. Lu, J. W. Clark, F. H. Ghorbel, D. L. Ware, and A. Bidani, “A human cardiopulmonary system model applied to the analysis of the Valsalva maneuver,” *Am J Physiol Heart Circ Physiol*, vol. 281, no. 6, pp. 2661–2679, 2001, doi: 10.1152/AJPHEART.2001.281.6.H2661/ASSET/IMAGES/LARGE/H41211209019.JPEG.

- [34] E. Azevedo and P. Castro, “Cerebral autoregulation,” *Manual of Neurosonology*, pp. 215–227, Apr. 2016, doi: 10.1017/CBO9781107447905.023.
- [35] R. Zhang, C. G. Crandall, and B. D. Levine, “Cerebral Hemodynamics during the Valsalva Maneuver: Insights from Ganglionic Blockade,” *Stroke*, vol. 35, no. 4, pp. 843–847, Apr. 2004, doi: 10.1161/01.STR.0000120309.84666.AE.
- [36] X. Liu *et al.*, “Assessment of cerebral autoregulation indices – a modelling perspective,” *Scientific Reports 2020 10:1*, vol. 10, no. 1, pp. 1–11, Jun. 2020, doi: 10.1038/s41598-020-66346-6.
- [37] J. Hayano, “Introduction to Heart Rate Variability,” *Clinical Assessment of the Autonomic Nervous System*, pp. 109–127, Jan. 2017, doi: 10.1007/978-4-431-56012-8\_7.
- [38] M. L. Sanders *et al.*, “Dynamic cerebral autoregulation reproducibility is affected by physiological variability,” *Front Physiol*, vol. 10, no. JUL, p. 461520, Jul. 2019, doi: 10.3389/FPHYS.2019.00865/BIBTEX.
- [39] J. A. Claassen *et al.*, “Transfer function analysis of dynamic cerebral autoregulation: A white paper from the International Cerebral Autoregulation Research Network,” *Journal of Cerebral Blood Flow and Metabolism*, vol. 36, no. 4, pp. 665–680, Jan. 2015, doi: 10.1177/0271678X15626425/ASSET/IMAGES/LARGE/10.1177\_0271678X15626425-FIG5.JPEG.
- [40] J. A. H. R. Claassen, B. D. Levine, and R. Zhang, “Dynamic cerebral autoregulation during repeated squat-stand maneuvers,” *J Appl Physiol*, vol. 106, no. 1, pp. 153–160, Jan. 2009, doi: 10.1152/JAPPLPHYSIOL.90822.2008/ASSET/IMAGES/LARGE/ZD G0010983020004.JPEG.
- [41] D. S. Nag, S. Sahu, A. Swain, and S. Kant, “Intracranial pressure monitoring: Gold standard and recent innovations,” *World J Clin Cases*, vol. 7, no. 13, p. 1535, Jul. 2019, doi: 10.12998/WJCC.V7.I13.1535.
- [42] A. Tariq, P. Aguilar-Salinas, R. A. Hanel, N. Naval, and M. Chmayssani, “The role of ICP monitoring in meningitis,” *Neurosurg Focus*, vol. 43, no. 5, Nov. 2017, doi: 10.3171/2017.8.FOCUS17419.
- [43] M. Czosnyka, Z. Czosnyka, and P. Smielewski, “Pressure reactivity index: journey through the past 20 years,” *Acta Neurochir (Wien)*, vol. 159, no. 11, pp. 2063–2065, Nov. 2017, doi: 10.1007/S00701-017-3310-1/METRICS.
- [44] F. A. Zeiler, J. Donnelly, P. Smielewski, D. K. Menon, P. J. Hutchinson, and M. Czosnyka, “Critical Thresholds of Intracranial Pressure-Derived Continuous Cerebrovascular Reactivity Indices for Outcome Prediction in Noncraniectomized Patients with Traumatic Brain Injury,” *J Neurotrauma*, vol. 35, no. 10, pp. 1107–1115, May 2018, doi: 10.1089/NEU.2017.5472/SUPPL\_FILE/SUPP\_APPENDIXE.DOCX.

- [45] E. F. M. Wijdicks, “Lundberg and his Waves,” *Neurocrit Care*, vol. 31, no. 3, pp. 546–549, Dec. 2019, doi: 10.1007/S12028-019-00689-5/METRICS.
- [46] Y. Hamarat *et al.*, “Location of the internal carotid artery and ophthalmic artery segments for non-invasive intracranial pressure measurement by multi-depth TCD,” *Libyan J Med*, vol. 12, no. 1, Jan. 2017, doi: 10.1080/19932820.2017.1384290.
- [47] Y. Hamarat *et al.*, “Graphical and statistical analyses of the oculocardiac reflex during a non-invasive intracranial pressure measurement,” *PLoS One*, vol. 13, no. 4, Apr. 2018, doi: 10.1371/JOURNAL.PONE.0196155.
- [48] A. Ragauskas *et al.*, “Clinical assessment of noninvasive intracranial pressure absolute value measurement method,” *Neurology*, vol. 78, no. 21, pp. 1684–1691, May 2012, doi: 10.1212/WNL.0B013E3182574F50.
- [49] B. Schmidt *et al.*, “Adaptive noninvasive assessment of intracranial pressure and cerebral autoregulation,” *Stroke*, vol. 34, no. 1, pp. 84–89, Jan. 2003, doi: 10.1161/01.STR.0000047849.01376.AE.
- [50] B. Schmidt *et al.*, “Comparison of Different Calibration Methods in a Non-invasive ICP Assessment Model,” *Acta Neurochir Suppl*, vol. 126, pp. 79–84, 2018, doi: 10.1007/978-3-319-65798-1\_17.
- [51] L. A. Calviello and M. Czosnyka, “Neurocritical Care Monitoring in ICU: Measurement of the Cerebral Autoregulation by Transcranial Doppler (TCD),” *Neurosonology in Critical Care: Monitoring the Neurological Impact of the Critical Pathology*, pp. 291–297, Jan. 2021, doi: 10.1007/978-3-030-81419-9\_16/COVER.
- [52] J. D. Kirsch, “Essentials of transcranial doppler ultrasound,” *Neurovascular Imaging: From Basics to Advanced Concepts*, pp. 47–66, Jan. 2016, doi: 10.1007/978-1-4614-9029-6\_36/COVER.
- [53] C. H. Lee, S. H. Jeon, S. J. Wang, B. S. Shin, and H. G. Kang, “Factors associated with temporal window failure in transcranial Doppler sonography,” *Neurol Sci*, vol. 41, no. 11, pp. 3293–3299, Nov. 2020, doi: 10.1007/S10072-020-04459-6.
- [54] K. A. Alswat, “Gender Disparities in Osteoporosis,” *J Clin Med Res*, vol. 9, no. 5, p. 382, 2017, doi: 10.14740/JOCMR2970W.
- [55] M. H. Olsen, C. G. Riberholt, J. Mehlsen, R. M. G. Berg, and K. Møller, “Reliability and validity of the mean flow index (Mx) for assessing cerebral autoregulation in humans: A systematic review of the methodology,” *J Cereb Blood Flow Metab*, vol. 42, no. 1, pp. 27–38, Jan. 2022, doi: 10.1177/0271678X211052588.
- [56] K. P. Budohoski *et al.*, “The relationship between cerebral blood flow autoregulation and cerebrovascular pressure reactivity after traumatic brain injury,” *Neurosurgery*, vol. 71, no. 3, pp. 652–660, Sep. 2012, doi: 10.1227/NEU.0B013E318260FEB1.

- [57] B. Goldstein, R. C. Tasker, and W. Wakeland, "From Lundberg to SIM-ICP: computational physiology and modeling intracranial pressure," *Sci Transl Med*, vol. 4, no. 129, Apr. 2012, doi: 10.1126/SCITRANSLMED.3003925.
- [58] F. Lange and I. Tachtsidis, "Clinical Brain Monitoring with Time Domain NIRS: A Review and Future Perspectives," *Applied Sciences 2019, Vol. 9, Page 1612*, vol. 9, no. 8, p. 1612, Apr. 2019, doi: 10.3390/APP9081612.
- [59] E. L. Vu *et al.*, "Cerebral Autoregulation during Orthostatic Challenge in Congenital Central Hypoventilation Syndrome," *Am J Respir Crit Care Med*, vol. 205, no. 3, pp. 340–349, Feb. 2022, doi: 10.1164/RCCM.202103-0732OC.
- [60] F. Abecasis, C. Dias, A. Zakrzewska, V. Oliveira, and M. Czosnyka, "Monitoring cerebrovascular reactivity in pediatric traumatic brain injury: comparison of three methods," *Childs Nerv Syst*, vol. 37, no. 10, pp. 3057–3065, Oct. 2021, doi: 10.1007/S00381-021-05263-Z.
- [61] "A method and apparatus for non-invasively deriving and indicating of dynamic characteristics of the human and animal intracranial media," Aug. 1994.
- [62] Y. Hamarat *et al.*, "Prospective Pilot Clinical Study of Noninvasive Cerebrovascular Autoregulation Monitoring in Open-Angle Glaucoma Patients and Healthy Subjects," *Transl Vis Sci Technol*, vol. 11, no. 2, Feb. 2022, doi: 10.1167/TVST.11.2.17.
- [63] V. Petkus *et al.*, "Non-invasive Cerebrovascular Autoregulation Assessment Using the Volumetric Reactivity Index: Prospective Study," *Neurocrit Care*, vol. 30, no. 1, pp. 42–50, Feb. 2019, doi: 10.1007/S12028-018-0569-X.
- [64] C. S. A. Weersink *et al.*, "Clinical and Physiological Events That Contribute to the Success Rate of Finding 'Optimal' Cerebral Perfusion Pressure in Severe Brain Trauma Patients," *Crit Care Med*, vol. 43, no. 9, pp. 1952–1963, Sep. 2015, doi: 10.1097/CCM.0000000000001165.
- [65] C. Lazaridis *et al.*, "Optimal cerebral perfusion pressure: are we ready for it?," *Neurol Res*, vol. 35, no. 2, pp. 138–148, 2013, doi: 10.1179/1743132812Y.0000000150.
- [66] A. H. Kramer, P. L. Couillard, D. A. Zygun, M. J. Aries, and C. N. Gallagher, "Continuous Assessment of 'Optimal' Cerebral Perfusion Pressure in Traumatic Brain Injury: A Cohort Study of Feasibility, Reliability, and Relation to Outcome," *Neurocrit Care*, vol. 30, no. 1, pp. 51–61, Feb. 2019, doi: 10.1007/S12028-018-0570-4.
- [67] V. Petkus *et al.*, "Optimal Cerebral Perfusion Pressure: Targeted Treatment for Severe Traumatic Brain Injury," *J Neurotrauma*, vol. 37, no. 2, pp. 389–396, Jan. 2020, doi: 10.1089/NEU.2019.6551.
- [68] B. K. J. A. S. K. V. P. E. C. M. Svagzdiene, "The optimal mean arterial blood pressure during cardiopulmonary bypass: does one fit all?," *Eur J Anaesthesiol*, vol. 39, p. 165, Jun. 2022.

- [69] J. H. Gibbon and J. D. Hill, "Part I. The Development of the First Successful Heart-Lung Machine," *Ann Thorac Surg*, vol. 34, no. 3, pp. 337–341, Sep. 1982, doi: 10.1016/S0003-4975(10)62507-6.
- [70] *Global Heart-lung Machines Market 2023-2027*. TechNavio, 2023.
- [71] "LivaNova Sorin S5 Heart-Lung Machine | Perfusion System."
- [72] S. Öztürk, M. Saçar, A. Baltalarlı, and İ. Öztürk, "Effect of the type of cardiopulmonary bypass pump flow on postoperative cognitive function in patients undergoing isolated coronary artery surgery," *Anatol J Cardiol*, vol. 16, no. 11, pp. 875–880, 2016, doi: 10.14744/ANATOLJCARDIOL.2015.6572.
- [73] K. Aykut, G. Albayrak, M. Guzeloglu, E. Hazan, M. Tufekci, and I. Erdoğan, "Pulsatile versus non-pulsatile flow to reduce cognitive decline after coronary artery bypass surgery: A randomized prospective clinical trial," *J Cardiovasc Dis Res*, vol. 4, no. 2, pp. 127–129, Jun. 2013, doi: 10.1016/J.JCDR.2013.05.005.
- [74] O. Desebbe *et al.*, "Quick Assessment of the Lower Limit of Cerebral Autoregulation Using Transcranial Doppler during Cardiopulmonary Bypass in Cardiac Surgery: A Feasibility Study," 2023, doi: 10.31083/j.rcm2406156.
- [75] L. Froese *et al.*, "The impact of sedative and vasopressor agents on cerebrovascular reactivity in severe traumatic brain injury," *Intensive Care Med Exp*, vol. 11, no. 1, p. 54, Aug. 2023, doi: 10.1186/S40635-023-00524-4.
- [76] J. D. Pollock, I. V. Murray, S. J. Bordes, and A. N. Makaryus, "Physiology, Cardiovascular Hemodynamics," *StatPearls*, Mar. 2023, Accessed: Aug. 12, 2023. [Online]. Available: <https://www.ncbi.nlm.nih.gov/books/NBK470310/>
- [77] Klein SP, De Sloovere V, Meyfroidt G, Depreitere B. Differential Hemodynamic Response of Pial Arterioles Contributes to a Quadriphasic Cerebral Autoregulation Physiology. *J Am Heart Assoc*. 2022 Jan 4;11(1):e022943. doi: 10.1161/JAHA.121.022943. Epub 2021 Dec 22. PMID: 34935426; PMCID: PMC9075199.



## **CURRICULUM VITAE**

### **Contacts**

Name, Surname: Edvinas Chaleckas

E-mail.: [edvinaschaleckas@gmail.com](mailto:edvinaschaleckas@gmail.com)

Address: K. Barsausko g. 59, A555, Kaunas, LT-51423

### **Education**

- |           |  |
|-----------|--|
| 2001–2009 | Kaunas A. Stulginskis Secondary School   |
| 2009–2013 | Kaunas Maironis University Gymnasium   |
| 2013–2017 | Kaunas University of Technology. Biomedical Electronics.<br>Bachelor's degree.           |
| 2015      | Vienna University of Technology, Erasmus exchange program.                               |
| 2017–2019 | Kaunas University of Technology. Biomedical Engineering.<br>Master's degree.             |
| 2019–2023 | Kaunas University of Technology. Electrical and Electronics<br>Engineering. PhD studies. |

### **Employment history**

- |           |   |
|-----------|---|
| 2020–2023 | Junior researcher – Kaunas University of Technology, Health<br>Telematics Science Institute |
|-----------|---|

### **Research interests**

Signal processing, human physiology, programming.

## LIST OF PUBLICATIONS

1. **Chaleckas Edvinas**; Putnynaite Vilma; Lapinskiene Indre; Preiksaitis Aidanas, Serpytis Mindaugas; Rocka Saulius; Bartusis Laimonas; Petkus Vytautas; Arminas Ragauskas. Impaired cerebral autoregulation detected in early prevasospasm period is associated with unfavorable outcome after spontaneous subarachnoid hemorrhage: an observational prospective pilot study. *The Ultrasound Journal*. Accepted 11 March 2024. DOI:10.1186/s13089-024-00371-8
2. Deimantavicius, Mantas; **Chaleckas, Edvinas**; Boere, Katherine; Putnynaite, Vilma; Tamosuitis, Tomas; Tamasauskas, Arimantas; Kavaliauskas, Mindaugas; Rocka, Saulius; Preiksaitis, Aidanas; Vosylius, Saulius; Krakauskaite, Solventa; Berskiene, Kristina; Petkus, Vytautas; Ragauskas, Arminas. Feasibility of the optimal cerebral perfusion pressure value identification without a delay that is too long // *Scientific reports*. Berlin :Nature. ISSN 2045-2322. 2022, vol. 12, iss. 1, art. no. 17724, p. 1-12. DOI: 10.1038/s41598-022-22566-6. [Science Citation Index Expanded (Web of Science); Scopus; MEDLINE] [IF: 4,600; AIF: 7,200; Q2(2022, InCites JCR SCIE)] [CiteScore: 7,50; SNIP: 1,312; SJR: 0,973; Q1 (2022, Scopus Sources)].
3. Petkus, Vytautas; Preiksaitis, Aidanas; **Chaleckas, Edvinas**; Chomskis, Romanas; Zubaviciute, Erika; Vosylius, Saulius; Rocka, Saulius; Rastenyte, Daiva; Aries, Marcel; Ragauskas, Arminas; Neumann, Jan-Oliver. Optimal cerebral perfusion pressure-targeted treatment for severe traumatic brain injury // *Journal of Neurotrauma*. NewYork : Mary Ann Liebert. ISSN 0897-7151. eISSN 1557-9042. 2020, vol. 37, no. 2, p. 389-396. DOI:10.1089/neu.2019.6551. [Science Citation Index Expanded (Web of Science); Scopus; MEDLINE] [IF: 5,269; AIF: 4,923; Q1 (2020, InCites JCR SCIE)] [CiteScore: 8,10; SNIP: 1,301; SJR: 1,653; Q1(2020, Scopus Sources)].

### List of conferences

1. V. Putnynaite, **E. Chaleckas**, R. Zakelis, L. Bartusis, B. Kumpaitiene, M. Svagzdiene, E. Sirvinskas, G. Kasputyte, M. Gailusis, R. Benetis, V. Petkus, A. Ragauskas. Non-invasive real time cerebral autoregulation monitoring technology for brain neuroprotection in cardiac surgery. *Brain & Brain PET, 2023*, Brisbane, Australia.
2. Hamarat, Yasin; **Chaleckas, Edvinas**; Krakauskaite, Solventa; Kumpaitiene, Birute; Svagzdiene, Milda; Sirvinskas, Edmundas; Petkus, Vytautas; Kasputyte, Greta; Gailiusas, Mindaugas; Benetis, Rimantas; Ragauskas, Arminas. Transient function of cerebral autoregulation monitoring during cardiac bypass surgery // *Actaphysiologica: Turkish society of physiological sciences 47th Turkish physiology congress*, 1-4 November 2022, Antalya, Turkey. Hoboken, NJ : John Wiley & sons. ISSN 1748-1708. eISSN 1748-1716. 2023, vol. 237, iss. S727, 4.1, p. 13. DOI: 10.1111/apha.13908. [Science Citation Index Expanded (Web of Science)] [CiteScore:11,40; SNIP: 1,288; SJR: 1,497; Q1 (2022, Scopus Sources)] [M.kr.: T 010, M 001].

3. **E. Chaleckas**, Y. Hamarat, A. Ragauskas. Monitoring of cerebral autoregulations transient function during cardiac bypass surgery (**best poster award**). Cerebrovascular Research Network 11<sup>th</sup> annual meeting, Leicester 2022.
4. **Chaleckas, E.**; Putnynaite, V.; Deimantavicius, M.; Boere, K.; Tamosuitis, T.; Kavaliauskas, M.; Preiksaitis, A.; Rocka, S.; Petkus, V.; Ragauskas, A. Increasing the efficiency of cerebrovascular autoregulation-guided neuroprotection for traumatic brain injury patients // Journal of Neurotrauma: abstracts from the 15th International Neurotrauma Symposium, July 17–20, 2022, Berlin, Germany. New Rochelle, NY : Mary Ann Liebert. ISSN0897-7151. eISSN 1557-9042. 2022, vol. 39, iss. 15-16, 55, p. A19-A20. [Science Citation Index Expanded (Web of Science)] [CiteScore: 9,40; SNIP: 1,288; SJR: 1,310; Q1 (2022, Scopus Sources)] [M.kr.: T 010, M 001].
5. Krakauskaitė, Solventa; Sirvinskas, Edmundas; Kasputyte, Greta; Kumpaitiene, Birute; Petkus, Vytautas; Gailiusas, Mindaugas; Svagzdiene, Milda; **Chaleckas, Edvinas**; Benetis, Rimantas; Ragauskas, Arminas. Noninvasive intracranial pressure dynamics during cardiac bypass surgery: prospective study // ICBET 2022: proceedings of 2022 12th international conference on biomedical engineering and technology, Tokyo, Japan, April 20-23, 2022. New York: Association for computing machinery, 2022. ISBN 9781450395779. p. 175-179. (ACM international conference proceeding series). DOI: 10.1145/3535694.3535723. [Scopus].
6. **Chaleckas, E.**; Putnynaite, V.; Petkus, V.; Deimantavicius, M.; Boere, K.; Tamosuitis, T.; Kavaliauskas, M.; Rocka, S.; Preiksaitis, A.; Ragauskas, A. Increasing the efficiency of cerebrovascular autoregulation-guided personalized management for traumatic brain injury patients // Journal of cerebral blood flow & metabolism: Brain and brain-pet 2022 abstracts. Thousands oaks, CA : SAGE. ISSN 0271-678X. eISSN 1559-7016. 2022, vol. [Science Citation Index Expanded (Web of Science)] [CiteScore: 11,40; SNIP: 1,519; SJR: 1,925; Q1 (2022, Scopus Sources)].

### List of patent applications

1. V. Petkus, **E. Chaleckas**, A. Ragauskas. Method and system for estimating status of human brain cerebral blood flow autoregulation for personalized brain perfusion management. E.U. Patent application No. EP EP23182135, 28 JUN 2023.
2. A. Ragauskas, V. Petkus, **E. Chaleckas**, R. Zakelis, L. Bartusis, V. Putnynaite, Y. Hamarat, S. Krakauskaitė, M. Deimantavicius, T. Tamosuitis. Method and apparatus for non-invasive determining intraorbital and intracranial compliance values. U.S. Patent application No. 18/129,887. 2023 04 21.
3. A. Ragauskas, V. Petkus, **E. Chaleckas**. Method and apparatus for human brain neuroprotection during surgery. EU. Patent application No. EP22160563, 07 MAR 2022.
4. A. Ragauskas, V. Petkus, **E. Chaleckas**. Method and apparatus for human brain neuroprotection during surgery. U.S. Patent application No. 17/683,943, 03 MAR 2022.

## ACKNOWLEDGMENTS

I would like to thank my supervisor Prof. Dr. Arminas Ragauskas, Prof., DSc., FBC, FLSHD, for such a fantastic opportunity to study PhD and giving a new perception of the world's view.

I would like to thank Dr. Vytautas Petkus for all the signal processing and the mathematical knowledge as well as life advices.

I would like to thank Dr. Laimonas Bartušis, Dr. Rolandas Žakelis, Vilma Putnynaitė for helping with the data collection in Kaunas Clinics and partners from Kaunas Clinics for the opportunity to collect the clinical data.

I would like to thank Dr. Yasin Hamarat for the best advices during writing of the thesis.

I would like to thank my family and friends for their support during these years.

UDK 616.831-073](043.3)

SL344. 20xx-xx-xx, xx leidyb. apsk. I. Tiražas xx egz. Užsakymas xxx.  
Išleido Kauno technologijos universitetas, K. Donelaičio g. 73, 44249 Kaunas  
Spausdino leidyklos „Technologija“ spaustuvė, Studentų g. 54, 51424 Kaunas